ABSTRACT

Title of Dissertation: Diversity in Cooperative Networks:
How to Achieve and Where to Exploit?

Karim G. Seddik, Doctor of Philosophy, 2008

Dissertation directed by: Professor K. J. Ray Liu
Department of Electrical and Computer Engineering

Recently, there has been much interest in modulation techniques to achieve transmit diversity motivated by the increased capacity of multiple-input multiple-output (MIMO) channels. To achieve transmit diversity the transmitter needs to be equipped with more than one antenna. The antennas should be well separated to have uncorrelated fading among the different antennas; hence, higher diversity orders and higher coding gains are achievable. It is affordable to equip base stations with more than one antenna, but it is difficult to equip the small mobile units with more than one antenna with uncorrelated fading. In such a case, transmit diversity can only be achieved through user cooperation leading to what is known as *cooperative diversity*. Cooperative diversity provides a new dimension over which higher diversity orders can be achieved. In this thesis, we consider the design of protocols that allow several terminals to cooperate via forwarding

each others' data, which can increase the system reliability by achieving spatial cooperative diversity. We consider the problem of "how to achieve and where to exploit diversity in cooperative networks?"

We first propose a cooperation protocol for the multi-node amplify-and-forward protocol. We derive symbol error rate (SER) and outage probability bounds for the proposed protocol. We derive an upper-bound for the SER of any multi-node amplify-and-forward protocol. We prove that the proposed protocol, where each rely only forwards the source signal, will achieve the SER upper-bound if the relays are close to the source node. Then, we consider the problem of power allocation among the source and relay nodes based on the derived SER and outage probability bounds to further enhance the system performance.

We consider the design of distributed space-time and distributed space-frequency codes in wireless relay networks is considered for different schemes, which vary in the processing performed at the relay nodes. We consider the problem of whether a space-time code that achieves full diversity and maximum coding gain over MIMO channels will achieve the same if used in a distributed fashion. Then, we consider the design of diagonal distributed space-time code (DDSTC) which relaxes the stringent synchronization requirement by allowing only one relay to transmit at any time slot. Then, we consider designing distributed space-frequency codes for the case of multipath fading relay channels that can exploit the multipath as well as the cooperative diversity of the channel.

Then, we consider studying systems that exhibit diversity of three forms: source coding diversity (when using a dual description encoder), channel coding diversity, and user-cooperation diversity. We derive expressions for the distortion exponent of several source-channel diversity achieving schemes. We analyze the tradeoff

between the diversity gain (number of relays) to the quality of the source encoder and find the optimum number of relays to help the source. Then, we consider comparing source coding diversity versus channel coding diversity.

Finally, we will consider the use of relay nodes in sensor networks. We will consider the use of relay nodes instead of some of the sensor nodes that are less-informative to the fusion center to relay the information for the other more-informative sensor nodes. Allowing some relay nodes to forward the measurements of the more-informative sensors will increase the reliability of these measurements at the expense of sending fewer measurements to the fusion center. This will create a tradeoff between the number of measurements sent to the fusion center and the reliability of the more-informative measurements.

Diversity in Cooperative Networks: How to Achieve and Where to Exploit?

by

Karim G. Seddik

Dissertation submitted to the Faculty of the Graduate School of the
University of Maryland, College Park in partial fulfillment
of the requirements for the degree of
Doctor of Philosophy
2008

Advisory Committee:

Professor K. J. Ray Liu, Chairman
Professor Prakash Narayan
Professor Alexander Barg
Professor Sennur Ulukus
Professor Amr Baz

PREFACE

All praise is due to Allah (God)

"The end of these two is never reached - knowledge and understanding", Imam Ali.

DEDICATION

To my Parents, my Family and my beloved Fiancee Nahed

ACKNOWLEDGEMENTS

A thesis is never solely the work of the author. I would not have been able to complete this work without the aid and support of countless people over the past four years. I must first express my gratitude towards my advisor, Prof. Ray Liu. His leadership, support, attention to detail, hard work, and scholarship have set an example I hope to match someday. Dr. Liu was always there to support, to guide, and to help, with his calming influence and amazing wisdom. I am extremely grateful to Dr. Liu for his support, encouragement, and understanding in various aspects.

I would like to thank the members in my dissertation committee. I would like to thank Prof. Prakash Narayan for accepting to be in my thesis committee and for so many fruitful discussions during one of my courses' projects. I also want to thank Prof. Alexander Barg, Prof. Sennur Ulukus and Prof. Amr Baz for agreeing to serve in my thesis committee.

I also thank all of my fellow PhD students in our Signals and Information group. They each helped make my time in the PhD program more fun and interesting. The atmosphere has always been a perfect source of motivation. I want to specially thank Dr. Weifeng Su, Dr. Ahmed Sadek, Ahmed Ibrahim, and Amr El Sherif for the so many inspiring discussions that we had during my PhD years.

Finally, I thank my parents and family without whom I would never have been able to achieve so much. I thank them for instilling in me confidence and a drive

for pursuing my PhD. I especially wish to express my love for my fiancee Nahed who only knows the real price of this dissertation.

TABLE OF CONTENTS

LIST OF TABLES

LIST OF FIGURES

Chapter 1

Introduction

The advent of future wireless multimedia services, requiring high signal quality and high data rate, has increased the attention toward the study of wireless channels. The wireless resources such as bandwidth and energy are scarce and it is difficult to meet the high data rate requirement unless some efficient techniques are employed. Also, the wireless channels have a lot of impairments such as fading, shadowing, and multiuser interference which can highly degrade the system performance. This has increased the thrill toward the study of wireless channels to overcome their impairments.

1.1 Wireless Fading Channels

One of the major challenges for communicating over wireless channels is the fading nature of that channels. Fading means the random fluctuations in the amplitude and phase of the received signal and is due to the effect of the reflections of the transmitted signal [1, 2]. As shown in Fig. 1.1, the received signal will be a superposition of reflected versions of the transmitted signal. If the transmitted

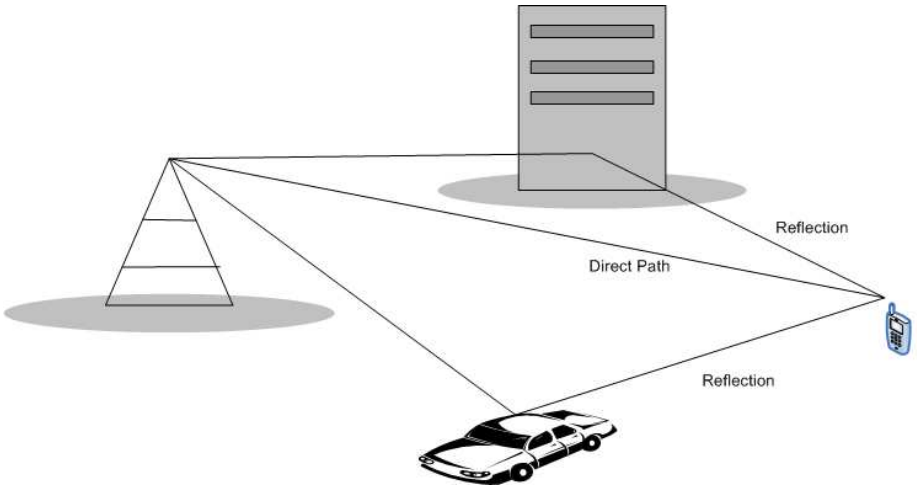

Figure 1.1: The wireless fading channel.

signal is $x(t)$ then the received signal $y(t)$ can be given by

$$y(t) = \sum_{l=1}^{L} h_l(t)x(t - \tau_l) + n(t), \tag{1.1}$$

where $h_l(t)$ is the channel coefficient for the l-th path at time t, L is the number of paths, τ_l is the delay of the l-th path and $n(t)$ is the receiver additive noise. The delay spread of the channel is defined as the time difference between the maximum and minimum delays of the channel paths, i.e., $\Delta\tau = \max_l \tau_l - \min_l \tau_l$ where $\Delta\tau$ is the channel delay spread. According to the value of the delay spread of the channel as compared to the transmitted symbol duration the channel can be either flat (frequency nonselective) fading channel or multipath (frequency selective) fading channel.

1.1.1 Flat-Fading Wireless Channels

If the delay spread of the channel is small compared to the symbol duration of the transmitted signal the channel is known to be flat (frequency nonselective) fading

channel. In this case the channel can be represented by a single parameter that multiplies the transmitted signal. In this case, the received signal can be given by

$$y(t) = h(t)x(t - \tau_l) + n(t), \tag{1.2}$$

where $h(t)$ is the channel coefficient.

1.1.2 Multipath Fading Wireless Channels

If the channel delay spread is larger than the symbol duration the channel can be represented by a linear filter with more than one non-zero tap. This will result in inter-symbol interference (ISI). In this case, the different frequency components of the transmitted signal will experience different fading values; therefore, the channel in this case is known as frequency selective fading channel. In this case, an equalizer is needed at the receiver side to remove the effect of ISI. Also, there exists some transmission schemes, such as orthogonal frequency-division multiplexing (OFDM), that can simplify the equalization at the receiver side.

Although the multipath fading channel causes ISI, which is undesirable phenomenon, however the multipath nature of the channel can be used to enhance the system performance. If we are able to resolve the different paths of the received signal we will have more than one copy of the transmitted signal and this can be considered as some form of achieving *Diversity*.

1.2 Diversity Schemes

One solution to the fading nature of the wireless channels is the use of diversity achieving schemes. Diversity means to provide the destination node with more than one copy of the transmitted data so if one or more copy is highly degraded

due to severe fading then the destination will be still able to decode the source signal using the other received copies. Diversity in the wireless system can be achieved through time diversity, frequency diversity, spatial diversity, etc. Time diversity can be achieved through the transmission of the same signal at different time slots; these time slots should be well separated to ensure that the channel coefficients at these slots are uncorrelated. This will cause a loss in the system data rate as well as an increase in the transmission delay. Frequency diversity can be achieved through the transmission of the same data on different frequency bands. In this case, there will a bandwidth loss due to the transmission of the same data on different frequency bands. Spatial diversity can be achieved through the use of multiple transmit and/or multiple receive antennas. Spatial diversity has proved to be an eminent candidate for achieving the signal quality and high data rate promised by the future multimedia services since it does not increase the overhead in the system in terms of the bandwidth or delay.

The diversity of any scheme is measured through the diversity order D of the system and is defined as

$$D = \lim_{SNR \to \infty} -\frac{\log SER}{\log SNR}, \tag{1.3}$$

where SER is the scheme symbol error rate (SER) and SNR is the system signal-to-noise ratio (SNR). The diversity order D measures the rate of decay of the system SER as a function of the SNR as the SNR tends to infinity.

1.2.1 Multiple-Input Multiple-Output (MIMO) Channels

The seminal works [3] and [4] revealed the increased capacity of the wireless channels by employing Multiple-Input Multiple-Output (MIMO) channels. The MIMO channels are constructed through the use of multiple transmit and/or multiple re-

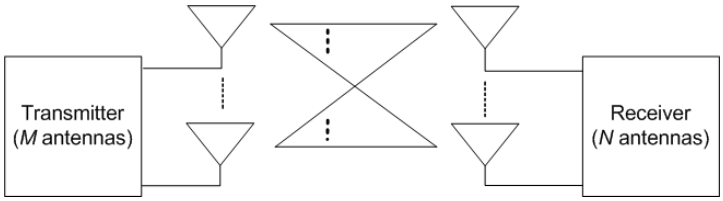

Figure 1.2: Multiple-Input Multiple-Output Channels.

ceive antennas as shown in Fig. 1.2. For the case of having M transmit antennas and N receive antennas, and assuming that the fading coefficients between the different antennas are Rayleigh distributed and uncorrelated, space-time codes can be designed such that the SER behaves as $c \cdot SNR^{-MN}$ at high SNRs for some constant c [5, 6]. In this case the maximum diversity order of the system is given by the product $M \times N$.

1.2.2 Cooperative Diversity

In wireless applications, it is affordable to have multiple antennas at the base station but it is difficult to equip the small mobile units with more than one antenna due to space constraints of the mobile units[1]. Hence, the use of multiple antennas at the mobile units is limited. This gave rise to what is known as *cooperative diversity* in which several nodes try to form a virtual multiple element transmit antenna. Cooperative diversity can be achieved through relay nodes helping the source by forwarding its information.

The classical relay channel model based on additive white Gaussian noise (AWGN) channels was presented in [7]. In this paper, the authors considered

[1]If the antennas are located close to each other, the channel fades may have some correlation which reduces the achievable diversity and/or coding gain.

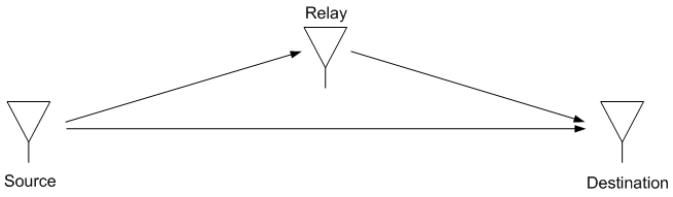

Figure 1.3: The single-relay channel.

calculation of the capacity of the single-relay channels. In this work, an upper-bound on the capacity based the cut-set upper bound has been provided. Also, achievable rates based on some schemes, which under certain conditions achieve the cut-set bound, have been provided. Recent results regarding the capacity of the multi-node relay channels can be found in [8].

Lately, the study of cooperative diversity achieving techniques has gained a lot of interest. The techniques of cooperative diversity have been introduced, for example, by Sendonaris in the context of Code-Division Multiple Access (CDMA) systems [9], [10]. In [11], different protocols were proposed to achieve spatial diversity through node cooperation and outage analyses for these protocols have been provided. Among those protocols are the decode-and-forward (DAF) and amplify-and-forward (AAF) protocols.

In the decode-and-forward protocol with one relay node shown in Fig. 1.3 the relay node decodes the source symbol before re-transmitting to the destination. In order to achieve a diversity of order two for the single-relay DAF protocol, the relay should be able to decide whether or not it has decoded correctly. This can be achieved through the use of error detecting codes or the use of appropriate SNR threshold at the relay node [12]. If the relay always forwards the source signal the system will achieve a diversity of order limited by errors at the relay node(s) and this is known as error propagation [13]. Symbol error rate performance analyses

for the single-node and multi-node decode-and-forward cooperation protocols were provided in [12, 14].

In the amplify-and-forward protocol with one relay node, the relay amplifies the received signal before retransmission to the destination. The amplify-and-forward protocol does not suffer from the error propagation problem because the relays do not perform any hard-decision operation on the received signal; however, in the AAF protocol noise accumulates with the desired signal along the transmission path.

The problem with the multi-node decode-and-forward protocol and the multi-node amplify-and-forward protocol is the loss in the data rate as the number of relay nodes increases. The use of orthogonal subchannels for the relay nodes transmissions, either through Time-Division Multiple Access (TDMA) or Frequency-Division Multiple Access (FDMA), results in a high loss of the system spectral efficiency. This leads to the use of what is known as distributed space-time coding, where relay nodes are allowed to simultaneously transmit over the same channel by emulating a space-time code. The term *distributed* comes from the fact that the virtual multi-antenna transmitter is distributed between randomly located relay nodes. It was proposed in [15] to use relay nodes to form a virtual multi-antenna transmitter to achieve diversity through the use of distributed space-time codes. In addition, an outage analysis was presented for the system. Several works have considered the application of the existing space-time codes in a distributed fashion for the wireless relay network [16–19].

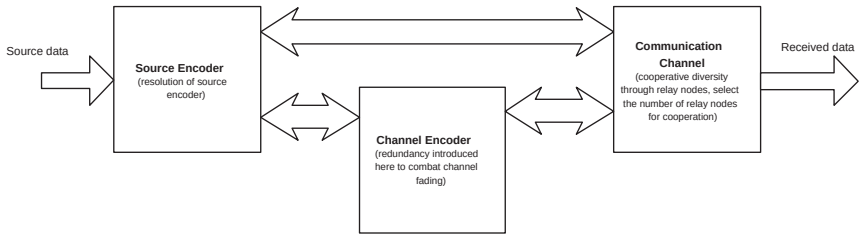

Figure 1.4: The interaction between the different blocks of a general cooperative system.

1.3 Dissertation Outline

In this thesis, we propose to develop and analyze efficient cooperation protocols over the wireless relay channels. Figure 1.4 shows the blocks of a general cooperative communication system. We try to answer the questions of how to achieve and where to exploit diversity in cooperative networks.

For the case of *multimedia communication*, where the most important performance measure is the end-to-end distortion, we study whether the source encoder resolution or the channel encoder redundancy is more important. We develop a general framework for the tradeoff between the source and channel encoders over relay channels. This framework will be used for optimal rate allocation between the source and channel encoders to minimize the end-to-end distortion as well as for selecting the optimal number of relay nodes for cooperation.

For *data communication*, where SER is the performance measure, we no more have the notion of source encoder. We consider achieving diversity through node cooperation. We develop and analyze efficient cooperation protocols based on the use of distributed space-time and space-frequency codes.

1.3.1 Multi-Node Amplify-and-Forward Cooperative Communications (Chapter 2)

In Chapter 2, we investigate the performance of the multi-node amplify-and-forward relay network protocol. We provide a symbol error rate (SER) bound for the multi-node amplify-and-forward protocol in Rayleigh fading channels in which each relay node only amplifies the source signal. The obtained SER bound is shown to be tight at high SNR. We prove that the multi-node amplify-and-forward protocol achieves a diversity of order $N + 1$ for N relay nodes helping the source. We then provide an analysis for a hypothetical system that represents an SER upper-bound for any multi-node amplify-and-forward protocol SER performance. We also prove that multi-node amplify-and-forward protocol, with each relay only amplifying the source signal, approximately achieves this SER upper-bound if the relay nodes are close to the source. Then, we provide outage probability analysis for the multi-node amplify-and-forward protocol. Based on the derived SER and outage probability bounds for the multi-node amplify-and-forward protocol, optimal power allocation is provided.

1.3.2 Distributed Space-Time and Space-Frequency Codings (Chapter 3)

In Chapter 3, the design of distributed space-time codes for wireless relay networks is considered. Distributed space-time coding (DSTC) can be achieved through node cooperation to emulate multiple antennas transmitter. First, the decode-and-forward protocol, in which each relay node decodes the symbols received from the source node before retransmission, is considered. A space-time code designed

to achieve full diversity and maximum coding gain over multiple-input multiple-output (MIMO) channels is proved to achieve full diversity but not necessarily maximizing the coding gain if used with the decode-and-forward protocol. Next, the amplify-and-forward protocol is considered; each relay node can only perform simple operations such as linear transformation of the received signal and then amplify the signal before retransmission. A space-time code designed to achieve full diversity and maximum coding gain over MIMO channels is proved to achieve full diversity and maximum coding gain if used with the amplify-and-forward protocol.

Next, the design of DSTC that can mitigate the relay nodes synchronization errors is considered. Most of the previous works on cooperative transmission assume perfect synchronization between the relay nodes, which means that the relays' timings, carrier frequencies, and propagation delays are identical. Perfect synchronization is difficult to achieve among randomly located relay nodes. To simplify the synchronization in the network, a diagonal structure is imposed on the space-time code used. The diagonal structure of the code bypasses the perfect synchronization problem by allowing only one relay node to transmit at any time slot. Hence, it is not necessary to synchronize simultaneous "in-phase" transmissions of randomly located relay nodes, which greatly simplifies the synchronization among the relay nodes. The code design criterion for distributed space-time codes based on the diagonal structure is derived. The work shows that the code design criterion is to maximize the minimum product distance.

Next, we consider the problem of the design of distributed space-frequency codes. Designing diversity achieving schemes over the wireless broadband fading relay channels is crucial to achieve higher diversity gains. These gains are achieved by exploiting the multipath (frequency) and cooperative diversities to combat the

fading nature of wireless channels. The challenge is how to design space-frequency codes, distributed among randomly located nodes that can exploit the frequency diversity of the wireless broadband channels. In this Chapter, the design of distributed space-frequency codes (DSFCs) for wireless relay networks is considered. The proposed DSFCs are designed to achieve the frequency and cooperative diversities of the wireless relay channels. The use of DSFCs with the decode-and-forward (DAF) and amplify-and-forward (AAF) protocols is considered. The code design criteria to achieve full diversity, based on the pairwise error probability (PEP) analysis, are derived. For DSFC with the DAF protocol, a two-stage coding scheme, with source node coding and relay nodes coding, is proposed. We derive sufficient conditions for the proposed code structures at the source and relay nodes to achieve full diversity of order NL, where N is the number of relay nodes and L is the number of paths per channel. For the case of DSFC with the AAF protocol, a structure for distributed space-frequency coding is proposed.

1.3.3 Source-Channel Diversity for Multi-Hop and Relay Channels (Chapter 4)

A key challenge in the design of real-time wireless multimedia systems is the presence of fading coupled with strict delay constraints. A very effective answer to this problem is the use of diversity achieving techniques. Chapter 4 focuses on studying systems that exhibit diversity of three forms: source coding diversity, channel coding diversity, and user-cooperation diversity (implemented through either relay channels or multi-hop channels, each with amplify-and-forward or decode-and-forward user cooperation). Consistent with the focus on real-time multimedia communications, performance is measured through the distortion exponent, which

measures the rate of decay of the end-to-end distortion at high signal-to-noise ratio (SNR). The results show that for both relay and multi-hop channels, channel coding diversity provides the best performance, followed by source coding diversity. The results also show a tradeoff between the quality (resolution) of the source encoder and the amount of cooperation, in that, as the bandwidth expansion factor increases (higher bandwidth) user cooperation diversity is the main limiting factor, not the source encoding distortion. Thus, the distortion exponent is improved by increasing the number of relays (increasing the diversity order). At low bandwidth expansion factor the source average end-to-end distortion is limited by the source encoder distortion and, in this case, using higher resolution source encoder will improve the performance, in terms of the distortion exponent, more than increasing the number of relay nodes.

1.3.4 Distributed Detection in Wireless Networks: A Sensor or a Relay? (Chapter 5)

In this Chapter, the problem of deploying relay nodes in sensor networks will be considered. A system consisting of a set of sensor nodes communicating to a fusion center, where decisions are made, is considered. As some sensor nodes provide "less-informative" measurements to the fusion center, assigning the system resources allocated for these sensors to relay nodes to forward the measurements of the other "more-informative" sensor nodes is considered. This introduces a new tradeoff in the system design between the number of measurements sent to the fusion center and the reliability of the more-informative measurements, which is enhanced by deploying more relay nodes in the network. We will analyze the performance of two protocols. In Protocol I, each sensor node directly transmits its

measurement to the fusion center. In Protocol II, instead of having each sensor directly transmitting its measurement, relay nodes will be used instead of some of the less-informative sensor nodes to forward the measurements of the more-informative sensor nodes. Hence, in Protocol II, the reliability of the more-informative measurements is enhanced at the expense of having fewer measurements sent to the fusion center and this creates the tradeoff between the number of measurements available at the fusion center and the reliability of the measurements. We analyze the performance of the two protocols over additive white Gaussian noise (AWGN) and Rayleigh flat-fading channels. Based on the analysis, the regions where the performance of one protocol is superior to the other are characterized. Also, asymptotic comparison results when the communication noise variance or the measurement noise variance tends to zero are provided. The results show that in some cases it is better to allocate some of the system resources to relay nodes, not to sensor nodes, to increase the reliability of the more-informative measurements and this leads to a better overall detection performance at the fusion center.

Chapter 2

Multi-Node Amplify-and-Forward Cooperative Communications

In the amplify-and-forward protocol with one relay node, the relay normalizes the received signal and then amplifies it before re-transmission. The amplify-and-forward protocol does not suffer from the error propagation problem because the relays do not perform any hard-decision operation to the received signal but noise accumulates with the desired signal along the transmission.

In this Chapter, the symbol error rate (SER) expressions for the multi-node amplify-and-forward protocol are derived. The SER analyses for the single-relay amplify-and-forward and decode-and-forward protocols can be found in [14] and for the multi-node decode-and-forward protocol can be found in [12]. The approach we adopt in this Chapter is based on deriving the exact moment generating function (MGF) of the scaled harmonic mean of two exponential random variables[1]. These exact MGF expressions can be used to get exact expressions for the SER.

[1]The harmonic mean of two numbers X_1 and X_2 is $\frac{2X_1X_2}{X_1+X_2}$.

Also, an outage probability analysis of the multi-node amplify-and-forward protocol with N relay nodes helping the source is presented. In [11], the outage probability of the single relay amplify-and-forward network was obtained based on the limiting behavior of the cumulative distribution function (CDF) of certain combinations of exponential random variables. The case of a single relay amplify-and-forward protocol in [11] can be considered as a special case of our analysis with $N = 1$.

2.1 System Models

In this section, we introduce the multi-node source-only and the maximum ratio combiner (MRC) based amplify-and-forward system models.

2.1.1 Source-Only Amplify-and-Forward System Model

The multi-node source-only amplify-and-forward system model is shown in Fig. 2.1. A cooperative strategy with two phases is considered. In phase 1, the source transmits its information to the destination, and due to the broadcast nature of the wireless channels the neighbor nodes receive the information. In phase 2, N users help the source by amplifying the source signal. In both phases the users transmit their information through orthogonal channels (through TDMA or FDMA). Perfect synchronization is assumed among the cooperating nodes.

In phase 1, the source broadcasts its information to the destination and N relay nodes. The received signals $y_{s,d}$ and y_{s,r_i} at the destination and the i-th relay can be written, respectively, as

$$y_{s,d} = \sqrt{P_s} h_{s,d} x + \eta_{s,d}, \tag{2.1}$$

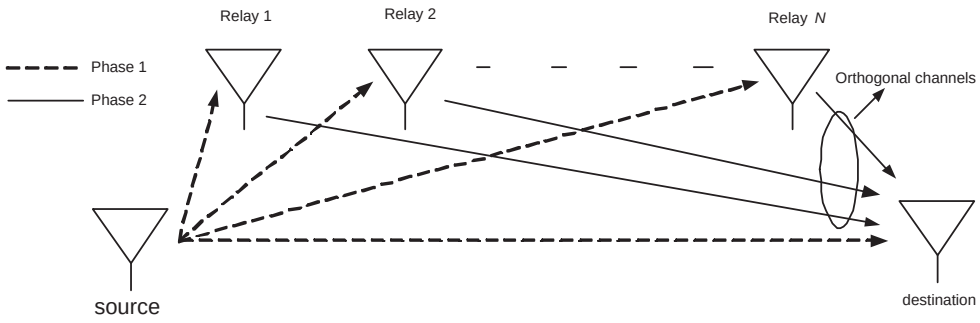

Figure 2.1: Multi-node amplify-and-forward system model.

$$y_{s,r_i} = \sqrt{P_s} h_{s,r_i} x + \eta_{s,r_i},\ i = 1, 2, ..., N, \tag{2.2}$$

where P_s is the transmitted source power, x is the transmitted source symbol with $E\{||x||^2\} = 1$ where $E\{\cdot\}$ denotes the expectation operator, $\eta_{s,d}$ and η_{s,r_i} denote the additive white Gaussian noise (AWGN) at the destination and the i-th relay, respectively, and $h_{s,d}$ and h_{s,r_i} are the channel coefficients from the source to destination and the i-th relay node, respectively. Each relay amplifies the received signal from the source and re-transmits it to the destination. The received signal at the destination node in phase 2 due to the i-th relay transmission is given by

$$y_{r_i,d} = \frac{\sqrt{P_i}}{\sqrt{P_s |h_{s,r_i}|^2 + N_0}} h_{r_i,d} y_{s,r_i} + \eta_{r_i,d}, \tag{2.3}$$

where P_i is the i-th relay node power, $h_{r_i,d}$ is the channel coefficient from the i-th relay node to the destination, and $\eta_{r_i,d}$ is the destination AWGN. The channel coefficients $h_{s,d}$, h_{s,r_i}, and $h_{r_i,d}$ are modeled as zero-mean circularly symmetric complex Gaussian random variables with variances $\delta^2_{s,d}$, δ^2_{s,r_i}, and $\delta^2_{r_i,d}$, respectively, i.e., a Rayleigh flat-fading channel model is considered. The channel coefficients are assumed to be available at the receiving nodes but not at the transmitting nodes. The noise terms are modeled as zero-mean complex Gaussian random variables with variance $N_0/2$ per dimension. Jointly combining the signals received from

the source in phase 1 and that from the relays in phase 2, the destination detects the transmitted symbols by the use of MRC detector [20].

2.1.2 MRC-Based Amplify-and-Forward System Model

In this subsection, we introduce the multi-node MRC-based amplify-and-forward system model. For simplicity of presentation, we will consider a system with two relay nodes which can be easily extended to the N relay nodes case. This system has three phases as follows. In phase 1, the source transmits its information to the destination and the two relay nodes. In phase 2, the first relay helps the source by amplifying and forwarding the received source signal in phase 1. In phase 3, the second relay applies an MRC to the two received signals from the previous two phases and sends to the destination an amplified version of the MRC output. Therefore, for the case of having N relay nodes helping the source we will have $N + 1$ phases. Each relay applies an MRC to the received signals from the source and all of the previous relays. MRC has the advantage of maximizing the signal-to-noise ratio (SNR) at the output of the detector under the condition that the noise terms at the input of the MRC are uncorrelated [20].

The system model for the MRC-based AAF protocol can be formulated as follows. In phase 1, the source broadcasts its information to the destination and all of the relay nodes. The received signals $y_{s,d}$ and y_{s,r_i} for $i = 1, 2$ are as given in (2.1) and (2.2), respectively. In phase 2, the received data at the destination due to the first relay node transmission is given as in (2.3). The received data at the second relay node due to the first relay node transmission is given by

$$y_{r_1,r_2} = \frac{\sqrt{P_1}}{\sqrt{P_s|h_{s,r_1}|^2 + N_0}} h_{r_1,r_2} y_{s,r_1} + \eta_{r_1,r_2}, \tag{2.4}$$

where the inter-relay channel coefficient h_{r_1,r_2} is modeled as zero-mean circularly

symmetric complex Gaussian random variable with variance $\delta^2_{r_1,r_2}$. The receiver noise η_{r_1,r_2} is modeled as zero-mean complex Gaussian random variables with variance $N_0/2$ per dimension.

In phase 3, the second relay node applies MRC to the received signals from phases 1 and 2. With the assumption of channel knowledge at the second relay node, the output of the MRC can be written as

$$\widetilde{y} = \widetilde{\alpha}_s y_{s,r_2} + \widetilde{\alpha}_1 y_{r_1,r_2}, \tag{2.5}$$

where $\widetilde{\alpha}_s = \sqrt{P_s} h^*_{s,r_2}/N_0$ and

$$\widetilde{\alpha}_1 = \frac{\sqrt{\frac{P_s P_1}{P_s|h_{s,r_1}|^2+N_0}} h^*_{s,r_1} h^*_{r_1,r_2}}{\left(\frac{P_1|h_{r_1,r_2}|^2}{P_s|h_{s,r_1}|^2+N_0}+1\right) N_0}.$$

Then, the received signal at the destination in phase 3 is given by

$$y_{r_2,d} = \sqrt{P_2} h_{r_2,d} \frac{\widetilde{y}}{\sqrt{K^2+K}} + \eta_{r_2,d}, \tag{2.6}$$

where

$$K = \frac{\frac{P_s P_1}{P_s|h_{s,r_1}|^2+N_0}|h_{s,r_1}|^2|h_{r_1,r_2}|^2}{\left(\frac{P_1|h_{r_1,r_2}|^2}{P_s|h_{s,r_1}|^2+N_0}+1\right) N_0} + \frac{P_s|h_{s,r_2}|^2}{N_0}. \tag{2.7}$$

Then the destination node applies an MRC-detector to the received signals from the different phases.

2.2 SER Performance Analysis

In this section, we derive a closed-form symbol error rate (SER) bound for the source-only amplify-and-forward cooperation protocol with M-PSK and square M-QAM signals. We also consider two scenarios for the MRC-based protocol to gain some insights into the performance of the MRC-based protocol.

2.2.1 Source-Only Amplify-and-Forward Protocol

With the knowledge of the channel state information, the output of the MRC detector can be written as

$$y = \alpha_s y_{s,d} + \sum_{i=1}^{N} \alpha_i y_{r_i,d}, \tag{2.8}$$

where $\alpha_s = \sqrt{P_s} h^*_{s,d}/N_0$ and

$$\alpha_i = \frac{\sqrt{\frac{P_s P_i}{P_s|h_{s,r_i}|^2+N_0}}\, h^*_{s,r_i} h^*_{r_i,d}}{\left(\frac{P_i|h_{r_i,d}|^2}{P_s|h_{s,r_i}|^2+N_0}+1\right) N_0}.$$

With our assumption of having source symbol x with unit average energy then the SNR at the MRC-detector output is

$$\gamma = \gamma_s + \sum_{i=1}^{N} \gamma_i \tag{2.9}$$

where $\gamma_s = P_s|h_{s,d}|^2/N_0$, and

$$\gamma_i = \frac{1}{N_0} \frac{P_s P_i |h_{s,r_i}|^2 |h_{r_i,d}|^2}{P_s|h_{s,r_i}|^2 + P_i|h_{r_i,d}|^2 + N_0}. \tag{2.10}$$

It has been shown in [21] that the instantaneous SNR γ_i can be tightly upper-bounded as

$$\widetilde{\gamma}_i = \frac{1}{N_0} \frac{P_s P_i |h_{s,r_i}|^2 |h_{r_i,d}|^2}{P_s|h_{s,r_i}|^2 + P_i|h_{r_i,d}|^2}, \tag{2.11}$$

which is a scaled harmonic mean of $P_s|h_{s,r_i}|^2/N_0$ and $P_i|h_{r_i,d}|^2/N_0$.

If M-PSK modulation is used in the system with the instantaneous SNR γ in (2.9) then the conditional SER given the channel state information (CSI) can be given as [22]

$$\begin{aligned} P^{CSI}_{PSK} &= \Psi_{PSK}(\gamma) \\ &= \frac{1}{\pi} \int_0^{(M-1)\pi/M} \exp\left(-\frac{b_{PSK}\gamma}{\sin^2\theta}\right) d\theta, \end{aligned} \tag{2.12}$$

where $b_{PSK} = \sin^2(\pi/M)$.

If M-QAM ($M = 2^k$ with k even) constellation is used in the system, the conditional SER is given by

$$P_{QAM}^{CSI} = \Psi_{QAM}(\gamma), \tag{2.13}$$

where

$$\Psi_{QAM}(\gamma) = 4RQ\left(\sqrt{b_{QAM}\gamma}\right) - 4R^2Q^2\left(\sqrt{b_{QAM}\gamma}\right), \tag{2.14}$$

in which $R = 1 - \frac{1}{\sqrt{M}}$, $b_{QAM} = 3/(M-1)$, and $Q(u) = \frac{1}{\sqrt{2\pi}}\int_u^\infty \exp\left(-\frac{t^2}{2}\right) dt$ is the Gaussian Q-function.

Averaging over the Rayleigh fading channel coefficients, the SER of the M-PSK signals and M-QAM signals can be given, respectively, by

$$P_{PSK} \approx \frac{1}{\pi}\int_0^{(M-1)\pi/M} M_{\gamma_s}\left(\frac{b_{PSK}}{\sin^2\theta}\right)\prod_{i=1}^{N} M_{\widetilde{\gamma}_i}\left(\frac{b_{PSK}}{\sin^2\theta}\right) d\theta, \tag{2.15}$$

and

$$\begin{aligned} P_{QAM} \approx & \frac{4R}{\pi}\int_0^{\pi/2} M_{\gamma_s}\left(\frac{b_{QAM}}{2\sin^2\theta}\right)\prod_{i=1}^{N} M_{\widetilde{\gamma}_i}\left(\frac{b_{QAM}}{2\sin^2\theta}\right) d\theta \\ & - \frac{4R^2}{\pi}\int_0^{\pi/4} M_{\gamma_s}\left(\frac{b_{QAM}}{2\sin^2\theta}\right)\prod_{i=1}^{N} M_{\widetilde{\gamma}_i}\left(\frac{b_{QAM}}{2\sin^2\theta}\right) d\theta, \end{aligned} \tag{2.16}$$

where $M_Z(s)$ denotes the moment generating function (MGF)[2] of the random variable Z.

We used the SNR approximation of $\widetilde{\gamma}_i$ in (2.11) to get the expressions in (2.15) and (2.16). To get the expression in (2.16), two special properties of the Gaussian

[2]The moment generating function (MGF) of a random variable Z is given by

$$M_Z(s) = \int_{-\infty}^{\infty} exp(-sz)\, p_Z(z)\, dz, \tag{2.17}$$

where $p_Z(z)$ is the probability density function (pdf) of the random variable Z.

Q-function as $Q(u) = \frac{1}{\pi}\int_0^{\pi/2} exp\left(-\frac{u^2}{2\sin^2\theta}\right) d\theta$ and $Q^2(u) = \frac{1}{\pi}\int_0^{\pi/4} exp\left(-\frac{u^2}{2\sin^2\theta}\right) d\theta$ for $u \geq 0$ were used [22].

The MGF of γ_s, which is an exponential random variable, can be simply given by

$$M_{\gamma_s} = \frac{1}{1 + \frac{sP_s\delta_{s,d}^2}{N_0}}. \tag{2.18}$$

The problem is how to get the MGF of $\widetilde{\gamma}_i$. It has been investigated in [21] by applying Laplace transform, in which a solution was given by using the hypergeometric functions. These expressions are hard to be used for analysis and for optimal power allocation. An alternative approach was proposed in [14] from which a closed-form expression for the MGF of $\widetilde{\gamma}_i$ can be obtained as follows.

Let X_1 and X_2 be two independent exponential random variables with parameters β_1 and β_2, respectively, and $Z = \frac{X_1X_2}{X_1+X_2}$ is a scaled harmonic mean of X_1 and X_2. Then, the MGF of Z is

$$M_Z(s) = \frac{(\beta_1 - \beta_2)^2 + (\beta_1 + \beta_2)s}{\Delta^2} + \frac{2\beta_1\beta_2 s}{\Delta^3}\ln\frac{(\beta_1 + \beta_2 + s + \Delta)^2}{4\beta_1\beta_2}, \tag{2.19}$$

where

$$\Delta = \sqrt{(\beta_1 - \beta_2)^2 + 2(\beta_1 + \beta_2)s + s^2}.$$

With $\beta_1 = N_0/P_s\delta_{s,r_i}^2$ and $\beta_2 = N_0/P_i\delta_{r_i,d}^2$, the MGF of $\widetilde{\gamma}_i$ is given by (2.19). At high enough SNR, the MGF can be further simplified to [14]

$$M_Z(s) \approx \frac{\beta_1 + \beta_2}{s}. \tag{2.20}$$

Substituting in (2.15) and (2.16), we can get the following result.

At high enough SNR, the SER of the source-only multi-node amplify-and-forward cooperative protocol with N relay nodes employing M-PSK or M-QAM

signals can be approximated as

$$P_{SER} \approx \frac{C\left(N\right) N_0^{N+1}}{b^{N+1}} . \frac{1}{P_s \delta_{s,d}^2} \prod_{i=1}^{N} \frac{P_s \delta_{s,r_i}^2 + P_i \delta_{r_i,d}^2}{P_s P_i \delta_{s,r_i}^2 \delta_{r_i,d}^2}, \tag{2.21}$$

where in case of M-PSK signals, $b = b_{PSK}$ and

$$C\left(N\right) = \frac{1}{\pi} \int_0^{(M-1)\pi/M} \sin^{2(N+1)} \theta d\theta, \tag{2.22}$$

while in case of M-QAM signals, $b = b_{QAM}/2$ and

$$C\left(N\right) = \frac{4R}{\pi} \int_0^{\pi/2} \sin^{2(N+1)} \theta d\theta - \frac{4R^2}{\pi} \int_0^{\pi/4} \sin^{2(N+1)} \theta d\theta. \tag{2.23}$$

Theorem 1 *The diversity order of source-only amplify-and-forward scheme with N relay nodes helping the source is $N + 1$.*

Proof To calculate the diversity order of the scheme, let P denote the total power and let $P_s = a_s P$ and $P_i = a_i P,\ i = 1, ..., N$ where $a_s + \sum_{i=1}^{N} a_i = 1,\ a_s > 0,\ a_i > 0,\ i = 1, ..., N$. Define the SNR as $SNR = P/N_0$. The diversity order of the protocol is defined as $d_{AF} = \lim_{SNR \to \infty} -\frac{\log P_{SER}}{\log SNR} = N + 1$ in our source-only multi-node amplify-and-forward protocol with N relay nodes helping the source.

2.2.2 MRC-based Amplify-and-Forward Protocol

In this subsection, we try to gain some insights into the performance of the MRC-based amplify-and-forward protocol. For the simple example of two relay nodes network and with the knowledge of the channel state information, the output of the MRC-detector at the destination node can be written as

$$y = \alpha_s y_{s,d} + \alpha_1 y_{r_1,d} + \alpha_2 y_{r_2,d}, \tag{2.24}$$

where α_s, α_1 are the same as the source-only amplify-and-forward protocol and α_2 is given by

$$\alpha_2 = \frac{\sqrt{P_2} h_{r_2,d}^* \frac{K}{\sqrt{K^2+K}}}{P_2 |h_{r_2,d}|^2 \frac{K}{K^2+K} + N_0},$$

where K is as defined in (2.7).

The SER analysis of this protocol is very complicated and intractable. Although this protocol is thought of to give better performance than the source-only amplify-and-forward protocol, it does not. The reason behind this is that the system suffers from the noise propagation problem [13]. For the simple example of two relays network, the noise terms at the destination in phases 2 and 3 contain a contribution from the noise generated at the first relay, η_{s,r_1}, in phase 1. So the noise components in the received signals during the several phases are no more uncorrelated and the MRC-detector is no more optimal. This noise propagation problem causes a degradation in the SER performance of the protocol. The problem is more severe for increased number of relays because we will have more correlated noise components that will propagate to the destination. The optimum receiver in this case is to apply a pre-whitening filtering to the received signals and then apply the MRC-detector. Of course the analysis of the system will become more complicated if we consider the noise propagation problem. Although the source-only amplify-and-forward protocol is less complex than the MRC-based amplify-and-forward protocol, we will show that it can give approximately the same, if not better, SER performance. This is because the benefit that we get from applying MRC at each relay node in the MRC-based protocol is diminished by the correlated noise propagation problem as will be described later. To see the effect of the noise propagation on the MRC-based protocol, we consider two extreme scenarios for the two relays network and compare the performances of the two protocols under these two scenarios.

1. $|h_{r_1,d}| = 0$: In this case, we do not have the noise propagation problem because the noise term η_{s,r_1} will be received only once in phase 3. In this

case the SNR at the destination of the MRC-based protocol can be written as

$$SNR_{MRC} \simeq \frac{P_s|h_{s,d}|^2}{N_0} + \frac{K\frac{P_2|h_{r_2,d}|^2}{N_0}}{K + \frac{P_2|h_{r_2,d}|^2}{N_0}}, \tag{2.25}$$

Similarly, the SNR at the destination of the source-only based protocol can be written as

$$SNR_{source-only} \simeq \frac{P_s|h_{s,d}|^2}{N_0} + \frac{\frac{P_s|h_{s,r_2}|^2}{N_0}.\frac{P_2|h_{r_2,d}|^2}{N_0}}{\frac{P_s|h_{s,r_2}|^2}{N_0} + \frac{P_2|h_{r_2,d}|^2}{N_0}}. \tag{2.26}$$

Clearly, $SNR_{MRC} > SNR_{source-only}$ because $K > \frac{P_s|h_{s,r_2}|^2}{N_0}$. Intuitively, because we do not have noise propagation in this case, it is better for relay 2 to combine the signals it received from both the source and relay 1 using MRC to maximize the SNR at its output instead of using only the source signal. Under this scenario the MRC-based protocol is better than the source-only protocol because it results in a higher SNR at the destination.

2. $|h_{r_1,d}| >>$, $|h_{r_2,d}| >>$, $|h_{r_1,r_2}| >>$ and $|h_{s,r_2}| = 0$: In this case, the relay-destination links can be approximated to be noise free. The output of the destination detector in the MRC-based protocol can be written as

$$y_{MRC} \simeq \left(\frac{P_s|h_{s,d}|^2}{N_0} + 2\frac{P_s|h_{s,r_1}|^2}{N_0}\right)x + \frac{\sqrt{P_s}h^*_{s,d}}{N_0}\eta_{s,d} + 2\frac{\sqrt{P_s}h^*_{s,r_1}}{N_0}\eta_{s,r_1}, \tag{2.27}$$

because the signal at the first relay in phase 1 is transmitted twice in phases 2 and 3. The output of the destination detector in the source-only based protocol can be written as

$$y_{source-only} \simeq \left(\frac{P_s|h_{s,d}|^2}{N_0} + \frac{P_s|h_{s,r_1}|^2}{N_0}\right)x + \frac{\sqrt{P_s}h^*_{s,d}}{N_0}\eta_{s,d} + \frac{\sqrt{P_s}h^*_{s,r_1}}{N_0}\eta_{s,r_1}. \tag{2.28}$$

Clearly, we have

$$SNR_{source-only} \simeq \frac{P_s|h_{s,d}|^2}{N_0} + \frac{P_s|h_{s,r_1}|^2}{N_0} > SNR_{MRC} \simeq \frac{\left(\frac{P_s|h_{s,d}|^2}{N_0} + 2\frac{P_s|h_{s,r_1}|^2}{N_0}\right)^2}{\frac{P_s|h_{s,d}|^2}{N_0} + 4\frac{P_s|h_{s,r_1}|^2}{N_0}}. \tag{2.29}$$

In this case, the source-only based protocol achieves better performance than the MRC-based protocol. This is because the MRC-based protocol combines the same signal twice (signals received in phases 2 and 3). Thus in this case, the noise propagation problem is highly severe and causes a high degradation in the system SER performance.

The above two scenarios give some insights about how the system performance is affected by the different channel coefficients. From the above two scenarios, intuition suggests that the source-only based protocol will give better performance than the MRC-based protocol if the relays become closer to the destination, because scenarios similar to the second scenario will dominate (occurs with higher probability). In the simulation section, we will simulate a system in which the relays are close to the destination and we will see that the source-only based protocol is always better than the MRC-based protocol, which proves our claim here.

2.2.3 SER Upper-Bound

In this section, we derive an SER upper-bound for any amplify-and-forward strategy. We will prove that this bound is achieved by the source-only amplify-and-forward protocol if the relays are close to the source. That is the source-only amplify-and-forward protocol will achieve the best performance that any amplify-and-forward protocol can achieve if the relay nodes are very close to the source. The best system that one can think of is a system in which the relay nodes from

2 to N, after power normalization, send the source symbol x. So the relay nodes from 2 to N will appear as source nodes. This does not apply to the first relay because it has only one copy of the transmitted data that is received from the source node so for any protocol it can not do better than what it does in the source-only amplify-and-forward protocol. But the relays from 2 to N may have more than one received signal that they could combine or do some processing to reduce the noise in the amplified transmitted signal. Of course this system is hypothetical and no system can achieve this noise suppression at the output of the relay nodes. But the SER performance of this system can be thought of as an SER upper-bound. In what follows we perform an SER performance analysis of this hypothetical system and prove that the source-only amplify-and-forward protocol will achieve this bound if the relays are close to the source. We assume that the relays from 2 to N transmit the source symbol x. With the knowledge of the channel state information, the of the MRC-detector can be written as

$$y = \alpha_s y_{s,d} + \alpha_1 y_{r_1,d} + \sum_{i=2}^{N} \alpha_i y_{r_i,d}, \tag{2.30}$$

where $\alpha_s = \sqrt{P_s} h^*_{s,d}/N_0$,

$$\alpha_1 = \frac{\sqrt{\frac{P_s P_1}{P_s|h_{s,r_1}|^2+N_0}} h^*_{s,r_1} h^*_{r_1,d}}{\left(\frac{P_1|h_{r_1,d}|^2}{P_s|h_{s,r_1}|^2+N_0}+1\right) N_0},$$

and $\alpha_i = \sqrt{P_i} h^*_{r_i,d}/N_0$ for $i = 2, \cdots, N$.

The SNR at the MRC-detector output is

$$\gamma = \gamma_s + \gamma_1 + \sum_{i=2}^{N} \gamma_i, \tag{2.31}$$

where $\gamma_s = P_s|h_{s,d}|^2/N_0$,

$$\gamma_1 = \frac{1}{N_0} \frac{P_s P_1 |h_{s,r_1}|^2 |h_{r_1,d}|^2}{P_s|h_{s,r_1}|^2 + P_1|h_{r_1,d}|^2 + N_0}, \tag{2.32}$$

and $\gamma_i = P_i|h_{r_i,d}|^2/N_0$, $i = 2, \cdots, N$. Following the analysis in Section 2.2.1, we can write the SER bound at high enough SNR of that system as

$$P_{SER} \approx \frac{C(N) N_0^{N+1}}{b^{N+1}} . \frac{1}{P_s \delta_{s,d}^2} . \frac{P_s \delta_{s,r_1}^2 + P_1 \delta_{r_1,d}^2}{P_s P_1 \delta_{s,r_1}^2 \delta_{r_1,d}^2} \prod_{i=2}^{N} \frac{1}{P_i \delta_{r_i,d}^2}, \tag{2.33}$$

where in case of M-PSK signals, $b = b_{PSK}$ and $C(N)$ is the same as in (2.22). While in case of M-QAM signals, $b = b_{QAM}/2$ and $C(N)$ is the same as in (2.23). In the expression of (2.33), it is clear that the relays from 2 to N appear as sources with the term $\frac{1}{P_i \delta_{r_i,d}^2}$. For the source-only amplify-and-forward protocol, each relay has a contribution in the SER by the term $\frac{P_s \delta_{s,r_i}^2 + P_i \delta_{r_i,d}^2}{P_s P_i \delta_{s,r_i}^2 \delta_{r_i,d}^2}$. If the relays are close to the source then

$$\frac{P_s \delta_{s,r_i}^2 + P_i \delta_{r_i,d}^2}{P_s P_i \delta_{s,r_i}^2 \delta_{r_i,d}^2} \xrightarrow{\delta_{s,r_i}^2 \uparrow} \frac{1}{P_i \delta_{r_i,d}^2}.$$

Intuitively, in the source-only amplify-and-forward protocol, the SNR of each source-relay-destination link is a scaled harmonic mean of the source-relay and relay-destination links SNR. If the relays are close to the source, the performance will be limited by the relay-destination link and the source-relay-destination link SNR is approximately that of the relay-destination link. So, in this case the relay nodes appear to be sources and they tend to transmit, after power normalization, the source symbols.

2.3 Source-Only Amplify-and-Forward Outage Probability Analysis

In this section, we provide the outage probability analysis of the source-only multi-node amplify-and-forward protocol.

2.4 Multi-node Amplify-and-Forward Relay Network Mutual Information

In this section, the source-only multi-node amplify-and-forward system model will be presented again but in a slightly different way to enable the calculation of the mutual information. In phase 1, the source broadcasts its information to the destination and N relay nodes. The received signals are the same as in (2.1) and (2.2). Each relay amplifies the received signal from the source and re-transmits to the destination. The received signal at the destination in phase 2 due to the i-th relay transmission is given by

$$y_{r_i,d} = h_{r_i,d}\beta_i y_{s,r_i} + \eta_{r_i,d}, \tag{2.34}$$

and β_i satisfies the power constraint, that is [11]

$$\beta_i \leq \sqrt{\frac{P_i}{P_s|h_{s,r_i}|^2 + N_0}}, \tag{2.35}$$

where all the channel coefficients and noise components are modeled as in Section 2.1.

Define the $(N+1) \times 1$ received data vector $\mathbf{y} = [y_{s,d}, y_{r_1,d}, ..., y_{r_N,d}]^T$. To calculate the mutual information expression, a simple trick is applied. We start by applying MRC to $\mathbf{y}$. The output of the MRC is given by

$$r = \alpha_s y_{s,d} + \sum_{i=1}^{N} \alpha_i y_{r_i,d}, \tag{2.36}$$

where now $\alpha_s = \sqrt{P_s}h^*_{s,d}/N_0$ and

$$\alpha_i = \frac{\sqrt{P_s}\beta_i h^*_{r_i,d} h^*_{s,r_i}}{\left(\beta_i^2|h_{r_i,d}|^2 + 1\right) N_0}.$$

We can write r in terms of x as

$$\begin{aligned} r = & \left(\frac{P_s |h_{s,d}|^2}{N_0} + \sum_{i=1}^{N} \frac{P_s \beta_i^2 |h_{r_i,d}|^2 |h_{s,r_i}|^2}{\left(\beta_i^2 |h_{r_i,d}|^2 + 1\right) N_0} \right) x \\ & + \frac{\sqrt{P_s} h_{s,d}^*}{N_0} \eta_{s,d} + \sum_{i=1}^{N} \frac{\sqrt{P_s} \beta_i h_{r_i,d}^* h_{s,r_i}^*}{\left(\beta_i^2 |h_{r_i,d}|^2 + 1\right) N_0} \left(\eta_{r_i,d} + h_{r_i,d} \beta_i \eta_{s,r_i} \right). \end{aligned} \tag{2.37}$$

The SNR at the MRC output is

$$SNR_{MRC} = \gamma_s + \sum_{i=1}^{N} \gamma_i \tag{2.38}$$

where $\gamma_s = P_s |h_{s,d}|^2 / N_0$, and

$$\gamma_i = \frac{P_s \beta_i^2 |h_{r_i,d}|^2 |h_{s,r_i}|^2}{\left(\beta_i^2 |h_{r_i,d}|^2 + 1\right) N_0}. \tag{2.39}$$

The probability density function (pdf) of $\mathbf{y}$ given x and the channel coefficients represents an exponential family of distributions [23]. Then, it can be easily shown that r, given the channel coefficients, is a sufficient statistics for x, that is

$$p_{\mathbf{y}/x,r} \left(\mathbf{y}/x, r \right) = p_{\mathbf{y}/r} \left(\mathbf{y}/r \right), \tag{2.40}$$

where $p_{\mathbf{y}/x,r} \left(\mathbf{y}/x, r \right)$ is the pdf of $\mathbf{y}$ given x and r, and $p_{\mathbf{y}/r} \left(\mathbf{y}/r \right)$ is the pdf of $\mathbf{y}$ given r. Since r is a sufficient statistics for x, then the mutual information between x and $\mathbf{y}$ equals the mutual information between x and r [24], that is

$$I \left(x; r \right) = I \left(x; \mathbf{y} \right). \tag{2.41}$$

Then, the average mutual information satisfies

$$I_{AF} \leq I \left(x; r \right) \leq \log \left(1 + \frac{P_s |h_{s,d}|^2}{N_0} + \sum_{i=1}^{N} \frac{P_s \beta_i^2 |h_{r_i,d}|^2 |h_{s,r_i}|^2}{\left(\beta_i^2 |h_{r_i,d}|^2 + 1\right) N_0} \right), \tag{2.42}$$

with equality for x zero-mean, circularly symmetric complex Gaussian random variable [3]. It is clear that (2.42) is increasing in β_i's, so to maximize the mutual information the constraint in (2.35) should be satisfied with equality yielding

$$I_{AF} = \log \left(1 + |h_{s,d}|^2 SNR_{s,d} + \sum_{i=1}^{N} f \left(|h_{s,r_i}|^2 SNR_{s,r_i}, |h_{r_i,d}|^2 SNR_{r_i,d} \right) \right), \tag{2.43}$$

where $SNR_{s,d} = SNR_{s,r_i} = P_s/N_0,\ i = 1, \cdots, N$ and $SNR_{r_i,d} = P_i/N_0,\ i = 1, \cdots, N$ and

$$f(v,u) = \frac{uv}{u+v+1}.$$

2.5 Outage Analysis of the Source-Only Multi-node Amplify-and-Forward Relay Network

In this subsection, the outage probability analysis of the source-only multi-node amplify-and-forward relay network of N relay nodes helping the source is provided. The outage probability for spectral efficiency R is defined as

$$P_{AF}^{out}(R) = \Pr\left\{\frac{1}{N+1} I_{AF} < R\right\}, \tag{2.44}$$

and the $1/(N+1)$ factor comes from the fact that the relays help the source through N uses of orthogonal channels. Defining the vector $\mathbf{p} = [P_s, P_1, P_2, ..., P_N]^T$, equation (2.44) can be rewritten as

$$P_{AF}^{out}(\mathbf{p}, R) = \Pr\left\{\left(\frac{P_s}{N_0}|h_{s,d}|^2 + \sum_{i=1}^{N} f\left(\frac{P_s}{N_0}|h_{s,r_i}|^2, \frac{P_i}{N_0}|h_{r_i,d}|^2\right)\right) < \left(2^{(N+1)R} - 1\right)\right\}. \tag{2.45}$$

At high SNR we can neglect the 1 term in the denominator of the $f(.,.)$ function [21]. We can now write the outage probability as

$$P_{AF}^{out}(\mathbf{p}, R) \simeq \Pr\left\{\left(\frac{P_s}{N_0}|h_{s,d}|^2 + \sum_{i=1}^{N} \frac{\frac{P_s}{N_0}|h_{s,r_i}|^2 \frac{P_i}{N_0}|h_{r_i,d}|^2}{\frac{P_s}{N_0}|h_{s,r_i}|^2 + \frac{P_i}{N_0}|h_{r_i,d}|^2}\right) < \left(2^{(N+1)R} - 1\right)\right\} \tag{2.46}$$

Define the random variables $w_1 = \frac{P_s}{N_0}|h_{s,d}|^2$ and $w_{i+1} = \frac{\frac{P_s}{N_0}|h_{s,r_i}|^2 \frac{P_i}{N_0}|h_{r_i,d}|^2}{\frac{P_s}{N_0}|h_{s,r_i}|^2 + \frac{P_i}{N_0}|h_{r_i,d}|^2},\ i = 1, \cdots, N$. The outage probability can now be given as

$$P_{AF}^{out}(\mathbf{p}, R) \simeq \Pr\left\{\sum_{j=1}^{N+1} w_j < \left(2^{(N+1)R} - 1\right)\right\}. \tag{2.47}$$

The random variable w_1 is an exponential r.v. with rate $\lambda_1 = \frac{N_0}{P_s \delta_{s,d}^2}$. To calculate the outage probability in (2.47), it is quite challenging to follow the approach in [11]. We consider an alternative approach based on approximating the scaled harmonic mean of two exponential random variables to be exponential random variable.

Each of the w_j's for $j = 2, \cdots, N+1$ is a scaled harmonic mean of two exponential random variables. The cumulative density function (CDF) for w_j, $j = 2, ..., N+1$ is given by [21]

$$P_{w_j}(w) = \Pr\{w_j < w\} = 1 - 2w\sqrt{\zeta_{j1}\zeta_{j2}} e^{-w(\zeta_{j1}+\zeta_{j2})} K_1\left(2w\sqrt{\zeta_{j1}\zeta_{j2}}\right), \quad (2.48)$$

where $\zeta_{j1} = \frac{N_0}{P_s \delta_{s,r_{j-1}}^2}$, $\zeta_{j2} = \frac{N_0}{P_{j-1}\delta_{s,r_{j-1}}^2}$ and $K_1(.)$ is the first order modified Bessel function of the second kind defined in [25]. The function $K_1(.)$ can be approximated as $K_1(x) \simeq \frac{1}{x}$ for small x [25], from which we can approximate the CDF of w_j at high SNR as

$$P_{w_j}(w) = \Pr\{w_j < w\} \simeq 1 - e^{-w(\zeta_{j1}+\zeta_{j2})}, \quad (2.49)$$

which is the CDF of an exponential random variable of rate $\lambda_j = \frac{N_0}{P_s \delta_{s,r_{j-1}}^2} + \frac{N_0}{P_{j-1}\delta_{r_{j-1},d}^2}$. Defining the random variable $W = \sum_{j=1}^{N+1} w_j$, the CDF of W, assuming the λ_i's to be distinct, can be proved to be given by

$$\Pr\{W \leq w\} \simeq \sum_{k=1}^{N+1} \left(\prod_{m=1, m\neq k}^{N+1} \frac{\lambda_m}{\lambda_m - \lambda_k} \right) \left(1 - e^{-\lambda_k w}\right). \quad (2.50)$$

The outage probability can be expressed in terms of the CDF of W as

$$P_{AF}^{out}(\mathbf{p}, R) \simeq \Pr\left\{W \leq \left(2^{(N+1)R} - 1\right)\right\}. \quad (2.51)$$

The CDF of W can now be written as

$$\Pr\{W \leq w\} = \sum_{k=1}^{N+1} \left(\prod_{m=1, m\neq k}^{N+1} \frac{\lambda_m}{\lambda_m - \lambda_k} \right) \left(\sum_{n=1}^{N+1} (-1)^{n+1} \lambda_k^n \frac{w^n}{n!} \right) + H.O.T., \quad (2.52)$$

where $H.O.T.$ stands for the higher order terms. Rearranging the terms in (2.52) we get

$$\Pr\{W \leq w\} = \sum_{n=1}^{N+1} \left(\sum_{k=1}^{N+1} \left(\prod_{m=1, m\neq k}^{N+1} \frac{\lambda_m}{\lambda_m - \lambda_k} \right) \lambda_k^n \right) (-1)^{n+1} \frac{w^n}{n!} + H.O.T. \quad (2.53)$$

To prove that the system achieves a diversity of order $N+1$ we need to have the coefficients of w^n's to be zeros for $n = 1, \cdots, N$. This requirement can be reformulated in a matrix form as

$$\underbrace{\begin{bmatrix} \lambda_1 & \dots & \lambda_{N+1} \\ \lambda_1^2 & \dots & \lambda_{N+1}^2 \\ \vdots & \vdots & \vdots \\ \lambda_1^{N+1} & \dots & \lambda_{N+1}^{N+1} \end{bmatrix}}_{\mathbf{V}} \underbrace{\begin{bmatrix} \prod_{m=2}^{N+1} \frac{\lambda_m}{\lambda_m - \lambda_1} \\ \prod_{m=1, m\neq 2}^{N+1} \frac{\lambda_m}{\lambda_m - \lambda_2} \\ \vdots \\ \prod_{m=1}^{N} \frac{\lambda_m}{\lambda_m - \lambda_{N+1}} \end{bmatrix}}_{\mathbf{q}} = \begin{bmatrix} 0 \\ 0 \\ \vdots \\ c_1 \end{bmatrix}. \quad (2.54)$$

To prove (2.54) consider the following system of equations

$$\mathbf{V}\mathbf{a} = \underbrace{[0, 0, \cdots, 1]^T}_{\mathbf{c}}, \quad (2.55)$$

where c_1 is some non-zero constant, and prove that $\mathbf{q} = c_1\mathbf{a}$. Noting that the columns of the $\mathbf{V}$ matrix are scaled versions of the columns of a Vandermonde matrix, i.e., it is a nonsingular matrix, the solution for the system of equations in (2.55) can be found as

$$a = \mathbf{V}^{-1}\mathbf{c} = \frac{1}{\det(\mathbf{V})} \mathrm{adj}(\mathbf{V})\, \mathbf{c}. \quad (2.56)$$

The determinant of a Vandermonde matrix is given by [26]

$$\det \begin{bmatrix} 1 & 1 & \dots & 1 \\ \lambda_1 & \lambda_2 & \dots & \lambda_{N+1} \\ \vdots & \vdots & \vdots & \vdots \\ \lambda_1^N & \lambda_2^N & \dots & \lambda_{N+1}^N \end{bmatrix} = \prod_{k=1}^{N+1} \prod_{m>k}^{N+1} (\lambda_m - \lambda_k), \quad (2.57)$$

from which we can express the determinant of the $\mathbf{V}$ matrix as

$$\det(\mathbf{V}) = \left(\prod_{j=1}^{N+1} \lambda_j\right) \prod_{k=1}^{N+1} \prod_{m>k}^{N+1} (\lambda_m - \lambda_k). \tag{2.58}$$

Due to the structure of the $\mathbf{c}$ vector, we are only interested in the last column of the $\mathtt{adj}(\mathbf{V})$ matrix. The i-th element of the $\mathbf{a}$ vector can be obtained as

$$a_i = \frac{(-1)^{N+i-1} \left(\prod_{j=1,j\neq i}^{N+1} \lambda_j\right) \prod_{k=1,k\neq i}^{N+1} \prod_{m>k,m\neq i}^{N+1} (\lambda_m - \lambda_k)}{\left(\prod_{j=1}^{N+1} \lambda_j\right) \prod_{k=1}^{N+1} \prod_{m>k}^{N+1} (\lambda_m - \lambda_k)} = \frac{(-1)^N}{\lambda_i} \prod_{j=1,j\neq i}^{N+1} \frac{1}{(\lambda_j - \lambda_i)}. \tag{2.59}$$

From (2.59), it is clear that $\mathbf{q} = c_1\mathbf{a}$ where

$$c_1 = (-1)^N \prod_{i=1}^{N+1} \lambda_i. \tag{2.60}$$

The outage probability can now be expressed as

$$\begin{aligned} P_{AF}^{out}(\mathbf{p}, R) &\simeq \Pr\left\{W < \left(2^{(N+1)R} - 1\right)\right\} \\ &= \frac{1}{(N+1)!} \left(\prod_{i=1}^{N+1} \lambda_i\right) \left(2^{(N+1)R} - 1\right)^{N+1} + H.O.T. \end{aligned} \tag{2.61}$$

Substituting for the λ_i's we get

$$P_{AF}^{out}(\mathbf{p}, R) \sim \frac{1}{(N+1)!} . \frac{1}{P_s \delta_{s,d}^2} . \prod_{i=1}^{N} \frac{P_s \delta_{s,r_i}^2 + P_i \delta_{r_i,d}^2}{P_s P_i \delta_{s,r_i}^2 \delta_{r_i,d}^2} \left(2^{(N+1)R} - 1\right)^{N+1} N_0^{N+1}. \tag{2.62}$$

For the special case of single relay node ($N = 1$) and let $SNR = P_s/N_0 = P_1/N_0$, we get

$$P_{AF}^{out}(SNR, R) \sim \frac{1}{2} . \frac{1}{\delta_{s,d}^2} . \frac{\delta_{s,r_1}^2 + \delta_{r_1,d}^2}{\delta_{s,r_1}^2 \delta_{r_1,d}^2} \left(\frac{2^{2R} - 1}{SNR}\right)^2, \tag{2.63}$$

which is consistent with the result obtained in [11] for that simple case of single-relay amplify-and-forward protocol.

From the expression in (2.62), let P be the total power and let $P_s = a_s P$ and $P_i = a_i P$ where $a_s + \sum_{i=1}^{N} a_i = 1,\ a_s > 0,\ a_i > 0,\ i = 1, ..., N$. Define the SNR as

$SNR = P/N_0$, the diversity order of the system, based on the outage probability, is defined as $d_{AF}^{out} = \lim_{SNR\to\infty} -\frac{\log P_{AF}^{out}(SNR,R)}{\log SNR} = N+1$. So the system achieves a diversity of order $N+1$, in terms of outage probability, for N relay nodes helping the source [27].

2.6 Optimal Power Allocation

The optimal power allocation is based on minimizing the outage probability bound in (2.62) under a total power constraint. Removing the fixed terms from the outage probability bound, our optimization problem can be written as

$$\mathbf{p}_{opt} = \min_{\mathbf{p}} \frac{1}{P_s^{N+1}} \prod_{i=1}^{N} \frac{P_s\delta_{s,r_i}^2 + P_i\delta_{r_i,d}^2}{P_i}, \tag{2.64}$$

$$\textbf{subject to } P_s + \textstyle\sum_{i=1}^{N} P_i \le P, \quad P_i \ge 0 \quad \forall i,$$

where $\mathbf{p}$ is as defined in the previous section and P is the maximum allowable total power for one symbol transmission.

It can be easily shown that the cost function in (2.64) is convex in $\mathbf{p}$ over the convex feasible set defined by the linear power constraints. The Lagrangian of this optimization problem can be written as

$$L = \frac{1}{P_s^{N+1}} \prod_{i=1}^{N} \frac{P_s\delta_{s,r_i}^2 + P_i\delta_{r_i,d}^2}{P_i} + \widetilde{\lambda}\left(P_s + \sum_{i=1}^{N} P_i - P\right) + \sum_{i=1}^{N} \mu_i \left(0 - P_i\right), \tag{2.65}$$

where the μ_i's serve as the slack variables. To minimize the outage probability bound, it is clear that we must have $P_i > 0 \ \forall i$. The complementary slackness imply that since $P_i > 0$ then $\mu_i = 0 \ \forall i$. Knowing that the log function is a monotone function and defining the $(N+1)\times 1$ vector $\mathbf{a} = [a_s, a_1, ..., a_N]$, where $a_s = P_s/P$ and $a_i = P_i/P \ \ i = 1, \cdots, N$, the Lagrangian of the optimization

problem in (2.64) can now be given as

$$f = -\log a_s + \sum_{i=1}^{N} \log\left(\frac{1}{a_i}\delta^2_{s,r_i} + \frac{1}{a_s}\delta^2_{r_i,d}\right) + \lambda\left(\mathbf{a}^T\mathbf{1}_{N+1} - 1\right), \tag{2.66}$$

where $\mathbf{1}_{N+1}$ is an all 1 $(N+1)\times 1$ vector. Applying first order optimality conditions, $\mathbf{a}_{opt}$ must satisfy

$$\frac{\partial f}{\partial a_s} = \frac{\partial f}{\partial a_i} = 0, \quad i = 1, \cdots, N, \tag{2.67}$$

from which we get

$$\frac{1}{a_s}\left[1 + \sum_{j=1}^{N} \frac{\delta^2_{r_j,d}}{\delta^2_{r_j,d} + \frac{a_s}{a_j}\delta^2_{s,r_j}}\right] = \frac{1}{a_i}\left[\frac{\delta^2_{s,r_i}}{\delta^2_{s,r_i} + \frac{a_i}{a_s}\delta^2_{r_i,d}}\right]. \tag{2.68}$$

Since $a_s > 0$ and $a_j > 0$, then we can easily show that $a_s > a_i$ i.e., $P_s > P_i\ \forall i$. This is due to the fact that the source power appears in all the SNR terms in (2.62) either through the source-destination direct link or through the scaled harmonic mean of the source-relay and relay-destination links.

Using (2.67) we have

$$\frac{1}{a_j}\left[\frac{\delta^2_{s,r_j}}{\delta^2_{s,r_j} + \frac{a_j}{a_s}\delta^2_{r_j,d}}\right] = \frac{1}{a_i}\left[\frac{\delta^2_{s,r_i}}{\delta^2_{s,r_i} + \frac{a_i}{a_s}\delta^2_{r_i,d}}\right],\ \forall i,\ j. \tag{2.69}$$

Define $c_i = \frac{a_i}{a_s} = \frac{P_i}{P_s},\ i = 1, \cdots, N$ and using (2.68), we get

$$\frac{\delta^2_{r_i,d}}{\delta^2_{s,r_i}}c_i^2 + c_i - c = 0,\ i = 1, \cdots, N, \tag{2.70}$$

for some constant c. From (2.69), the constant c should satisfy the following equation

$$f(c) = c - \frac{1}{1 + \sum_{j=1}^{N} \frac{\delta^2_{r_j,d}}{\delta^2_{r_j,d} + \frac{1}{c_j(c)}\delta^2_{s,r_j}}} = 0. \tag{2.71}$$

Since $P_i < P_s,\ \forall i$, then $c_i < 1,\ \forall i$. Hence, using (2.70), we have $c \in \left(0, 1 + \min_i \frac{\delta^2_{r_i,d}}{\delta^2_{s,r_i}}\right)$. So we have reduced the $(N+1)$-dimensional problem to a single-dimension search

over the parameter c which can be done using a simple numerical search or any other standard method such as the Newton's method.

Convexity of both the cost function and the feasible set in (2.64) imply global optimality of the solution of (2.71) over the desired feasible set. It is worth noting that minimizing the outage probability bound derived in this Chapter will also result in minimizing the SER bound in (2.21).

Table 2.1 gives numerical results for the optimal power allocation for one and two relays helping the source. From the results in Table 2.1, it is clear that equal power allocation is not optimal. As the relays get closer to the source the equal power allocation scheme tends to be optimal. If the relays are close to the destination optimal power allocation can result in a significant performance improvement, in terms of SER, compared to the conventional equal power allocation scheme as will be seen in the simulation section.

Table 2.1: Optimal power allocation for one and two relays ($\delta_{s,d}^2 = 1$ in all cases).

	$\delta_{s,r_i}^2 = 10, \delta_{r_i,d}^2 = 1$ relays close to the source	$\delta_{s,r_i}^2 = 1, \delta_{r_i,d}^2 = 10$ relays close to the destination
one relay	$P_s/P = 0.5393$ $P_1/P = 0.4607$	$P_s/P = 0.8333$ $P_1/P = 0.1667$
two relays	$P_s/P = 0.3830$ $P_1/P = P_2/P = 0.3085$	$P_s/P = 0.75$ $P_1/P = P_2/P = 0.125$

2.7 Simulation Results

In this section, we present extensive simulations to prove the theoretical analysis presented in the previous sections. We will compare the performance of the differ-

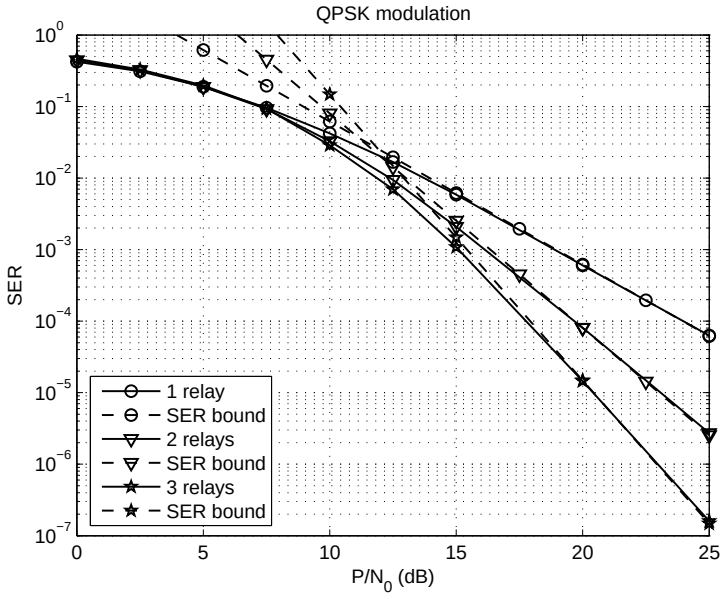

Figure 2.2: SER performance for BPSK signals, $\delta^2_{s,d} = 1, \delta^2_{s,r_i} = 1, \delta^2_{r_i,d} = 1, \delta^2_{r_i,r_l} = 1$, and equal power allocation.

ent amplify-and-forward strategies. In all simulations, unless otherwise stated, we assume equal power assignment between the source and the relay nodes. Fig. 2.2 shows the performance for binary phase shift keying (BPSK) signals ($M = 2$) for the case of having two relay nodes and three relay nodes helping the source. In Fig. 2.2 all the channels variances are equal to 1 (including the inter-relay channels). From that figure it is clear that the MRC based protocol, although more complex, does not give any performance improvement over the source-only amplify-and-forward protocol even if we used pre-whitening before applying the destination MRC detector. This is due to the correlated noise propagation problem discussed before which causes a degradation in the system performance.

Next, we simulate BPSK for relay nodes that are close to the source. Relay node close to the source means that the source-relay channel variance is high.

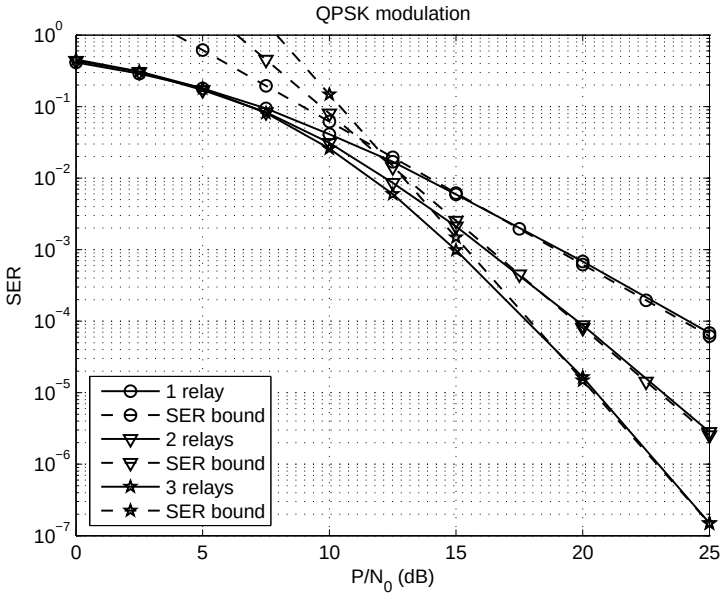

Figure 2.3: SER performance for BPSK signals with relays close to the source, $\delta^2_{s,d} = 1, \delta^2_{s,r_i} = 10, \delta^2_{r_i,d} = 1, \delta^2_{r_i,r_l} = 10$, and equal power allocation.

Fig. 2.3 shows that case of relay nodes close to the source. The channel variance between the source and any relay is taken to be $\delta^2_{s,r_i} = 10\ \forall i$ and each inter-relay channel has a variance of 10. From that figure it is clear that the bound in (2.21) is tight at high SNR. Again there is no improvement in the performance by using the MRC-based protocol. Furthermore, in the case of relays close to the source, the system achieves the SER upper-bound given in (2.33). So in this case the source-only amplify-and-forward protocol achieves the best you can get from any amplify-and-forward protocol and there is approximately no gain in going to a more complex combining techniques.

Fig. 2.4 shows the performance for quadrature phase shift keying (QPSK) signals ($M = 4$) for the case of having two relay nodes and three relay nodes helping the source. In Fig. 2.4, all the channels variances are equal to 1 (including

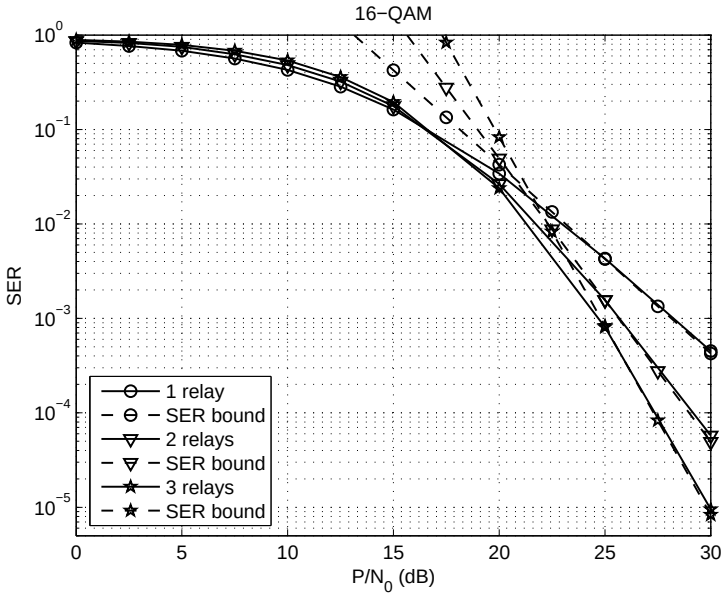

Figure 2.4: SER performance for QPSK signals,$\delta^2_{s,d} = 1, \delta^2_{s,r_i} = 1, \delta^2_{r_i,d} = 1, \delta^2_{r_i,r_l} = 1$, and equal power allocation.

the inter-relay channels). Again we have the same observations clarified before of no gain in using MRC-based amplify-and-forward protocol.

Then, we simulate QPSK for relay nodes that are close to the source. Fig. 2.5 shows that case of relay nodes close to the source. The channel variance between the source and any relay is taken to be $\delta^2_{s,r_i} = 10\ \forall i$ and each inter-relay channel has a variance of 10. From that figure it is clear that the bound in (2.21) is tight at high SNR. Again there is no performance gain by using the MRC-based protocol. Furthermore, in this case of relays close to the source, the protocol achieves the SER upper-bound given in (2.33).

Fig. 2.6 shows the performance for 16-QAM signals ($M = 16$) for the case of having two relay nodes and three relay nodes helping the source. In Fig. 2.6, all the channels variances are equal to 1 (including the inter-relay channels). Again we

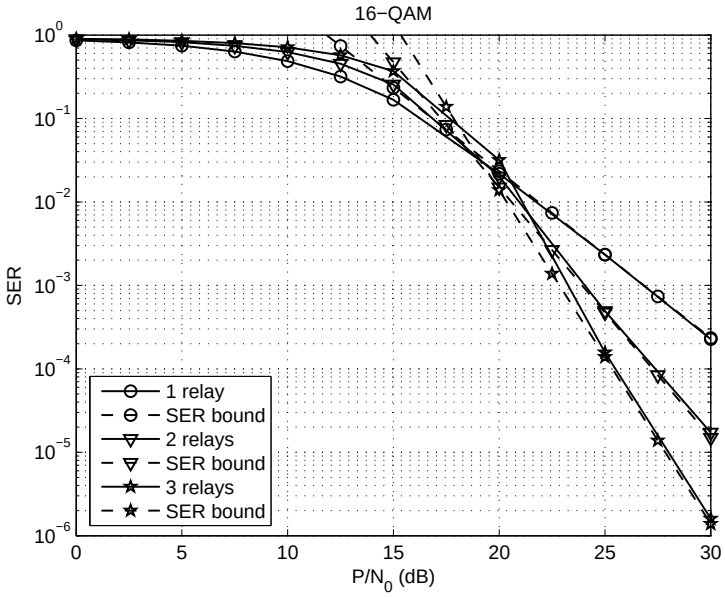

Figure 2.5: SER performance for QPSK signals with relays close to the source, $\delta^2_{s,d} = 1, \delta^2_{s,r_i} = 10, \delta^2_{r_i,d} = 1, \delta^2_{r_i,r_l} = 10$, and equal power allocation.

have the same observations of having approximately no gain in using MRC-based amplify-and-forward protocol.

Then, we simulate 16-QAM for relay nodes that are close to the source. Fig. 2.7 shows the case of having relay nodes close to the source. The channel variance between the source and any relay is taken to be $\delta^2_{s,r_i} = 10 \ \forall i$ and each inter-relay channel has a variance of 10. From that figure it is clear that the bound in (2.21) is tight at high SNR. Again there is no significant performance gains by using the MRC-based protocol. Similarly, in this case of relays close to the source the protocol achieves the SER upper-bound given in (2.33).

Next, to illustrate the severity of the correlated noise propagation problem when the relays become close to the destination, we simulate QPSK for two and three relay nodes. Fig. 2.8 shows that case of relay nodes close to the destination. The

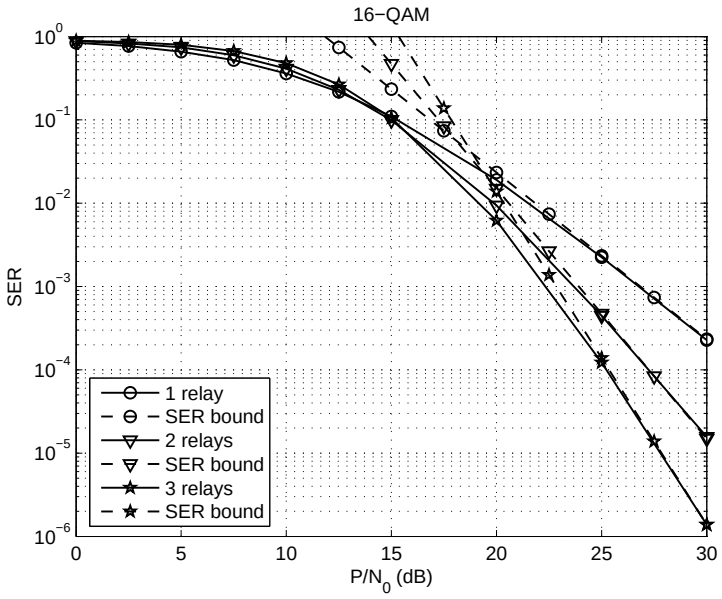

Figure 2.6: SER performance for 16-QAM signals, $\delta^2_{s,d} = 1, \delta^2_{s,r_i} = 1, \delta^2_{r_i,d} = 1, \delta^2_{r_i,r_l} = 1$, and equal power allocation.

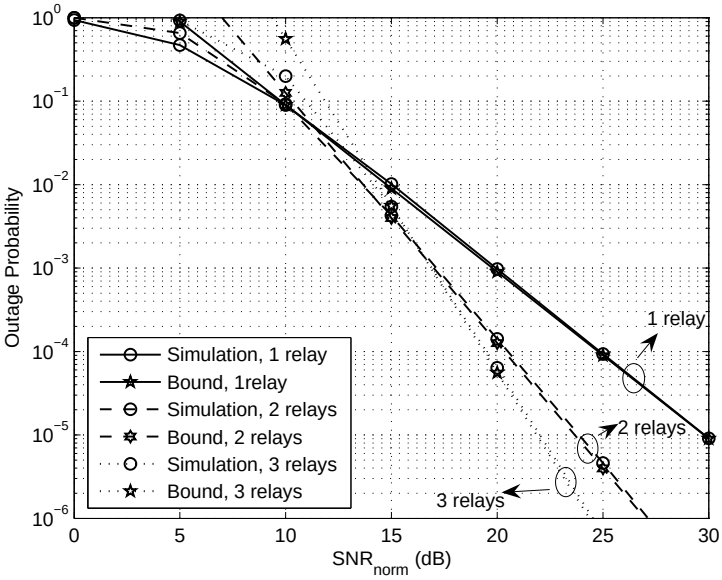

Figure 2.7: SER performance for 16-QAM signals with relays close to the source, $\delta^2_{s,d} = 1, \delta^2_{s,r_i} = 10, \delta^2_{r_i,d} = 1, \delta^2_{r_i,r_l} = 10$, and equal power allocation.

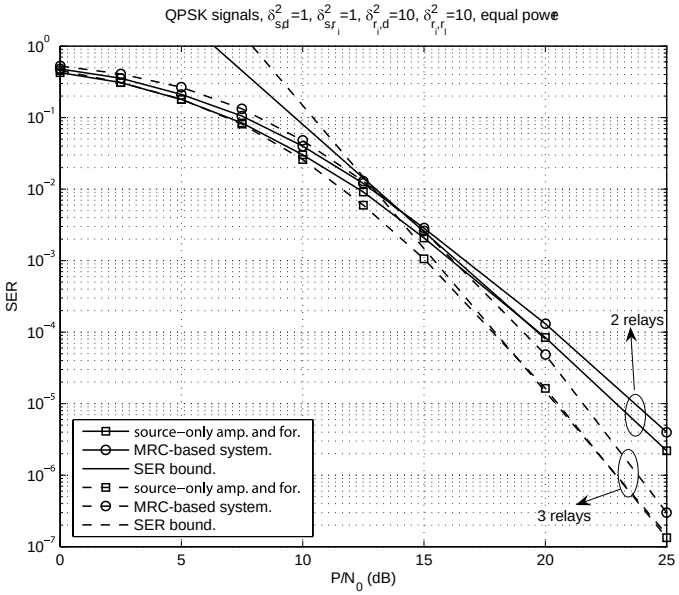

Figure 2.8: SER performance for QPSK signals with relays close to the destination, $\delta^2_{s,d} = 1, \delta^2_{s,r_i} = 1, \delta^2_{r_i,d} = 10, \delta^2_{r_i,r_l} = 10$, and equal power allocation.

channel variance between any relay and the destination is taken to be $\delta^2_{r_i,d} = 10\ \forall i$ and each inter-relay channel has a variance of 10. From this figure it is clear that the source-only based protocol gives a better SER performance than the MRC-based protocol. This is because of the correlated noise propagation problem becomes more severe as claimed in Section 2.2.2.

Fig. 2.9 shows the outage probability for one, two and three relay nodes helping the source versus SNR_{norm} defined as [28]

$$SNR_{norm} = \frac{SNR}{2^R - 1}, \tag{2.72}$$

which is the SNR normalized by the minimum SNR required to achieve spectral efficiency R for complex additive white Gaussian noise (AWGN) channel. In the simulations, we used $R = 1$ (small R regime). For the single relay case all the channel variances are taken to be 1. For the case of two relay nodes all the channel

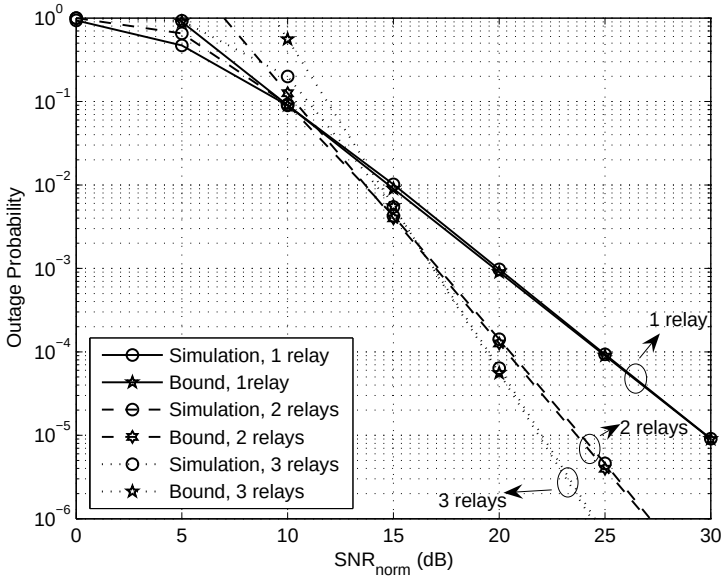

Figure 2.9: Outage probability for one, two and three nodes source-only amplify-and-forward relay network.

variances are taken to be 1 except for the channel between the source and the second relay for which the channel variance is taken to be $\delta^2_{s,r_2} = 10$, which means that the second relay is close to the source. For the case of three relay nodes all the channel variances are taken to be 1 except for the channel between the source and the second relay for which the channel variance is taken to be $\delta^2_{s,r_2} = 10$ and the channel between the source and the third relay for which the channel variance is taken to be $\delta^2_{s,r_3} = 5$. From Fig. 2.9 it is clear that the bound in (2.62) is tight at high SNR and that the source-only amplify-and-forward protocol achieves full diversity of order $N + 1$ in terms of outage probability.

Next we illustrate the gains of using our optimal power allocation scheme as compared to the equal power allocation scheme. Fig. 2.10 shows a comparison between the equal power and optimal power allocation schemes for relays close to

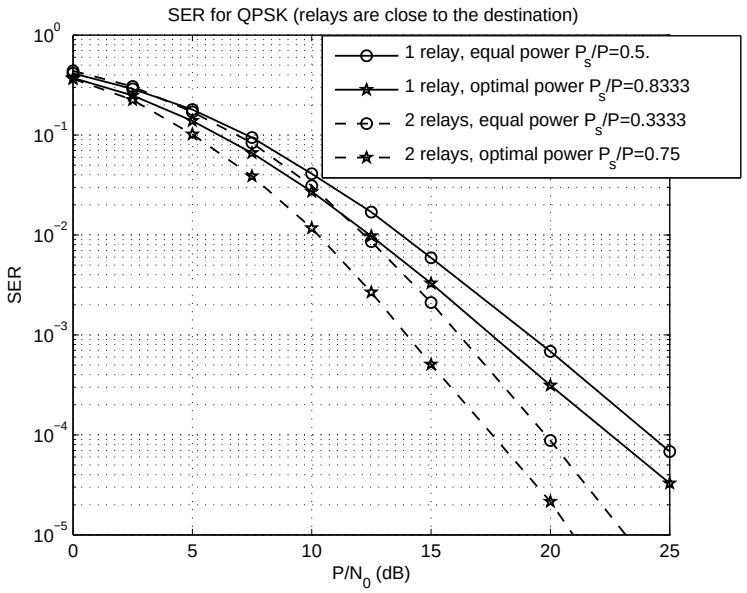

Figure 2.10: Comparison of the SER for QPSK modulation using equal power allocation and the optimal power allocation for relays close to the destination.

the destination ($\delta^2_{s,r_1} = \delta^2_{s,r_2} = 1$, $\delta^2_{r_1,d} = \delta^2_{r_2,d} = 10$ and $\delta^2_{s,d} = 1$). From Fig. 2.10 we can see that, using the optimal power allocation scheme, we can get about 1 dB improvement for the single relay case and about 2 dB improvement for the two relays case over the equal power assignment scheme.

Chapter 3

Distributed Space-Time and Space-Frequency Codings

The main problem with the multi-node decode-and-forward (DAF) protocol and the multi-node amplify-and-forward (AAF) protocol, presented in Chapter 2, is the loss in the data rate as the number of relay nodes increases. The use of orthogonal subchannels for the relay node transmissions, either through TDMA or FDMA, results in a high loss of the system spectral efficiency. This leads to the use of what is known as distributed space-time coding (DSTC) and distributed space-frequency coding (DSFC), where relay nodes are allowed to simultaneously transmit over the same channel by emulating a space-time or a space-frequency code. The term *distributed* comes from the fact that the virtual multi-antenna transmitter is distributed between randomly located relay nodes. Employing DSTCs or DSFCs reduces the data rate loss due to relay nodes transmissions without sacrificing the system diversity order as will be seen in this Chapter [29–34].

3.1 Distributed Space-Time Coding (DSTC)

Several works have considered the application of the existing space-time codes in a distributed fashion for the wireless relay network [16–19]. All of these works have considered a two-hop relay network where a direct link between the source and the destination nodes does not exist. In [16], space-time block codes were used in a completely distributed fashion. Each relay node transmits a randomly selected column from the space-time code matrix. This system achieves a diversity of order one, as the signal-to-noise (SNR) tends to infinity, limited by the probability of having all of the relay nodes selecting to transmit the same column of the space-time code matrix. In [17], distributed space-time coding based on the Alamouti scheme and amplify-and-forward cooperation protocol was analyzed. An expression for the average symbol error rate (SER) was derived. In [18], a performance analysis of the gain of using cooperation among nodes was considered assuming that the number of relays available for cooperation is a Poisson random variable. The authors compared the performance of different distributed space-time codes designed for the MIMO channels under this assumption. In [19], the performance the linear dispersion (LD) space-time codes of [35] was analyzed when used for distributed space-time coding in wireless relay networks. These works did not account for the code design criteria for the space-time codes when employed in a distributed fashion. In this section, we answer the question of whether or not a space-time code, which achieves full diversity and maximum coding gain over MIMO channels, can also achieve full diversity and maximum coding gain if used in a distributed fashion.

In this section, the design of distributed space-time codes for wireless relay networks is considered. A two-hop relay network model depicted in Fig. 3.1,

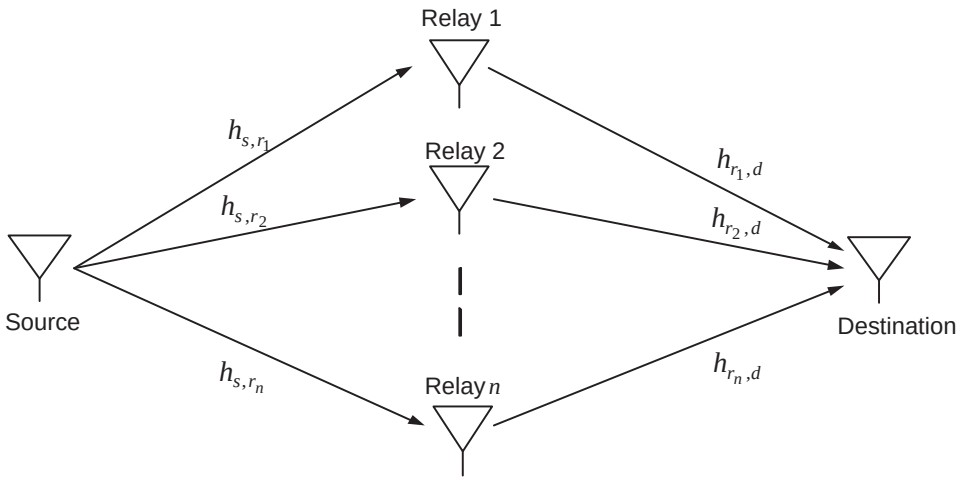

Figure 3.1: Simplified system model for the two-hop distributed space-time codes.

where the system lacks a direct link from the source to destination node, is considered. Distributed space-time (space-frequency) coding can be achieved through node cooperation to emulate multiple antennas transmitter. First, the decode-and-forward protocol, in which each relay node decodes the symbols received from the source node before retransmission, is considered. A space-time code designed to achieve full diversity and maximum coding gain over multiple-input multiple-output (MIMO) channels is shown to achieve full diversity but not necessarily maximizing the coding gain if used with the decode-and-forward protocol. Next, the amplify-and-forward protocol is considered; each relay node can only perform simple operations such as linear transformation of the received signal and then amplify the signal before retransmission. A space-time code designed to achieve full diversity and maximum coding gain over MIMO channels is shown to achieve full diversity and maximum coding gain if used with the amplify-and-forward protocol.

Next, the design of DSTC that can mitigate the relay nodes synchronization errors is considered. Most of the works on cooperative transmission assume perfect

synchronization between the relay nodes, which means that the relays' timings, carrier frequencies, and propagation delays are identical. Perfect synchronization is difficult to achieve among randomly located relay nodes. To simplify the synchronization in the network, a diagonal structure is imposed on the space-time code used. The diagonal structure of the code bypasses the perfect synchronization problem by allowing only one relay to transmit at any time slot (assuming TDMA). Hence, it is not necessary to synchronize simultaneous in-phase transmissions of randomly located relay nodes, which greatly simplifies the synchronization among the relay nodes.

3.1.1 DSTC with the Decode-and-Forward Protocol

In this section, the system model for DSTC with decode-and-forward cooperation protocol is presented, and a system performance analysis is provided. The notation $\mathbf{x} \sim \mathcal{CN}(\mathbf{m}, \mathbf{C})$ is used to denote that the random vector $\mathbf{x}$ is a circularly symmetric complex Gaussian random vector with mean $\mathbf{m}$ and covariance matrix $\mathbf{C}$.

DSTC with the Decode-and-Forward Protocol System Model

The source node is assumed to have n relay nodes assigned for cooperation. The system has two phases given as follows. In phase 1, the source transmits data to the relay nodes with power P_1. The received signal at the k-th relay is modeled as

$$\mathbf{y}_{s,r_k} = \sqrt{P_1} h_{s,r_k} \mathbf{s} + \mathbf{v}_{s,r_k}, \quad k = 1, 2, \cdots, n, \tag{3.1}$$

where $\mathbf{s}$ is an $L \times 1$ transmitted data vector with a power constraint $||\mathbf{s}||_F^2 \leq L$, where $|| \cdot ||_F^2$ denotes the Frobenius norm[1] and $h_{s,r_k} \sim \mathcal{CN}(0, \delta_{s,r_k}^2)$ denotes the

[1]The Frobenius norm of the $m \times n$ matrix $\mathbf{A}$ is defined as $||\mathbf{A}||_F^2 = \sum_{i=1}^{m} \sum_{j=1}^{n} |\mathbf{A}(i,j)|^2 = TR(\mathbf{A}\mathbf{A}^{\mathcal{H}}) = TR(\mathbf{A}^{\mathcal{H}}\mathbf{A})$, where $TR(\cdot)$ is the trace of a matrix and $\mathbf{A}^{\mathcal{H}}$ is the Hermitian transpose

channel gain between the source node and the k-th relay node. The channel gains from the source node to the relay nodes are assumed to be independent. All channel gains are fixed during the transmission of one data packet and can vary from one packet to another, i.e., a block flat-fading channel model is assumed. In (3.1), $\mathbf{v}_{s,r_i} \sim \mathcal{CN}(\mathbf{0}, N_o\mathbf{I}_n)$ denotes additive white Gaussian noise (AWGN), where $\mathbf{I}_n$ denotes the $n \times n$ identity matrix.

The n relay nodes try to decode the received signals from the source node. Each relay node is assumed to be capable of deciding whether or not it has decoded correctly. If a relay node decodes correctly, it will forward the source data in the second phase of the cooperation protocol; otherwise, it remains idle. This can be achieved through the use of cyclic redundancy check (CRC) codes [36]. Alternatively, this performance can be approached by setting a SNR threshold at the relay nodes, and the relay will only forward the source data if the received SNR is larger than that threshold [12]. For the analysis in this section, the relay nodes are assumed to be synchronized either by a centralized or a distributed algorithm.

In phase 2, the relay nodes that have decoded correctly re-encode the data vector $\mathbf{s}$ with a pre-assigned code structure. In the subsequent development no specific code design will be assumed, instead a generic space-time (ST) code structure is considered. The ST code is distributed among the relays such that each relay will emulate a single antenna in a multiple-antenna transmitter. Hence, each relay will generate a column in the corresponding ST code matrix. Let $\mathbf{X}_r$ denote the $K \times n$ space-time code matrix with $K \geq n$. Column k of $\mathbf{X}_r$ represents the code transmitted from the k-th relay node. The signal received at the destination

---

of $\mathbf{A}$.

is given by

$$\mathbf{y_d} = \sqrt{P_2}\mathbf{X}_r\mathbf{D_I}\mathbf{h}_d + \mathbf{v}_d, \tag{3.2}$$

where

$$\mathbf{h}_d = [h_{r_1,d}, h_{r_2,d}, \cdots, h_{r_n,d}]^T$$

is an $n \times 1$ channel gains vector from the n relays to the destination, $h_{r_k,d} \sim \mathcal{CN}(0, \delta^2_{r_k,d})$, and P_2 is the relay node power where equal power allocation among the relay nodes is assumed. The channel gains from the relay nodes to the destination node are assumed to be statistically independent as the relays are spatially separated. The $K \times 1$ vector $\mathbf{v}_d \sim \mathcal{CN}(\mathbf{0}, N_o\mathbf{I}_K)$ denotes AWGN at the destination node. The matrix $\mathbf{D_I}$ is the state matrix, which will be defined later.

The state of the k-th relay, i.e., whether it has decoded correctly or not, is denoted by the random variable I_k $(1 \leq k \leq n)$, which takes values 1 or 0 if the relay decodes correctly or erroneously, respectively. Let

$$\mathbf{I} = [I_1, I_2, \cdots, I_n]^T$$

denote the state vector of the relay nodes and $n_\mathbf{I}$ denote the number of relay nodes that have decoded correctly corresponding to a certain realization $\mathbf{I}$. The random variables I_k's are statistically independent as the state of each relay depends only on its channel conditions to the source node, which are independent from other relays. The matrix

$$\mathbf{D_I} = \text{diag}\,(()\, I_1, I_2, \cdots, I_n)$$

in (3.2) is defined as the state matrix of the relay nodes. An energy constraint is imposed on the generated ST code such that $||\mathbf{X}_r||^2_F \leq L$, and this guarantees that the transmitted power per source symbol is less than or equal to $P_1 + P_2$.

DSTC with the Decode-and-Forward Protocol Performance Analysis

In this section, the pairwise error probability (PEP) performance analysis for the cooperation scheme described in Section 3.1.1 is provided. The diversity and coding gain achieved by the protocol are then analyzed.

The random variable I_k can be easily seen to be a Bernoulli random variable. Therefore, the probability distribution of I_k is given by

$$I_k = \begin{cases} 0 & \text{with probability} = 1 - (1 - SER_k)^L \\ \\ 1 & \text{with probability} = (1 - SER_k)^L, \end{cases} \tag{3.3}$$

where SER_k is the un-coded SER at the k-th relay node and is modulation dependent. For M-ary quadrature amplitude modulation (M-QAM, $M = 2^p$ with p even), the exact expression can be shown to be upper-bounded by [37]

$$SER_k \leq \frac{2N_o g}{bP_1\delta^2_{s,r_k}}, \tag{3.4}$$

where $b = 3/(M-1)$ and $g = \frac{4R}{\pi}\int_0^{\pi/2}\sin^2\theta d\theta - \frac{4R^2}{\pi}\int_0^{\pi/4}\sin^2\theta d\theta$, in which $R = 1 - \frac{1}{\sqrt{M}}$.

The destination is assumed to have perfect channel state information (CSI) as well as the relay nodes state vector. The destination applies a maximum likelihood (ML) receiver, which will be a minimum distance rule. The conditional pairwise error probability (PEP) is given by

$$\begin{aligned} &\Pr\left(\mathbf{X}_1 \rightarrow \mathbf{X}_2 | \mathbf{I},\ \mathbf{h}_d\right) = \\ &\Pr\left(\|\mathbf{y_d} - \sqrt{P_2}\mathbf{X}_1\mathbf{D_I}\mathbf{h}_d\|_F^2 > \|\mathbf{y_d} - \sqrt{P_2}\mathbf{X}_2\mathbf{D_I}\mathbf{h}_d\|_F^2 | \mathbf{I},\ \mathbf{h}_d,\ \mathbf{X}_1 \text{was transmitted}\right), \end{aligned} \tag{3.5}$$

where $\mathbf{X}_1$ and $\mathbf{X}_2$ are two possible transmitted codewords. The conditional PEP can be expressed as quadratic form of a complex Gaussian random vector as

$$\Pr\left(\mathbf{X}_1 \rightarrow \mathbf{X}_2 | \mathbf{I},\ \mathbf{h}_d\right) = \Pr\left(q < 0 | \mathbf{I},\ \mathbf{h}_d\right), \tag{3.6}$$

where

$$q = \begin{bmatrix} \mathbf{w}_1^{\mathcal{H}} & \mathbf{w}_2^{\mathcal{H}} \end{bmatrix} \begin{bmatrix} \mathbf{I}_n & \mathbf{0} \\ \mathbf{0} & -\mathbf{I}_n \end{bmatrix} \begin{bmatrix} \mathbf{w}_1 \\ \mathbf{w}_2 \end{bmatrix},$$

$\mathbf{w}_1 = \sqrt{P_2}\left(\mathbf{X}_1 - \mathbf{X}_2\right)\mathbf{D}_{\mathbf{I}}\mathbf{h}_d + \mathbf{v}_d$, $\mathbf{w}_2 = \mathbf{v}_d$. The random vectors $\mathbf{h}_d$ and $\mathbf{I}$ are mutually independent as they arise from independent processes. First, the conditional PEP was averaged over the channel realizations $\mathbf{h}_d$. By defining the signal matrix

$$\mathbf{C}_{\mathbf{I}} = \left(\mathbf{X}_1 - \mathbf{X}_2\right)\mathbf{D}_{\mathbf{I}}\mathrm{diag}\left(()\,\delta_{r_1,d}^2, \delta_{r_2,d}^2, \cdots, \delta_{r_n,d}^2\right)\mathbf{D}_{\mathbf{I}}\left(\mathbf{X}_1 - \mathbf{X}_2\right)^{\mathcal{H}}, \tag{3.7}$$

the conditional PEP in (3.6) can be tightly upper-bounded by [38]

$$\Pr\left(\mathbf{X}_1 \to \mathbf{X}_2|\mathbf{I}\right) \leq \frac{\begin{pmatrix} 2\Delta(\mathbf{I}) - 1 \\ \Delta(\mathbf{I}) - 1 \end{pmatrix} N_0^{\Delta(\mathbf{I})}}{P_2^{\Delta(\mathbf{I})} \prod_{i=1}^{\Delta(\mathbf{I})} \lambda_i^{\mathbf{I}}}, \tag{3.8}$$

where $\Delta(\mathbf{I})$ is the number of nonzero eigenvalues of the signal matrix and $\lambda_i^{\mathbf{I}}$'s are the nonzero eigenvalues of the signal matrix corresponding to the state vector $\mathbf{I}$. The non-zero eigenvalues of the signal matrix are the same as the nonzero eigenvalues of the matrix [26]

$$\mathbf{\Gamma}\left(\mathbf{X}_1, \mathbf{X}_2\right) = \mathrm{diag}\left(\delta_{r_1,d}, \delta_{r_2,d}, \cdots, \delta_{r_n,d}\right)\ \mathbf{D}_{\mathbf{I}}\mathbf{\Phi}\left(\mathbf{X}_1, \mathbf{X}_2\right)\mathbf{D}_{\mathbf{I}}\ \mathrm{diag}\left(\delta_{r_1,d}, \delta_{r_2,d}, \cdots, \delta_{r_n,d}\right),$$

where

$$\mathbf{\Phi}\left(\mathbf{X}_1, \mathbf{X}_2\right) = \left(\mathbf{X}_1 - \mathbf{X}_2\right)^{\mathcal{H}}\left(\mathbf{X}_1 - \mathbf{X}_2\right).$$

The employed space-time code is assumed to achieve full diversity and maximum coding gain over MIMO channels, which means that the matrix $\mathbf{\Phi}\left(\mathbf{X}_1, \mathbf{X}_2\right)$ is full rank of order n for any pair of distinct codewords $\mathbf{X}_1$ and $\mathbf{X}_2$. Achieving maximum coding gain means that the minimum of the products $\prod_{i=1}^{n} \lambda_i$, where the λ_i's are the eigenvalues of the matrix $\mathbf{\Phi}\left(\mathbf{X}_1, \mathbf{X}_2\right)$, is maximized over all the pairs of distinct codewords [5].

Clearly, if the matrix $\mathbf{\Phi}(\mathbf{X}_1, \mathbf{X}_2)$ has a rank of order n then the matrix $\mathbf{\Gamma}(\mathbf{X}_1, \mathbf{X}_2)$ will have a rank of order $n_{\mathbf{I}}$, which is the number of relays that have decoded correctly. Equation (3.8) can now be rewritten as

$$\Pr(\mathbf{X}_1 \to \mathbf{X}_2|\mathbf{I}) \leq \frac{\begin{pmatrix} 2n_{\mathbf{I}} - 1 \\ n_{\mathbf{I}} - 1 \end{pmatrix} N_0^{n_{\mathbf{I}}}}{P_2^{n_{\mathbf{I}}} \prod_{i=1}^{n_{\mathbf{I}}} \lambda_i^{\mathbf{I}}}. \tag{3.9}$$

Second, the conditional PEP was averaged over the relays' state vector $\mathbf{I}$. The dependence of the expression in (3.9) on $\mathbf{I}$ appears through the set of nonzero eigenvalues $\left\{\lambda_i^{\mathbf{I}}\right\}_{i=1}^{n_{\mathbf{I}}}$, which depends on the number of relays that have decoded correctly and their realizations. The state vector $\mathbf{I}$ of the relay nodes determines which columns from the ST code matrix are replaced with zeros and thus affect the resulting eigenvalues.

The probability of having a certain realization of $\mathbf{I}$ is given by

$$\Pr(\mathbf{I}) = \left(\prod_{k \in CR(\mathbf{I})} (1 - SER_k)^L\right) \left(\prod_{k \in ER(\mathbf{I})} \left(1 - (1 - SER_k)^L\right)\right), \tag{3.10}$$

where $CR(\mathbf{I})$ is the set of relays that have decoded correctly and $ER(\mathbf{I})$ is the set of relays that have decoded erroneously corresponding to the $\mathbf{I}$ realization. For simplicity of presentation symmetry is assumed between all relays, that is $\delta_{s,r_k}^2 = \delta_{s,r}^2$ and $\delta_{r_k,d}^2 = \delta_{r,d}^2$ for all k. Averaging over all realizations of the states of the relays, gives the PEP at high SNR as

$$\begin{aligned} PEP &= \Pr(\mathbf{X}_1 \to \mathbf{X}_2) \\ &\leq \sum_{k=0}^{n} \left((1 - SER)^L\right)^k \left(1 - (1 - SER)^L\right)^{n-k} \sum_{\mathbf{I}:\, n_{\mathbf{I}} = k} \frac{\begin{pmatrix} 2k - 1 \\ k - 1 \end{pmatrix} N_0^k}{P_2^k \prod_{i=1}^{k} \lambda_i^{\mathbf{I}}}, \end{aligned} \tag{3.11}$$

where SER is now the symbol error rate at any relay node due to the symmetry assumption.

The diversity order of a system determines the average rate with which the error probability decays at high enough SNR. In order to compute the diversity order of the system, the PEP in (3.11) is rewritten in terms of the SNR defined as $SNR = P/N_o$, where $P = P_1 + P_2$ is the transmitted power per source symbol. Let $P_1 = \alpha P$ and $P_2 = (1-\alpha)P$, where $\alpha \in (0,1)$. Substituting these definitions along with the SER expressions at the relay nodes from (3.4) into (3.11) and considering high SNR, the PEP can be upper-bounded as

$$\Pr(\mathbf{X}_1 \rightarrow \mathbf{X}_2) \leq SNR^{-n} \sum_{k=0}^{n} \left(\frac{2Lg}{b\alpha\delta_{s,r}^2} \right)^{n-k} \sum_{\mathbf{I}:\, n_{\mathbf{I}}=k} \frac{\begin{pmatrix} 2k-1 \\ k-1 \end{pmatrix}}{(1-\alpha)^k \prod_{i=1}^{k} \lambda_i^{\mathbf{I}}}, \tag{3.12}$$

where at high SNR $1-(1-SER)^L \approx L \cdot SER$ and upper-bounding $1 - L \cdot SER$ by 1. The diversity gain is defined as $d = \lim_{SNR\rightarrow\infty} -\frac{\log(PEP)}{\log(SNR)}$. Applying this definition to the PEP in (3.12), when the number of cooperating nodes is n, gives

$$d_{DF} = \lim_{SNR\rightarrow\infty} -\frac{\log(PEP)}{\log(SNR)} = n. \tag{3.13}$$

Hence, any code that is designed to achieve full diversity over MIMO channels will achieve full diversity in the distributed relay network if it is used in conjunction with the decode-and-forward protocol. Some of these codes can be found in [5, 6, 35, 39, 40].

If full diversity is achieved, the coding gain is

$$C_{DF} = \left(\sum_{k=0}^{n} \left(\frac{2ng}{b\alpha\delta_{s,r}^2} \right)^{n-k} \sum_{\mathbf{I}:\, n_{\mathbf{I}}=k} \frac{\begin{pmatrix} 2k-1 \\ k-1 \end{pmatrix}}{(1-\alpha)^k \prod_{i=1}^{k} \lambda_i^{\mathbf{I}}} \right)^{-\frac{1}{n}}, \tag{3.14}$$

which is a term that does not depend on the SNR. To minimize the PEP bound the coding gain of the distributed space-time code needs to be maximized. This is different from the determinant criterion in the case of MIMO channels [5]. Hence, a space-time code designed to achieve full diversity and maximum coding gain over MIMO channels will achieve full diversity but not necessarily maximizing the coding gain if used in a distributed fashion with the decode-and-forward protocol. Intuitively, the difference is due to the fact that in the case of distributed space-time codes with decode-and-forward protocol, not all of the relays will always transmit their corresponding code matrix columns. The design criterion used in the case of distributed space-time codes makes sure that the coding gain is significant over all sets of possible relays that have decoded correctly. Although it is difficult to design codes to maximize the coding gain as given by (3.14), this expression gives insight on how to design good codes. The code design should take into consideration the fact that not all of the relays will always transmit in the second phase.

3.1.2 DSTC with the Amplify-and-Forward Protocol

In this section, the distributed space-time coding based on the amplify-and-forward protocol is introduced. In this case, the relay nodes do not perform any hard-decision operation on the received data vectors. The system model is presented and a performance analysis is provided.

DSTC with the Amplify-and-Forward Protocol System Model

The system has two phases as follows. In phase 1, if n relays are assigned for cooperation, the source transmits data to the relays with power P_1 and the signal received at the k-th relay is as modeled in (3.1) with $L = n$. For simplicity of presentation, symmetry of the relay nodes is assumed, i.e., $h_{s,r_k} \sim \mathcal{CN}(0, \delta^2_{s,r}),\ \forall k$ and $h_{r_k,d} \sim \mathcal{CN}(0, \delta^2_{r,d}),\ \forall k$. In the amplify-and-forward protocol, relay nodes do not decode the received signals. Instead, the relays can only amplify the received signal and perform simple operations such as permutations of the received symbols or other forms of *unitary* linear transformations. Let $\mathbf{A}_k$ denote the $n \times n$ unitary transformation matrix at the k-th relay node. Each relay will normalize the received signal by the factor $\sqrt{\frac{P_2/n}{P_1\delta^2_{s,r}+N_0}}$ to satisfy a long term-power constraint. It can be easily shown that this normalization will give a transmitted power per symbol of $P = P_1 + P_2$.

The $n \times 1$ received data vector from the relay nodes at the destination node can be modeled as

$$\mathbf{y_d} = \sqrt{\frac{P_2/n}{P_1\delta^2_{s,r} + N_0}}\widetilde{\mathbf{X}}_r\mathbf{h}_d + \mathbf{v}_d, \tag{3.15}$$

where $\mathbf{h}_d = [h_{r_1,d}, h_{r_2,d}, \cdots, h_{r_n,d}]^T$ is an $n \times 1$ vector channel gains from the n relays to the destination where $h_{r_i,d} \sim \mathcal{CN}(0, \delta^2_{r,d})$, $\widetilde{\mathbf{X}}_r$ is the $n \times n$ code matrix given by

$$\widetilde{\mathbf{X}}_r = [h_{s,r_1}\mathbf{A}_1\mathbf{s}, h_{s,r_2}\mathbf{A}_2\mathbf{s}, \cdots, h_{s,r_n}\mathbf{A}_n\mathbf{s}],$$

and $\mathbf{v}_d$ denotes additive white Gaussian noise. Each element of $\mathbf{v}_d$ given the channel coefficients has the distribution of $\mathcal{CN}\left(0, N_0\left(1 + \frac{P_2/n}{P_1\delta^2_{s,r}+N_o}\sum_{i=1}^{n}|h_{r_i,d}|^2\right)\right)$, and $\mathbf{v}_d$ accounts for both the noise propagated from the relay nodes as well as the noise generated at the destination. It can be easily shown that restricting the linear transformations at the relay nodes to be unitary causes the elements of the vector

$\mathbf{v}_d$, given the channel coefficients, to be mutually independent.

Now, the received vector in (3.15) can be rewritten as

$$\mathbf{y_d} = \sqrt{\frac{P_2 P_1/n}{P_1\delta_{s,r}^2 + N_0}}\mathbf{X}_r\mathbf{h} + \mathbf{v}_d, \tag{3.16}$$

where

$$\mathbf{h} = [\ h_{s,r_1}h_{r_1,d}, h_{s,r_2}h_{r_2,d}, \cdots, h_{s,r_n}h_{r_n,d}]^T$$

and

$$\mathbf{X}_r = [\mathbf{A}_1\mathbf{s}, \mathbf{A}_2\mathbf{s}, \cdots, \mathbf{A}_n\mathbf{s}]$$

plays the role of the space-time codeword.

DSTC with the Amplify-and-Forward Protocol Performance Analysis

In this section, a pairwise error probability analysis is made to derive the code design criteria. With the ML decoder, the PEP of mistaking $\mathbf{X}_1$ by $\mathbf{X}_2$ can be upper-bounded by the following Chernoff bound

$$\Pr(\mathbf{X}_1 \to \mathbf{X}_2) \leq$$
$$E\left\{\exp\left(-\frac{P_1P_2/n}{4N_0\left(P_1\delta_{s,r}^2 + N_o + \frac{P_2}{n}\sum_{i=1}^{n}|h_{r_i,d}|^2\right)}\mathbf{h}^{\mathcal{H}}(\mathbf{X}_1-\mathbf{X}_2)^{\mathcal{H}}(\mathbf{X}_1-\mathbf{X}_2)\mathbf{h}\right)\right\}, \tag{3.17}$$

where the expectation is over the channel coefficients. Taking the expectation in (3.17) over the source-to-relay channel coefficients, which are complex Gaussian random variables, gives

$$\Pr(\mathbf{X}_1 \to \mathbf{X}_2) \leq E\Bigg\{\det{}^{-1}\Bigg[\mathbf{I}_n + \frac{\delta_{s,r}^2 P_1P_2/n}{4N_0\left(P_1\delta_{s,r}^2 + N_o + \frac{P_2}{n}\sum_{i=1}^{n}|h_{r_i,d}|^2\right)} \tag{3.18}$$
$$(\mathbf{X}_1-\mathbf{X}_2)^{\mathcal{H}}(\mathbf{X}_1-\mathbf{X}_2)\mathrm{diag}\left(()\,|h_{r_1,d}|^2, |h_{r_2,d}|^2, \cdots, |h_{r_n,d}|^2\right)\Bigg]\Bigg\},$$

where $\mathbf{I}_n$ is the $n \times n$ identity matrix.

To evaluate the expectation in (3.18), define the matrix

$$\mathbf{M} = \frac{\delta_{s,r}^2 P_1 P_2/n}{4N_0\left(P_1\delta_{s,r}^2 + N_o + \frac{P_2}{n}\sum_{i=1}^{n}|h_{r_i,d}|^2\right)} \times \Phi(\mathbf{X}_1, \mathbf{X}_2)\text{diag}\left(()\,|h_{r_1,d}|^2, |h_{r_2,d}|^2, \cdots, |h_{r_n,d}|^2\right),$$

where

$$\Phi(\mathbf{X}_1, \mathbf{X}_2) = (\mathbf{X}_1 - \mathbf{X}_2)^{\mathcal{H}}(\mathbf{X}_1 - \mathbf{X}_2).$$

The bound in (3.18) can be written in terms of the eigenvalues of $\mathbf{M}$ as

$$\Pr(\mathbf{X}_1 \to \mathbf{X}_2) \leq E\left\{\frac{1}{\prod_{i=1}^{n}(1+\lambda_{M_i})}\right\}, \tag{3.19}$$

where λ_{M_i} is the i-th eigenvalue of the matrix $\mathbf{M}$. If $P_1 = \alpha P$ and $P_2 = (1-\alpha)P$, where P is the power per symbol for some $\alpha \in (0,1)$ and define $SNR = P/N_0$, the eigenvalues of $\mathbf{M}$ increase with the increase of the SNR. Now assuming that the matrix $\mathbf{M}$ has full rank of order n the following approximations hold at high SNR

$$\begin{aligned}\prod_{i=1}^{n}(1+\lambda_{M_i}) &\simeq 1 + \prod_{i=1}^{n}\lambda_{M_i} \\ &= 1 + \left(\frac{\delta_{s,r}^2 P_1 P_2/n}{4N_0\left(P_1\delta_{s,r}^2 + N_o + \frac{P_2}{n}\sum_{i=1}^{n}|h_{r_i,d}|^2\right)}\right)^n \prod_{i=1}^{n}\lambda_i \prod_{i=1}^{n}|h_{r_i,d}|^2 \\ &\simeq \prod_{i=1}^{n}\left(1 + \frac{\delta_{s,r}^2 P_1 P_2/n}{4N_0\left(P_1\delta_{s,r}^2 + N_o + \frac{P_2}{n}\sum_{i=1}^{n}|h_{r_i,d}|^2\right)}\lambda_i|h_{r_i,d}|^2\right),\end{aligned} \tag{3.20}$$

where λ_i's are the eigenvalues of the matrix $\Phi(\mathbf{X}_1, \mathbf{X}_2)$. The determinant of a matrix equals the product of the matrix eigenvalues and that the determinant of the multiplication of two matrices equals the product of the individual matrices' determinants.

The PEP in (3.19) can now be approximated at high SNR as

$$\Pr(\mathbf{X}_1 \to \mathbf{X}_2) \leq E\left\{ \frac{1}{\prod_{i=1}^{n}(1+\frac{\delta_{s,r}^2 P_1 P_2/n}{4N_0\left(P_1\delta_{s,r}^2+N_o+\frac{P_2}{n}\sum_{i=1}^{n}|h_{r_i,d}|^2\right)}\lambda_i|h_{r_i,d}|^2)} \right\}. \quad (3.21)$$

Consider now the term $h=\sum_{i=1}^{n}|h_{r_i,d}|^2$ in (3.21), which can be reasonably approximated as $\sum_{i=1}^{n}|h_{r_i,d}|^2 \approx n\delta_{r,d}^2$, especially for large n [19] (by the strong law of large numbers). Averaging the expression in (3.21) over the exponential distribution of $|h_{r_i,d}|^2$ gives

$$\begin{aligned}\Pr(\mathbf{X}_1 \to \mathbf{X}_2) &\leq \prod_{i=1}^{n}\left(\frac{(\delta_{s,r}^2\delta_{r,d}^2 P_1P_2/n)\lambda_i}{4N_0\left(P_1\delta_{s,r}^2+N_o+P_2\delta_{r,d}^2\right)}\right)^{-1} \\ &\times \prod_{i=1}^{n}\left[-\exp\left(-\frac{4N_0\left(P_1\delta_{s,r}^2+N_o+P_2\delta_{r,d}^2\right)}{(\delta_{s,r}^2\delta_{r,d}^2P_1P_2/n)\lambda_i}\right)\mathbf{Ei}\left(-\frac{4N_0\left(P_1\delta_{s,r}^2+N_o+P_2\delta_{r,d}^2\right)}{(\delta_{s,r}^2\delta_{r,d}^2P_1P_2/n)\lambda_i}\right)\right],\end{aligned} \quad (3.22)$$

where $\mathbf{Ei}(.)$ is the exponential integral function defined as [41]

$$\mathbf{Ei}(\mu) = \int_{-\infty}^{\mu}\frac{\exp(t)}{t}dt, \quad \mu<0. \quad (3.23)$$

The exponential integral function can be approximated as μ tends to 0 as $-\mathbf{Ei}(\mu) \approx \ln\left(-\frac{1}{\mu}\right)$, $\mu<0$ [41]. At high SNR (high P) $\exp\left(-\frac{4N_0\left(P_1\delta_{s,r}^2+N_o+P_2\delta_{r,d}^2\right)}{(\delta_{s,r}^2\delta_{r,d}^2P_1P_2/n)\lambda_i}\right) \approx 1$, and using the approximation for the $\mathbf{Ei}(.)$ function provides the bound in (3.22) as

$$\Pr(\mathbf{X}_1 \to \mathbf{X}_2) \leq \prod_{i=1}^{n}\left(\frac{(\delta_{s,r}^2\delta_{r,d}^2 P_1P_2/n)\lambda_i}{4N_0\left(P_1\delta_{s,r}^2+P_2\delta_{r,d}^2\right)}\right)^{-1}\prod_{i=1}^{n}\ln\left(\frac{(\delta_{s,r}^2\delta_{r,d}^2 P_1P_2/n)\lambda_i}{4N_0\left(P_1\delta_{s,r}^2+P_2\delta_{r,d}^2\right)}\right). \quad (3.24)$$

Let $P_1=\alpha P$ and $P_2=(1-\alpha)P$, where P is the power per symbol, for some $\alpha\in(0,1)$. With the definition of the SNR as $SNR=P/N_0$, the bound in (3.24) can be given as

$$\begin{aligned}\Pr(\mathbf{X}_1 \to \mathbf{X}_2) &\leq a_{AF}\frac{1}{\prod_{i=1}^{n}\lambda_i}SNR^{-n}\prod_{i=1}^{n}\left(\ln(SNR)+\ln(C_i)\right) \\ &\backsimeq a_{AF}\frac{1}{\prod_{i=1}^{n}\lambda_i}SNR^{-n}\left(\ln(SNR)\right)^n,\end{aligned} \quad (3.25)$$

where

$$C_i = \frac{(\delta_{s,r}^2 \delta_{r,d}^2 \alpha(1-\alpha)/n)\lambda_i}{4\left(\alpha\delta_{s,r}^2 + (1-\alpha)\delta_{r,d}^2\right)},\ i = 1, \cdots, n,$$

are constant terms that do not depend on the SNR and a_{AF} is a constant that depends on the power allocation parameter α and the variances of the channels. The $\ln(C_i)$ terms are neglected at high SNRs resulting in the last bound in (3.25). The diversity order of the system can be calculated as $d_{AF} = \lim_{SNR\to\infty} -\frac{\log(PEP)}{\log(SNR)} = n$. The system will achieve a full diversity of order n if the matrix $\mathbf{M}$ is full rank, that is the code matrix $\Phi(\mathbf{X}_1, \mathbf{X}_2)$ must be full rank of order n over all distinct pairs of codewords $\mathbf{X}_1$ and $\mathbf{X}_2$. It can be easily shown, following the same approach, that if the code matrix $\Phi(\mathbf{X}_1, \mathbf{X}_2)$ is rank deficient, then the system will not achieve full diversity. So any code that is designed to achieve full diversity over MIMO channels will achieve full diversity in the case of amplify-and-forward distributed space-time coding scheme.

If full diversity is achieved, the coding gain is given as

$$C_{AF} = \left(a_{AF}\frac{1}{\prod_{i=1}^{n}\lambda_i}\right)^{-\frac{1}{n}}.$$

To maximize the coding gain of the amplify-and-forward distributed space-time codes the product $\prod_{i=1}^{n}\lambda_i$ needs to be maximized, which is the same as the determinant criterion used over MIMO channels [5]. So if a space-time code is designed to maximize the coding gain over MIMO channels, it will also maximize the coding gain if it can be used in a distributed fashion with the amplify-and-forward protocol.

3.1.3 Synchronization-Aware Distributed Space-Time Codes

In this section, the design of distributed space-time codes that relax the stringent synchronization requirement is considered. Most of the work on cooperative trans-

mission assumed perfect synchronization between the relay nodes, which means that the relays' timings, carrier frequencies, and propagation delays are identical. To simplify the synchronization in the network a diagonal structure is imposed on the space-time code used (refer to the diagonal space-time codes presented in Section 2.1.2). Fig. 3.2 shows the time frame structure for the conventional decode -and-forward (amplify-and-forward) distributed space-time codes and the diagonal distributed space-time codes (DDSTCs). The diagonal structure of the code bypasses the perfect synchronization problem by allowing only one relay to transmit at any time slot. Hence, synchronizing simultaneous in-phase transmissions of randomly distributed relay nodes is not necessary.

This greatly simplifies the synchronization since nodes can maintain slot synchronization, which means that coarse slot synchronization is available[2]. However, fine synchronization is more difficult to be achieved. Guard intervals are introduced to ensure that the transmissions from different relays are not overlapped. One relay is allowed to consecutively transmit its part of the space-time code from different data packets. This allows the overhead introduced by the guard intervals to be neglected. Fig 3.3 shows the effect of propagation delay on the received signal from two relays. The sampling time in Fig 3.3 is the optimum sampling time for the first relay signal, but clearly it is not optimal for the second relay signal.

DDSTC System Model

In this subsection, the system model with n relay nodes, which helps the source by emulating a diagonal STC, is introduced. The system has two phases with the

[2]For example, any synchronization scheme that is used for TDMA systems can be employed to achieve synchronization in the network.

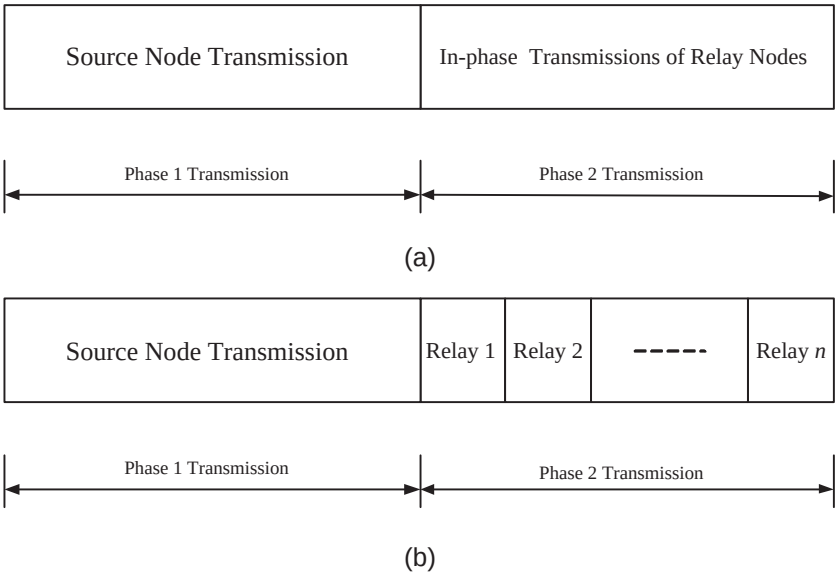

Figure 3.2: Time frame structure for (a) decode-and-forward (amplify-and-forward) based system (b) DDSTC based system.

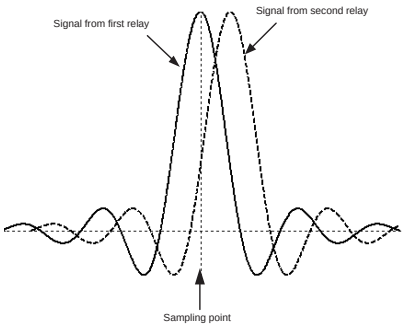

Figure 3.3: Baseband signals (each is raised cosine pulse-shaped) from two relays at the receiver.

time frame structure shown in Fig. 3.2(b). In phase 1, the received signals at the relay nodes are modeled as in (3.1) with $L = n$.

In phase 2, the k-th relay applies a linear transformation $\mathbf{t}_k$ to the received data vector, where $\mathbf{t}_k$ is an $1 \times n$ row vector, as

$$\begin{aligned} y_{r_k} &= \mathbf{t}_k \mathbf{y}_{s,r_k} \\ &= \sqrt{P_1} h_{s,r_k} \mathbf{t}_k \mathbf{s} + \mathbf{t}_k \mathbf{v}_{s,r_k} \\ &= \sqrt{P_1} h_{s,r_k} x_k + v_{r_k}, \end{aligned} \tag{3.26}$$

where $x_k = \mathbf{t}_k \mathbf{s}$ and $v_{r_k} = \mathbf{t}_k \mathbf{v}_{s,r_k}$. If the linear transformations are restricted to have unit norm, i.e., $||\mathbf{t}_k||^2 = 1$ for all k, then v_{r_k} is $\mathcal{CN}(0, N_o)$. The relay then multiplies y_{r_k} by the factor

$$\beta_k \leq \sqrt{\frac{P_2}{P_1 |h_{s,r_k}|^2}} \tag{3.27}$$

to satisfy a power constraint of $P = P_1 + P_2$ transmitted power per source symbol [11]. The received signal at the destination due to the k-th relay transmission is given by

$$\begin{aligned} y_k &= h_{r_k,d} \beta_k \sqrt{P_1} h_{s,r_k} x_k + h_{r_k,d} \beta_k v_{r_k} + \widetilde{v}_k \\ &= h_{r_k,d} \beta_k \sqrt{P_1} h_{s,r_k} x_k + z_k, \qquad k = 1, \cdots, n, \end{aligned} \tag{3.28}$$

where $\widetilde{v}_k$ is modeled as $\mathcal{CN}(0, N_0)$ and hence, z_k, given the channel coefficients is $\mathcal{CN}(0, (\beta_k^2 |h_{r_k,d}|^2 + 1) N_0),\ k = 1, \cdots, n$.

3.1.4 DDSTC Performance Analysis

In this subsection, the code design criterion of the DDSTC based on the PEP analysis is derived. In the following, the power constraint in (3.27) is set to be satisfied with equality.

Now, we start deriving a PEP upper-bound to derive the code design criterion. Let σ_k^2 denote the variance of z_k in (3.28) and is given as

$$\sigma_k^2 = \left(\frac{P_2 |h_{r_k,d}|^2}{P_1 |h_{s,r_k}|^2} + 1 \right) N_0, \ k = 1, \cdots, n. \tag{3.29}$$

Then, define the codeword vector $\mathbf{x}$ from (3.26) as

$$\mathbf{x} = \underbrace{\left[\mathbf{t}_1^T, \mathbf{t}_2^T, \cdots, \mathbf{t}_n^T \right]^T}_{\mathbf{T}} \mathbf{s} = \mathbf{T}\mathbf{s}, \tag{3.30}$$

where $\mathbf{T}$ is an $n \times n$ linear transformation matrix. From $\mathbf{x}$ define the $n \times n$ code matrix $\mathbf{X} = \text{diag}\left((\,) \mathbf{x} \right)$, which is a diagonal matrix with the elements of $\mathbf{x}$ on its diagonal. Let $\mathbf{y} = [y_1, y_2, \cdots, y_n]^T$ denote the received data vector at the destination node as given from (3.28).

Using our system model assumptions, the pdf of $\mathbf{y}$ given the source data vector $\mathbf{s}$ and the channel state information (CSI) is given by

$$p(\mathbf{y}|\mathbf{s}, CSI) = \left(\prod_{i=1}^{n} \frac{1}{\pi \sigma_i^2} \right) \exp \left(- \sum_{i=1}^{n} \frac{1}{\sigma_i^2} \left| y_i - \sqrt{\frac{P_1 P_2}{P_1 |h_{s,r_i}|^2}} h_{s,r_i} h_{r_i,d} x_i \right|^2 \right). \tag{3.31}$$

From which, the maximum likelihood (ML) decoder can be expressed as

$$\arg \max_{\mathbf{s} \in \mathcal{S}} p(\mathbf{y}|\mathbf{s}, CSI) = \arg \min_{\mathbf{s} \in \mathcal{S}} \sum_{i=1}^{n} \frac{1}{\sigma_i^2} \left| y_i - \sqrt{\frac{P_1 P_2}{P_1 |h_{s,r_i}|^2}} h_{s,r_i} h_{r_i,d} x_i \right|^2, \tag{3.32}$$

where $\mathcal{S}$ is the set of all possible transmitted source data vectors.

The PEP of mistaking $\mathbf{X}_1$ by $\mathbf{X}_2$ can be upper-bounded as [23]

$$\Pr(\mathbf{X}_1 \to \mathbf{X}_2) \leq E \left\{ \exp \left(\lambda [\ln p(\mathbf{y}|\mathbf{s}_2) - \ln p(\mathbf{y}|\mathbf{s}_1)] \right) \right\}, \tag{3.33}$$

where $\mathbf{X}_1$ and $\mathbf{X}_2$ are the code matrices corresponding to the source data vectors $\mathbf{s}_1$ and $\mathbf{s}_2$, respectively. Equation (3.33) applies for any λ which is a parameter

that can be adjusted to get the tightest bound. Now, the PEP can be written as

$$\Pr(\mathbf{X}_1 \to \mathbf{X}_2) \leq E\Bigg\{ \exp\Bigg(-\lambda\Bigg[\sum_{i=1}^{n} \frac{1}{\sigma_i^2} \Bigg(\sqrt{\frac{P_1P_2}{P_1|h_{s,r_i}|^2}} h_{s,r_i} h_{r_i,d}(x_{1i} - x_{2i}) z_i^* + \sqrt{\frac{P_1P_2}{P_1|h_{s,r_i}|^2}} h_{s,r_i}^* h_{r_i,d}^* (x_{1i} - x_{2i})^* z_i + \frac{P_1P_2}{P_1|h_{s,r_i}|^2} |h_{s,r_i}|^2 |h_{r_i,d}|^2 |x_{1i} - x_{2i}|^2 \Bigg) \Bigg] \Bigg) \Bigg\}, \tag{3.34}$$

where the expectation is over the noise and channel coefficients statistics and x_{ij} is the j-th element of the i-th code vector.

To average the expression in (3.34) over the noise statistics, define the receiver noise vector $\mathbf{z} = [z_1, z_2, \cdots, z_n]^T$, where z_i's are as defined in (3.28). The pdf of $\mathbf{z}$ given the channel state information is given by

$$p(\mathbf{z}|CSI) = \left(\prod_{i=1}^{n} \frac{1}{\pi\sigma_i^2} \right) \exp\left(- \sum_{i=1}^{n} \frac{1}{\sigma_i^2} z_i z_i^* \right). \tag{3.35}$$

Taking the expectation in (3.34) over $\mathbf{z}$ given the channel coefficients yields

$$\begin{aligned} \Pr(\mathbf{X}_1 \to \mathbf{X}_2) &\leq E\Bigg\{ \exp\left(-\lambda(1-\lambda) \sum_{i=1}^{n} \frac{1}{\sigma_i^2} \frac{P_1P_2}{P_1|h_{s,r_i}|^2} \left(|h_{s,r_i}|^2 |h_{r_i,d}|^2 |x_{1i} - x_{2i}|^2 \right) \right) \\ &\int_{\mathbf{z}} \left(\prod_{i=1}^{n} \frac{1}{\pi\sigma_i^2} \right) \exp\left(- \sum_{i=1}^{n} \frac{1}{\sigma_i^2} |z_i + \lambda \sqrt{\frac{P_1P_2}{P_1|h_{s,r_i}|^2}} h_{s,r_i} h_{r_i,d}(x_{1i} - x_{2i})|^2 \right) d\mathbf{z} \Bigg\} \\ &= E\left\{ \exp\left(-\lambda(1-\lambda) \sum_{i=1}^{n} \frac{1}{\sigma_i^2} \frac{P_1P_2}{P_1|h_{s,r_i}|^2} \left(|h_{s,r_i}|^2 |h_{r_i,d}|^2 |x_{1i} - x_{2i}|^2 \right) \right) \right\}. \end{aligned} \tag{3.36}$$

Choose $\lambda = 1/2$ that maximizes the term $\lambda(1-\lambda)$, i.e., minimizes the PEP upper-

bound. Substituting for σ_i^2's from (3.29), the PEP can be upper-bounded as

$$\Pr(\mathbf{X}_1 \to \mathbf{X}_2) \leq E\left\{\exp\left(-\frac{1}{4}\sum_{i=1}^{n}\frac{P_1|h_{s,r_i}|^2 P_2|h_{r_i,d}|^2}{(P_1|h_{s,r_i}|^2 + P_2|h_{r_i,d}|^2)N_0}|x_{1i} - x_{2i}|^2\right)\right\}. \tag{3.37}$$

To get the expression in (3.37), let us define the variable

$$\gamma_i = \frac{P_1|h_{s,r_i}|^2 P_2|h_{r_i,d}|^2}{(P_1|h_{s,r_i}|^2 + P_2|h_{r_i,d}|^2)N_0},\ i = 1, ..., n,$$

which is the scaled harmonic mean[3] of the two exponential random variables $\frac{P_1|h_{s,r_i}|^2}{N_0}$ and $\frac{P_2|h_{r_i,d}|^2}{N_0}$. Averaging the expression in (3.37) over the channel coefficients, the upper-bound on the PEP can be expressed as

$$\Pr(\mathbf{X}_1 \to \mathbf{X}_2) \leq \prod_{i=1, x_{1i}\neq x_{2i}}^{n} M_{\gamma_i}\left(\frac{1}{4}|x_{1i} - x_{2i}|^2\right), \tag{3.38}$$

where $M_{\gamma_i}(.)$ is the moment generating function (MGF) of the random variable γ_i. The problem now is to get an expression for $M_{\gamma_i}(.)$. To get $M_{\gamma_i}(.)$, let y_1 and y_2 be two independent exponential random variables with parameters α_1 and α_2, respectively. Let $y = \frac{y_1 y_2}{y_1 + y_2}$ be the scaled harmonic mean of y_1 and y_2. Then the MGF of y is [14]

$$M_y(s) = \frac{(\alpha_1 - \alpha_2)^2 + (\alpha_1 + \alpha_2)s}{\Delta^2} + \frac{2\alpha_1\alpha_2 s}{\Delta^3}\ln\frac{(\alpha_1 + \alpha_2 + s + \Delta)^2}{4\alpha_1\alpha_2}, \tag{3.39}$$

where

$$\Delta = \sqrt{(\alpha_1 - \alpha_2)^2 + 2(\alpha_1 + \alpha_2)s + s^2}.$$

Using the expression in (3.39), the MGF for γ_i can be approximated at high enough SNR to be [14]

$$M_{\gamma_i}(s) \simeq \frac{\zeta_i}{s}, \tag{3.40}$$

[3]The scaling factor is 1/2 since the harmonic mean of two numbers, g_1 and g_2, is $\frac{2g_1 g_2}{g_1 + g_2}$.

where

$$\zeta_i = \frac{N_0}{P_1\delta_{s,r}^2} + \frac{N_0}{P_2\delta_{r,d}^2}.$$

The PEP can now be upper-bounded as

$$\Pr(\mathbf{X}_1 \to \mathbf{X}_2) \leq N_0^n \left(\prod_{i=1, x_{1i}\neq x_{2i}}^{n} \left(\frac{1}{P_1\delta_{s,r}^2} + \frac{1}{P_2\delta_{r,d}^2} \right) \right) \left(\prod_{i=1, x_{1i}\neq x_{2i}}^{n} \frac{1}{4}|x_{1i} - x_{2i}|^2 \right)^{-1}. \tag{3.41}$$

Let $P_1 = \alpha P$ and $P_2 = (1-\alpha)P$, where P is the power per symbol, for some $\alpha \in (0,1)$ and define $SNR = P/N_0$. The diversity order d_{DDSTC} of the system is

$$d_{DDSTC} = \lim_{SNR\to\infty} -\frac{\log(PEP)}{\log(SNR)} = \min_{m\neq j} rank(\mathbf{X}_m - \mathbf{X}_j), \tag{3.42}$$

where $\mathbf{X}_m$ and $\mathbf{X}_j$ are two possible code matrices. To achieve a diversity order of n, the matrix $\mathbf{X}_m - \mathbf{X}_j$ should be of full rank for any $m \neq j$ (that is $x_{mi} \neq x_{ji}$ $\forall m \neq j$, $\forall i = 1, \cdots, n$). Intuitively, if two code matrices exist for which the rank of the matrix $\mathbf{X}_m - \mathbf{X}_j$ is not n this means that they have at least one diagonal element that is the same in both matrices. Clearly, this element can not be used to decide between these two possible transmitted code matrices and hence, the diversity order of the system is reduced. This criterion implies that each element in the code matrix is unique to that matrix and any other matrix will have a different element at that same location and this is really the source of diversity. Furthermore, to minimize the PEP bound in (3.41) we need to maximize

$$\min_{m\neq j} \left(\prod_{i=1}^{n} |x_{mi} - x_{ji}|^2 \right)^{1/n}, \tag{3.43}$$

which is called the minimum product distance of the set of symbols $\mathbf{s} = [s_1, s_2, ..., s_n]^T$ [42], [43]. A linear mapping is used to form the transmitted codeword, that is

$$\mathbf{x} = \mathbf{T}\mathbf{s}. \tag{3.44}$$

Several works have considered the design of the $n \times n$ transformation matrix $\mathbf{T}$ to maximize the minimum product distance. It was proposed in [44] and [45] to use both Hadamard transforms and Vandermonde matrices to design the $\mathbf{T}$ matrix. The transforms based on the Vandermonde matrices were shown to give larger minimum product distance than the Hadamard-based transforms. Some of the best known transforms based on the Vandermonde matrices [46] are summarized. Two classes of optimum transforms were proposed in [44]

1. If $n = 2^k$ $(k \geq 1)$, the optimum transform is given by

$$\mathbf{T}_{opt} = \frac{1}{\sqrt{n}} \text{vander}(\theta_1, \theta_2, ..., \theta_n),$$

where $\theta_1, \theta_2, ..., \theta_n$ are the roots of the polynomial $\theta^n - j$ over the field $\mathbf{Q}[j] \triangleq \{c + dj \ : \ \text{both } c \ \text{ and } d \text{ are rational numbers}\}$ and they are determined as $\theta_i = e^{j\frac{4i-3}{2n}\pi}, \quad i = 1, 2, ..., n.$

2. If $n = 3.2^k$ $(k \geq 0)$, the optimum transform is given by

$$\mathbf{T}_{opt} = \frac{1}{\sqrt{n}} \text{vander}(\theta_1, \theta_2, ..., \theta_n),$$

where $\theta_1, \theta_2, ..., \theta_n$ are the roots of the polynomial $\theta^n + w$ over the field $\mathbf{Q}[w] \triangleq \{c + dw \ : \ \text{both } c \ \text{ and } d \text{ are rational numbers}\}$ and they are determined as $\theta_i = e^{j\frac{6i-1}{3n}\pi}, \quad i = 1, 2, ..., n.$

The signal constellation from $\mathbf{Z}[j]$ such as M-QAM, M-PSK and PAM constellations are of practical interest. Moreover, in [45], some non-optimal transforms were proposed for some n's not satisfying any of the above two cases.

3.1.5 Simulation Results for DSTCs

In this section, simulation results for the distributed space-time coding schemes from the previous sections are presented. In the simulations, the variance of any

source-relay or relay-destination channel is taken to be 1. The performance of the different schemes with two relays helping the source are compared. Fig. 3.4 shows the simulations for two decode-and-forward systems using the Alamouti scheme (DAF Alamouti) and the diagonal STC (DAF DAST), distributed space-time codes based on the linear dispersion (LD) space-time codes (LD-DSTC) [19] which are based on the AAF scheme, the orthogonal distributed space-time codes (O-DSTC) proposed in [47] and [48], and DDSTC. The O-DSTCs are based on a generalized AAF scheme where relay nodes apply linear transformation to the received data as well as their complex conjugate. All of these systems have a data rate of (1/2). QPSK modulation is used, which means that a rate of one transmitted bit per symbol (1 bit/sym) is achieved. For the decode-and-forward system the power of the relay nodes that have decoded erroneously is not re-allocated to other relay nodes. Clearly, decode-and-forward based systems outperform amplify-and-forward based systems [4] but this is under the assumption that each relay node can decide whether it has decoded correctly or not. Intuitively, the decode-and-forward will deliver signals that are less noisy to the destination. The noise is suppressed at the relay nodes by transmitting a noise-free version of the signal. The amplify-and-forward delivers more noise to the destination due to noise propagation from the relay nodes. However, the assumption of correct decision at the relay nodes imposes practical limitations on the decode-and-forward systems, otherwise, error propagation [11] may occur caused by errors at the relay nodes. Error propagation would highly degrade the system bit error rate (BER) performance. Fig. 3.5 shows the simulation results for two decode-and-forward systems using the $\mathcal{G}_3$ ST block code of [6] and the diagonal STC (DAF DAST), LD-DSTC, and the DDSTC. For

[4]DDSTC is based on amplify-and-forward protocol.

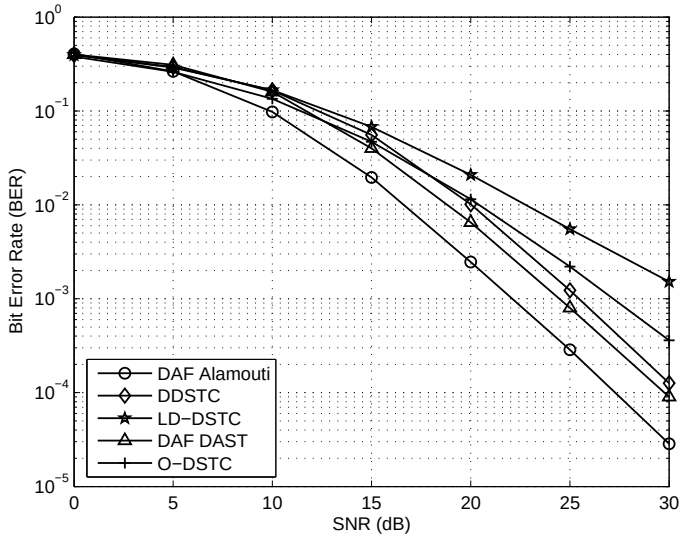

Figure 3.4: BER for two relays with data rate 1 bit/sym.

fair comparison the number of transmitted bits per symbol is fixed to be 1 bit/sym. The $\mathcal{G}_3$ ST block code has a data rate of (1/2) [6], which results in an overall system data rate of (1/3). Therefore, 8-PSK modulation is employed for the system that uses the $\mathcal{G}_3$ ST block code. For the other three systems QPSK modulation is used as these systems have a data rate of (1/2). For the decode-and-forward system the power of the relay nodes that decoded erroneously is not re-allocated. Clearly, decode-and-forward based systems outperform amplify-and-forward based systems under the same constraints stated previously. It is noteworthy that the performance of the LD-DSTC is not optimized since the LD matrices are randomly selected based on the isotropic distribution on the space of $n \times n$ unitary matrices as in [19].

In the sequel, the effect of the synchronization errors on the system BER performance is investigated. Fig. 3.6 shows the case of having two relays helping the source and propagation delay mismatches of $T_2 = 0.2T,\ 0.4T$ and $0.6T$, where T

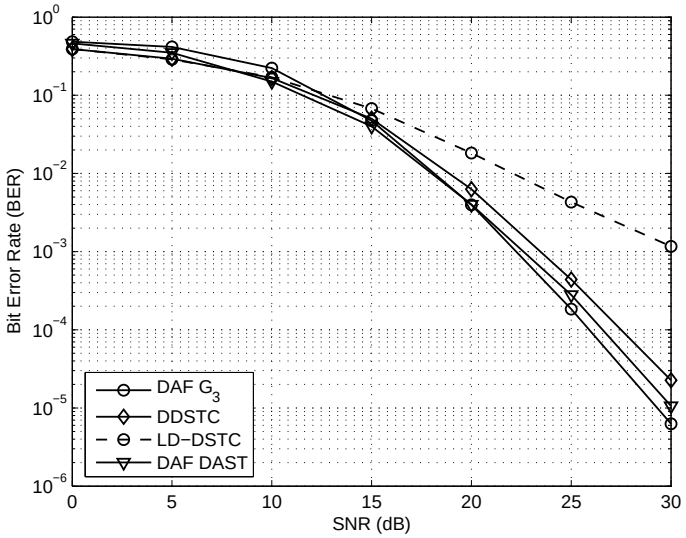

Figure 3.5: BER for three relays with data rate 1 bit/sym.

is the time slot duration. Raised cosine pulse-shaped waveforms were used with roll-off factor of 0.2 and QPSK modulation. Clearly, the BER performance of the system highly deteriorates as the propagation delay mismatch becomes larger. Fig. 3.7 shows the case of having three relays helping the source for different propagation delay mismatches. Decode-and-forward (DAF) system using the $\mathcal{G}_3$ ST block code of [6] and the DDSTC were compared. For fair comparison the number of transmitted bits per symbol is fixed to be 1 bit/sym. Again, the $\mathcal{G}_3$ ST block code has a data rate of (1/2) [6], which results in an overall system data rate to be (1/3). Therefore, 8-PSK modulation is employed for the system that uses the $\mathcal{G}_3$ ST block code. For the DDSTC, QPSK modulation is used as the system has a data rate of (1/2). Raised cosine pulse-shaped waveforms with roll-off factor of 0.2 are used. Clearly, the system performance is highly degraded as the propagation delay mismatch becomes larger. From Figures 3.6 and 3.7 it is clear that the synchronization errors can highly deteriorate the system BER performance. The

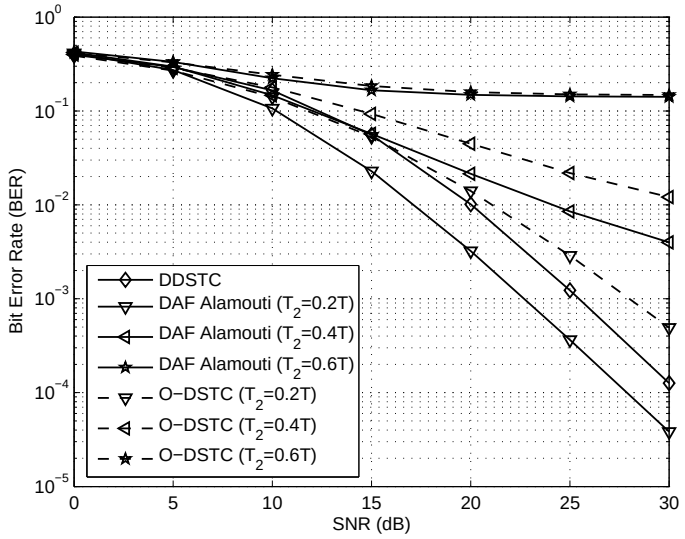

Figure 3.6: BER performance with propagation delay mismatch: two relays case.

DDSTC bypasses this problem by allowing only one relay transmission at any time slot.

3.2 Distributed Space-Frequency Coding (DSFC)

In this section, we will consider the design of distributed space-frequency coding (DSFC) for broadband multipath fading channels to exploit the frequency diversity of the channel. The presence of multipaths in broadband channels provides another means for achieving diversity across the frequency axis. Exploiting the frequency axis diversity can highly improve the system performance by achieving higher diversity orders. The main problem for the wireless relay network is how to design space-frequency codes distributed among *spatially separated* relay nodes while guaranteeing to achieve full diversity at the destination node. The spatial separation of the relay nodes presents other challenges for the design of DSFCs

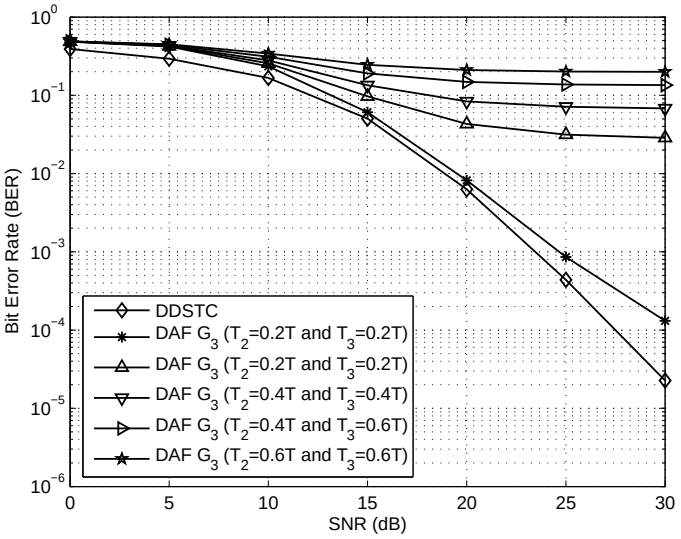

Figure 3.7: BER performance with propagation delay mismatch: three relays case.

such as time synchronization and carrier offset synchronization.

In this section, we will present some structures for distributed space-frequency codes (DSFCs) over wireless broadband relay networks. The presented DSFCs are designed to achieve the frequency and cooperative diversities of the wireless relay channels. The use of DSFCs with the decode-and-forward (DAF) and amplify-and-forward (AAF) protocols is considered. The code design criteria to achieve full diversity, based on the pairwise error probability (PEP) analysis, are derived. For DSFC with the DAF protocol, a two-stage coding scheme, with source node coding and relay nodes coding, is presented. We derive sufficient conditions for the code structures at the source and relay nodes to achieve full diversity of order NL, where N is the number of relay nodes and L is the number of paths per channel. For the case of DSFC with the AAF protocol, a structure for distributed space-frequency coding will be presented and sufficient conditions for that structure to

achieve full diversity will then be derived.

3.2.1 DSFC with the DAF Protocol

In this section, the design and performance analysis for DSFCs with the DAF protocol are presented. A two-stage structure is proposed for the DSFCs with the DAF protocol. Sufficient conditions for the proposed code structure to achieve full diversity are derived.

System Model

In this section, the system model for the DSFCs with the DAF protocol is presented. We use $\lfloor x \rfloor$ to denote the largest integer that is less that x. $\mathbf{diag}(\mathbf{y})$, where $\mathbf{y}$ is a $T \times 1$ vector, is the $T \times T$ diagonal matrix with the elements of $\mathbf{y}$ on its diagonal. $\mathbf{A} \otimes \mathbf{B}$ denotes the tensor product of the two matrices $\mathbf{A}$ and $\mathbf{B}$. $||\mathbf{A}||_F^2$ of the $m \times n$ matrix $\mathbf{A}$ is the Frobenius norm of the matrix defined as $||\mathbf{A}||_F^2 = \sum_{i=1}^{m} \sum_{j=1}^{n} |\mathbf{A}(i,j)|^2 = \mathcal{TR}\left(\mathbf{A}\mathbf{A}^{\mathcal{H}}\right) = \mathcal{TR}\left(\mathbf{A}^{\mathcal{H}}\mathbf{A}\right)$ where $\mathcal{TR}(\cdot)$ is the trace of a matrix.

Without loss of generality, we assume a two-hop relay channel model, where there is no direct link from the source node to the destination node. The case when a direct link exists between the source node and the destination node will be discussed in Section 3.2.3. A schematic system model is depicted in Fig. 3.8. The system is based on orthogonal frequency division multiplexing (OFDM) modulation with K subcarriers. The channel between the source node and the n-th relay node is modeled as a multipath fading channel with L paths as

$$h_{s,r_n}(\tau) = \sum_{l=1}^{L} \alpha_{s,r_n}(l)\delta(\tau - \tau_l), \tag{3.45}$$

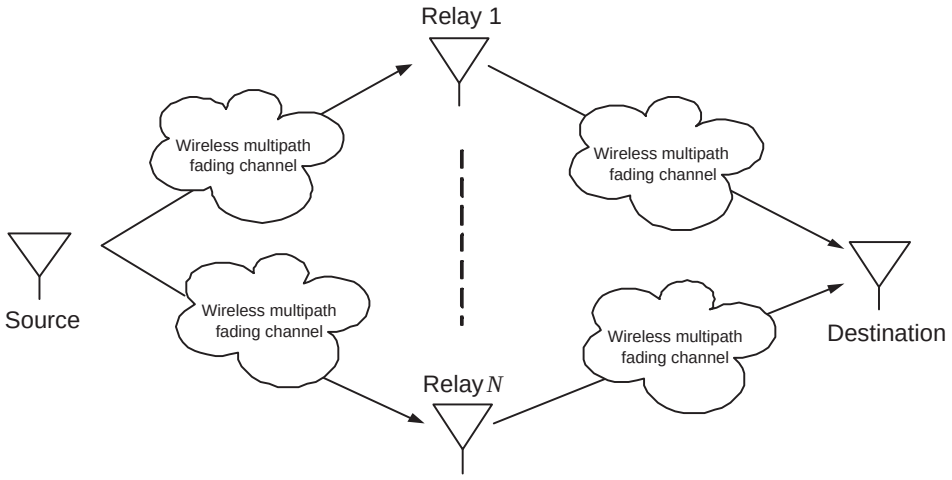

Figure 3.8: Simplified system model for the distributed space-frequency codes.

where τ_l is the delay of the l-th path, $\delta(\cdot)$ is the Dirac delta function, and $\alpha_{s,r_n}(l)$ is the complex amplitude of the l-th path. The $\alpha_{s,r_n}(l)$'s are modeled as zero-mean complex Gaussian random variables with variance $E\left[|\alpha_{s,r_n}(l)|^2\right] = \sigma^2(l)$, where we assume symmetry between the relay nodes for simplicity of presentation; the analysis can be easily extended to the asymmetric case. The channels are normalized such that the channel variance $\sum_{l=1}^{L} \sigma^2(l) = 1$. A cyclic prefix is introduced to convert the multipath frequency-selective fading channels to flat fading subchannels on the subcarriers.

The system has two phases as follows. In phase 1, the source node broadcasts the information to the N relays. The received signal in the frequency domain on the k-th subcarrier at the n-th relay node is given by

$$y_{s,r_n}(k) = \sqrt{P_1} H_{s,r_n}(k) s(k) + \eta_{s,r_n}(k), \quad k = 1, \cdots, K; \quad n = 1, \cdots, N, \quad (3.46)$$

where P_1 is the transmitted source node power, $H_{s,r_n}(k)$ is the channel attenuation of the source node to the n-th relay node channel on the k-th subcarrier, $s(k)$ is the transmitted source node symbol on the k-th subcarrier with $E\left\{|s(k)|^2\right\} = 1$,

and $\eta_{s,r_n}(k)$ is the n-th relay node additive white Gaussian noise on the k-th subcarrier that is modeled as zero-mean circularly symmetric complex Gaussian random variable with variance $N_0/2$ per dimension. The subcarrier noise terms are statistically independent assuming that the time-domain noise samples are statistically independent and identically distributed[5]. In (3.46), $H_{s,r_n}(k)$ is given by

$$H_{s,r_n}(k) = \sum_{l=1}^{L} \alpha_{s,r_n}(l) e^{-j2\pi(k-1)\Delta f \tau_l},\ k = 1, \cdots, K, \tag{3.47}$$

where $\Delta f = 1/T$ is the subcarrier frequency separation and T is the OFDM symbol duration. We assume perfect channel state information at any receiving node but no channel information at transmitting nodes.

In phase 2, relays that have decoded correctly in phase 1 will forward the source node information. Each relay is assumed to be able to decide whether it has decoded correctly or not. This can be achieved through the use of error detecting codes such as the *Cyclic Redundancy* codes (CRC) [36], [12].

The transmitted $K \times N$ space-frequency (SF) codeword from the relay nodes

[5]Fast Fourier Transform (FFT), which is used to transform the received data from the time-domain to the frequency-domain, can be represented by a unitary matrix multiplication. Unitary transformation of a Gaussian random vector, whose components are statistically independent and identically distributed, results in a Gaussian random vector with statistically independent and identically distributed components.

is given by[6]

$$\mathbf{C}_r = \begin{pmatrix} C_r(1,1) & C_r(1,2) & \cdots & C_r(1,N) \\ C_r(2,1) & C_r(2,2) & \cdots & C_r(2,N) \\ \vdots & \vdots & \ddots & \vdots \\ C_r(K,1) & C_r(K,2) & \cdots & C_r(K,N) \end{pmatrix}, \tag{3.48}$$

where $C_r(k,n)$ is the symbol transmitted by the n-th relay node on the k-th subcarrier. The SF is assumed to satisfy the power constraint $||\mathbf{C}_r||_F^2 \leq K$.

The received signal at the destination node on the k-th subcarrier is given by

$$y_d(k) = \sqrt{P_2} \sum_{n=1}^{N} H_{r_n,d}(k) C_r(k,n) I_n + \eta_{r_n,d}(k), \tag{3.49}$$

where P_2 is the relay node power, $H_{r_n,d}(k)$ is the attenuation of the channel between the n-th relay node and the destination node on the k-th subcarrier, $\eta_{r_n,d}(k)$ is the destination additive white Gaussian noise on the k-th subcarrier, and I_n is the state of the n-th relay. I_n will equal 1 if the n-th relay has decoded correctly in phase 1, otherwise, I_n will equal 0.

Performance Analysis

It is now necessary to develop sufficient code design criteria for the DSFC to achieve full diversity of order NL. Unlike the case of MIMO space-frequency coding, we will need a two-stage coding to achieve full diversity at the destination node. Therefore, the proposed DSFCs will have two stages of coding: the first stage is coding at the source node and the second stage is coding at the relay nodes. The transmitted source node code will be designed to guarantee a diversity of order L

[6] $\mathbf{C}_r$ will be SF code transmitted by the relay nodes if all of them have decoded correctly in phase 1.

at any relay node, and this will in turn cause the proposed DSFC to achieve full diversity of order NL as will be shown later.

Source Node Coding

Due to the symmetry assumption, the pairwise error probability (PEP) is the same at any relay node. For two distinct transmitted source node symbols, $\mathbf{s}$ and $\widetilde{\mathbf{s}}$, the PEP can be tightly upper-bounded as [38, 46]

$$PEP(\mathbf{s} \to \widetilde{\mathbf{s}}) \leq \begin{pmatrix} 2\nu - 1 \\ \nu \end{pmatrix} \left(\prod_{i=1}^{\nu} \lambda_i \right)^{-1} \left(\frac{P_1}{N_0} \right)^{-\nu} \tag{3.50}$$

and ν is the rank of the matrix $\mathbf{C} \circ \mathbf{R}$ where

$$\mathbf{C} = (\mathbf{s} - \widetilde{\mathbf{s}})(\mathbf{s} - \widetilde{\mathbf{s}})^{\mathcal{H}},$$

$$\mathbf{R} = E\left\{ \mathbf{H}_{s,r_n} \mathbf{H}_{s,r_n}^{\mathcal{H}} \right\},$$

and $\mathbf{H}_{s,r_n} = [H_{s,r_n}(1), \cdots, H_{s,r_n}(K)]^T$. Here λ_i's are the non-zero eigenvalues of the matrix $\mathbf{C} \circ \mathbf{R}$, where $\circ$ denotes the Hadamard product[7].

The correlation matrix, $\mathbf{R}$, of the channel impulse response can be found as

$$\begin{aligned} \mathbf{R} &= E\left\{ \mathbf{H}_{s,r_n} \mathbf{H}_{s,r_n}^{\mathcal{H}} \right\} \\ &= \mathbf{W} E\left\{ \alpha_{s,r_n} \alpha_{s,r_n}^{\mathcal{H}} \right\} \mathbf{W}^{\mathcal{H}} \\ &= \mathbf{W} \mathbf{diag}\{\sigma^2(1), \sigma^2(2), \cdots, \sigma^2(L)\} \mathbf{W}^{\mathcal{H}}, \end{aligned} \tag{3.51}$$

where

$$\alpha_{s,r_n} = [\alpha_{s,r_n}(1), \alpha_{s,r_n}(2), \cdots, \alpha_{s,r_n}(L)]^T,$$

[7] If $\mathbf{A} = \{a_{i,j}\}$ and $\mathbf{B} = \{b_{i,j}\}$ are two $m \times n$ matrices, the Hadamard product is defined as $\mathbf{D} = \mathbf{A} \circ \mathbf{B} = \{d_{i,j}\}$, where $d_{i,j} = a_{i,j} b_{i,j}$.

$$\mathbf{W} = \begin{pmatrix} 1 & 1 & \cdots & 1 \\ w^{\tau_1} & w^{\tau_2} & \cdots & w^{\tau_L} \\ \vdots & \vdots & \ddots & \vdots \\ w^{(K-1)\tau_1} & w^{(K-1)\tau_2} & \cdots & w^{(K-1)\tau_L} \end{pmatrix},$$

and $w = e^{-j2\pi\Delta f}$.

The coding at the source node is implemented to guarantee a diversity of order L, which is the maximum achievable diversity order at any relay node. We propose to partition the transmitted $K \times 1$ source node code into subblocks of length L and we will design the subblocks to guarantee a diversity of order L at any relay node as will be seen later. Let $M = \lfloor K/L \rfloor$ denote the number of subblocks in the source node transmitted OFDM block. The transmitted $K \times 1$ source node code is given as

$$\mathbf{s} = [s(1), s(2), \cdots, s(K)]^T = [\mathbf{F}_1^T, \mathbf{F}_2^T, \cdots, \mathbf{F}_M^T, \mathbf{0}_{K-ML}^T]^T, \tag{3.52}$$

where $\mathbf{F}_i = [F_i(1), \cdots, F_i(L)]^T$ is the i-th subblock of dimension $L \times 1$. Zeros are padded if K is not an integer multiple of L. For any two distinct source codewords, $\mathbf{s}$ and $\widetilde{\mathbf{s}} = [\widetilde{\mathbf{F}}_1^T, \widetilde{\mathbf{F}}_2^T, \cdots, \widetilde{\mathbf{F}}_M^T, \mathbf{0}_{K-ML}^T]^T$, at least one index p_0 exists for which $\mathbf{F}_{p_0}$ is not equal to $\widetilde{\mathbf{F}}_{p_0}$.

Based on the proposed structure of the transmitted code from the source node, sufficient conditions for the code to achieve a diversity of order L at the relay nodes are derived. We assume for $\mathbf{s}$ and $\widetilde{\mathbf{s}}$ that $\mathbf{F}_p = \widetilde{\mathbf{F}}_p$ for all $p \neq p_0$, which corresponds to the worst-case PEP. This does not decrease the rank of the matrix $\mathbf{C} \circ \mathbf{R}$ [46]. Define the $L \times L$ matrix $\mathbf{Q} = \{q_{i,j}\}$ as $q_{i,j} = \sum_{l=1}^{L} \sigma^2(l) w^{(i-j)\tau(l)}, \quad 1 \leq i, j \leq L$. Note that the non-zero eigenvalues of the matrix $\mathbf{C} \circ \mathbf{R}$ are the same as those of

the matrix $\left(\mathbf{F}_{p_0} - \widetilde{\mathbf{F}}_{p_0}\right)\left(\mathbf{F}_{p_0} - \widetilde{\mathbf{F}}_{p_0}\right)^{\mathcal{H}} \circ \mathbf{Q}$. Hence, we have

$$\begin{aligned}
&\left(\mathbf{F}_{p_0} - \widetilde{\mathbf{F}}_{p_0}\right)\left(\mathbf{F}_{p_0} - \widetilde{\mathbf{F}}_{p_0}\right)^{\mathcal{H}} \circ \mathbf{Q} \\
&\qquad = \left[\mathbf{diag}\left(\mathbf{F}_{p_0} - \widetilde{\mathbf{F}}_{p_0}\right)\mathbf{1}_{L\times L}\mathbf{diag}\left(\mathbf{F}_{p_0} - \widetilde{\mathbf{F}}_{p_0}\right)^{\mathcal{H}}\right] \circ \mathbf{Q} \qquad (3.53)\\
&\qquad = \mathbf{diag}\left(\mathbf{F}_{p_0} - \widetilde{\mathbf{F}}_{p_0}\right)\ \mathbf{Q}\ \mathbf{diag}\left(\mathbf{F}_{p_0} - \widetilde{\mathbf{F}}_{p_0}\right)^{\mathcal{H}}
\end{aligned}$$

where $\mathbf{1}_{L\times L}$ is the $L \times L$ matrix whose all elements are ones. The last equality follows from a property of the Hadamard product ([49], p.304).

If all of the eigenvalues of the matrix $\left(\mathbf{F}_{p_0} - \widetilde{\mathbf{F}}_{p_0}\right)\left(\mathbf{F}_{p_0} - \widetilde{\mathbf{F}}_{p_0}\right)^{\mathcal{H}} \circ \mathbf{Q}$ are non-zero, then their product can be calculated as

$$\begin{aligned}
&\det\left(\left(\mathbf{F}_{p_0} - \widetilde{\mathbf{F}}_{p_0}\right)\left(\mathbf{F}_{p_0} - \widetilde{\mathbf{F}}_{p_0}\right)^{\mathcal{H}} \circ \mathbf{Q}\right) \\
&\quad = \det\left(\mathbf{diag}\left(\mathbf{F}_{p_0} - \widetilde{\mathbf{F}}_{p_0}\right)\right)\det\left(\mathbf{Q}\right)\det\left(\mathbf{diag}\left(\mathbf{F}_{p_0} - \widetilde{\mathbf{F}}_{p_0}\right)^{\mathbf{H}}\right) \qquad (3.54)\\
&\quad = \prod_{l=1}^{L}\left|F_{p_0}(l) - \widetilde{F}_{p_0}(l)\right|^2 \left(\det(Q)\right).
\end{aligned}$$

The matrix $\mathbf{Q}$ is non-singular. Hence, if the product $\prod_{l=1}^{L}\left|F_{p_0}(l) - \widetilde{F}_{p_0}(l)\right|^2$ is non-zero over all possible pairs of distinct transmitted source codewords, $\mathbf{s}$ and $\widetilde{\mathbf{s}}$, then a diversity of order L will be achieved at each relay node.

In phase 2, relays that have decoded correctly in phase 1 will forward the source node information. The received signal at the destination node on the k-th subcarrier is as given in (3.49). The state of the n-th relay node I_n is a Bernoulli random variable with a probability mass function (pmf) given by

$$I_n = \begin{cases} 0 & \text{with probability} = SER \\ \\ 1 & \text{with probability} = 1 - SER, \end{cases} \qquad (3.55)$$

where SER is the symbol error rate at the n-th relay node. Note that SER is the same for any relay node due to the symmetry assumption. If the transmitted code

from the source node is designed such that the product $\prod_{l=1}^{L}\left|F_{p_0}(l)-\widetilde{F}_{p_0}(l)\right|^2$ is non-zero, for at least one index p_0, over all the possible pairs of distinct transmitted source codewords, $\mathbf{s}$ and $\widetilde{\mathbf{s}}$, then the SER at the n-th relay node can be upper-bounded as

$$\begin{aligned} SER &= \sum_{\mathbf{s}\in\mathcal{S}} \Pr\{\mathbf{s}\} \Pr\{\text{error given that } \mathbf{s} \text{ was transmitted}\} \\ &\leq \sum_{\mathbf{s}\in\mathcal{S}} \Pr\{\mathbf{s}\} \sum_{\widetilde{\mathbf{s}}\in\mathcal{S},\widetilde{\mathbf{s}}\neq\mathbf{s}} PEP(\mathbf{s}\rightarrow\widetilde{\mathbf{s}}) \\ &\leq c\times SNR^{-L}, \end{aligned} \tag{3.56}$$

where $\mathcal{S}$ is the set of all possible transmitted source codewords and c is a constant that does not depend on the SNR. The first inequality follows from the union upper-bound and the second inequality follows from (3.50), where SNR is defined as $SNR = P_1/N_0$.

Relay Nodes Coding

Next, the design of the SF code at the relay nodes to achieve a diversity of order NL is considered. We propose to design SF codes constructed from the concatenation of block diagonal matrices, which is similar to the structure used in [46] to design full-rate, full-diversity space-frequency codes over MIMO channels. We will derive sufficient conditions for the proposed code structure to achieve full diversity at the destination node.

Let $P = \lfloor K/NL \rfloor$ denote the number of subblocks in the transmitted OFDM block from the relay nodes. The transmitted $K \times N$ SF codeword from the relay nodes, if all relays decoded correctly, is given by

$$\mathbf{C}_r = [\mathbf{G}_1^T, \mathbf{G}_2^T, \cdots, \mathbf{G}_P^T, \mathbf{0}_{K-PLN}^T]^T, \tag{3.57}$$

where $\mathbf{G}_i$ is the i-th subblock of dimension $NL \times N$. Zeros are padded if K is not an integer multiple of NL. Each $\mathbf{G}_i$ is a block diagonal matrix that has the structure

$$\mathbf{G}_i = \begin{pmatrix} \mathbf{X}_{1_{L\times 1}} & \mathbf{0}_{L\times 1} & \cdots & \mathbf{0}_{L\times 1} \\ \mathbf{0}_{L\times 1} & \mathbf{X}_{2_{L\times 1}} & \cdots & \mathbf{0}_{L\times 1} \\ \vdots & \vdots & \ddots & \vdots \\ \mathbf{0}_{L\times 1} & \mathbf{0}_{L\times 1} & \cdots & \mathbf{X}_{N_{L\times 1}} \end{pmatrix} \tag{3.58}$$

and let $\mathbf{X} = [\mathbf{X}_1^T, \mathbf{X}_2^T, \cdots, \mathbf{X}_N^T] = [x(1), x(2), \cdots, x(NL)]$.

For two distinct transmitted source codewords, $\mathbf{s}$ and $\widetilde{\mathbf{s}}$, and a given realization of the relays states $\mathbf{I} = [I_1, I_2, \cdots, I_n]^T$, the conditional PEP can be tightly upper-bounded as

$$PEP(\mathbf{s} \to \widetilde{\mathbf{s}}/\mathbf{I}) \leq \begin{pmatrix} 2\kappa - 1 \\ \\ \kappa \end{pmatrix} \left(\prod_{i=1}^{\kappa} \eta_i \right)^{-1} \left(\frac{P_2}{N_0} \right)^{-\kappa}, \tag{3.59}$$

and κ is the rank of the matrix $\mathbf{C}(\mathbf{I}) \circ \mathbf{R}$ where

$$\mathbf{C}(\mathbf{I}) = (\mathbf{C}_r - \widetilde{\mathbf{C}}_r)\mathbf{diag}(\mathbf{I})(\mathbf{C} - \widetilde{\mathbf{C}}_r)^{\mathcal{H}}.$$

For two source codewords, $\mathbf{s}$ and $\widetilde{\mathbf{s}}$, at least one index p_0 exists for which $\mathbf{G}_{p_0} \neq \widetilde{\mathbf{G}}_{p_0}$. We assume for $\mathbf{s}$ and $\widetilde{\mathbf{s}}$ that $\mathbf{G}_p = \widetilde{\mathbf{G}}_p$ for all $p \neq p_0$. As for the source node coding case, this does not decrease the rank of the matrix $\mathbf{C}(\mathbf{I}) \circ \mathbf{R}$ that corresponds to any realization $\mathbf{I}$ of the relays states.

Define the $NL \times NL$ matrix $\mathbf{S} = \{s_{i,j}\}$ as

$$s_{i,j} = \sum_{l=1}^{L} \sigma^2(l) w^{(i-j)\tau(l)}, \quad 1 \leq i, j \leq NL.$$

Note that the non-zero eigenvalues of the matrix $\mathbf{C}(\mathbf{I}) \circ \mathbf{R}$ are the same as the non-zero eigenvalues of the matrix $\left(\mathbf{G}_{p_0}(\mathbf{I}) - \widetilde{\mathbf{G}}_{p_0}(\mathbf{I})\right)\left(\mathbf{G}_{p_0}(\mathbf{I}) - \widetilde{\mathbf{G}}_{p_0}(\mathbf{I})\right)^{\mathcal{H}} \circ \mathbf{S}$ where

$\mathbf{G}_{p_0}(\mathbf{I})$ is formed from $\mathbf{G}_{p_0}$ by setting the columns corresponding to the relays that have decoded erroneously to zeros. Hence,

$$\begin{aligned}
&\left(\mathbf{G}_{p_0}(\mathbf{I}) - \widetilde{\mathbf{G}}_{p_0}(\mathbf{I})\right)\left(\mathbf{G}_{p_0}(\mathbf{I}) - \widetilde{\mathbf{G}}_{p_0}(\mathbf{I})\right)^{\mathcal{H}} \circ \mathbf{S} \\
&= \left(\mathbf{diag}(\mathbf{X} - \widetilde{\mathbf{X}})\left(\mathbf{diag}(\mathbf{I}) \otimes \mathbf{1}_{L\times 1}\right)\left(\mathbf{diag}(\mathbf{I}) \otimes \mathbf{1}_{L\times 1}\right)^{\mathcal{H}} \mathbf{diag}(\mathbf{X} - \widetilde{\mathbf{X}})^{\mathcal{H}}\right) \circ \mathbf{S} \\
&= \left(\mathbf{diag}(\mathbf{X} - \widetilde{\mathbf{X}})\left(\mathbf{diag}(\mathbf{I}) \otimes \mathbf{1}_{L\times L}\right)\mathbf{diag}(\mathbf{X} - \widetilde{\mathbf{X}})^{\mathcal{H}}\right) \circ \mathbf{S} \\
&= \mathbf{diag}(\mathbf{X} - \widetilde{\mathbf{X}})\left[\left(\mathbf{diag}(\mathbf{I}) \otimes \mathbf{1}_{L\times L}\right) \circ \mathbf{S}\right]\mathbf{diag}(\mathbf{X} - \widetilde{\mathbf{X}})^{\mathcal{H}},
\end{aligned} \tag{3.60}$$

where the second and the third equalities follow from the properties of the tensor and Hadamard products [49].

Let $n_{\mathbf{I}} = \sum_{n=1}^{N} I_n$ denote the number of relays that have decoded correctly corresponding to a realization $\mathbf{I}$ of the relays states. Using (3.60), the product of the non-zero eigenvalues of the matrix $\mathbf{C}(\mathbf{I}) \circ \mathbf{R}$ can be found as

$$\prod_{i=1}^{\kappa} \eta_i = \left(\prod_{i=1,\, i\in\mathcal{I}}^{NL} |x(i) - \widetilde{x}(i)|^2\right) \cdot \left(\det(\mathbf{S}_0)\right)^{n_{\mathbf{I}}} \tag{3.61}$$

where $\mathcal{I}$ is the index set of symbols that are transmitted from the relays that have decoded correctly corresponding to the realization $\mathbf{I}$ and $\mathbf{S}_0 = \{s_{i,j}\},\ 1 \le i, j \le L$. The result in (3.61) is based on the assumption that the product $\prod_{i=1,\, i\in\mathcal{I}\}}^{NL} |x(i) - \widetilde{x}(i)|^2$ is non-zero. The first product in (3.61) is over $n_{\mathbf{I}}L$ terms. The matrix $\mathbf{S}_0$ is always full rank of order L. Hence, designing the product $\prod_{i=1,\, i\in\mathcal{I}}^{NL} |x(i) - \widetilde{x}(i)|^2$ to be non-zero will guarantee a rate of decay, at high SNR, of the conditional PEP as $SNR^{-n_{\mathbf{I}}L}$, where SNR is now defined as $SNR = P_2/N_0$. To guarantee that this rate of decay, $SNR^{-n_{\mathbf{I}}L}$, is always achieved irrespective of the state realization $\mathbf{I}$ of the relay nodes then the product $\prod_{i=1}^{NL} |x(i) - \widetilde{x}(i)|^2$ should be non-zero. Hence, designing the product $\prod_{i=1}^{NL} |x(i) - \widetilde{x}(i)|^2$ to be non-zero for any pair of distinct

source codewords is a sufficient condition for the conditional PEP to decay as $SNR^{-n_{\mathbf{I}}L}$ for any realization $\mathbf{I}$, where $n_{\mathbf{I}}$ is the number of relays that have decoded correctly corresponding to $\mathbf{I}$.

Now, we calculate the PEP at the destination node for our proposed DSFC structure. Let c_r denote the number of relays that have decoded correctly. Then c_r follows a Binomial distribution as[8]

$$\Pr\{c_r = k\} = \begin{pmatrix} N \\ k \end{pmatrix} (1 - SER)^k SER^{N-k}, \tag{3.62}$$

where SER is the symbol error rate at the relay nodes. The destination PEP is given by

$$\begin{aligned} PEP(\mathbf{s} \to \widetilde{\mathbf{s}}) &= \sum_{\mathbf{I}} \Pr\{\mathbf{I}\} PEP(\mathbf{s} \to \widetilde{\mathbf{s}}/\mathbf{I}) \\ &= \sum_{k=0}^{N} \Pr\{c_r = k\} \sum_{\{\mathbf{I}: n_{\mathbf{I}} = k\}} PEP(\mathbf{s} \to \widetilde{\mathbf{s}}/\mathbf{I}) \\ &= \sum_{k=0}^{N} \begin{pmatrix} N \\ k \end{pmatrix} (1 - SER)^k SER^{N-k} \sum_{\{\mathbf{I}: n_{\mathbf{I}} = k\}} PEP(\mathbf{s} \to \widetilde{\mathbf{s}}/\mathbf{I}), \end{aligned} \tag{3.63}$$

Using the upper-bound on the SER at the relay nodes given in (3.56) and the expression for the conditional PEP at the destination node in (3.59), and upper-bounding $(1 - SER)$ by 1, it can be shown that

$$PEP(\mathbf{s} \to \widetilde{\mathbf{s}}) \leq constant \times SNR^{-NL}. \tag{3.64}$$

Hence, our proposed structure for DSFCs with two-stage coding at the source node and the relay nodes achieves a diversity of order NL, which is the rate of decay of the PEP at high SNR.

[8] c_r is a Binomial random variable as it is the sum of independent, identically distributed Bernoulli random variables.

3.2.2 DSFC with the AAF Protocol

In this section, the design and performance analysis for DSFCs with the AAF protocol are presented. A structure is proposed and sufficient conditions for the proposed structure to achieve full diversity are then derived for some special cases.

System Model

In this section, we describe the system model for DSFC with the AAF protocol. The received signal model at the relay nodes and the channel gains are modeled as in Section 3.2.1. The transmitted data from the source node is parsed into subblocks of size $NL \times 1$. Let $P = \lfloor K/NL \rfloor$ denote the number of subblocks in the transmitted OFDM block. The transmitted $K \times 1$ source codeword is given by

$$\mathbf{s} = [s(1), s(2), \cdots, s(K)]^T = [\mathbf{B}_1^T, \mathbf{B}_2^T, \cdots, \mathbf{B}_P^T, \mathbf{0}_{K-PLN}^T]^T, \tag{3.65}$$

where $\mathbf{B}_i$ is the i-th subblock of dimension $NL \times 1$. Zeros are padded if K is not an integer multiple of NL. For each subblock, $\mathbf{B}_i$, the n-th relay only forwards the data on L subcarriers. For example, relay 1 will only forward $[\mathbf{B}_i(1), \cdots, \mathbf{B}_i(L)]$ for all i's and send zeros on the remaining set of subcarriers. In general, the n-th relay will only forward $[\mathbf{B}_i((n-1)L+1), \cdots, \mathbf{B}_i((n-1)L+L)]$ for all i's.

At the relay nodes, each node will normalize the received signal on the subcarriers that it will forward before retransmission and send zeros on the remaining set of subcarriers. If the k-th subcarrier is to be forwarded by the n-th relay, the relay will normalize the received signal on that subcarrier by the factor $\beta(k) = \sqrt{\frac{1}{P_1|H_{s,r_n}(k)|^2+N_0}}$ [11]. The relay nodes will use OFDM modulation for transmission to the destination node. At the destination node, the received signal

on the k-th subcarrier, assuming it was forwarded by the n-th relay, is given by

$$y(k) = H_{r_n,d}(k)\sqrt{P_2}\left(\sqrt{\frac{1}{P_1|H_{s,r_n}(k)|^2+N_0}}\left(\sqrt{P_1}H_{s,r_n}(k)s(k)+\eta_{s,r_n}(k)\right)\right)+\eta_{r_n,d}(k), \tag{3.66}$$

where P_2 is the relay node power, $H_{r_n,d}(k)$ is the attenuation of the channel between the n-th relay node and the destination node on the k-th subcarrier, and $\eta_{s,r_n}(k)$ is the destination noise on the k-th subcarrier. The $\eta_{r_n,d}(k)$'s are modeled as zero-mean, circularly symmetric complex Gaussian random variables with a variance of $N_0/2$ per dimension.

Performance Analysis

In this section, the PEP of the DSFC with the AAF protocol is presented. Based on the PEP analysis, code design criteria are derived. The received signal at destination on the k-th subcarrier given by (3.66) can be rewritten as

$$y(k) = H_{r_n,d}(k)\sqrt{P_2}\left(\sqrt{\frac{1}{P_1|H_{s,r_n}(k)|^2+N_0}}\sqrt{P_1}H_{s,r_n}(k)s(k)\right)+z_{r_n,d}(k), \tag{3.67}$$

where $z_{r_n,d}(k)$ accounts for the noise propagating from the relay node as well as the destination noise. $z_{r_n,d}(k)$ follows a circularly symmetric complex Gaussian random variable with a variance $\delta_z^2(k)$ of $\left(\frac{P_2|H_{r_n,d}(k)|^2}{P_1|H_{s,r_n}(k)|^2+N_0}+1\right)N_0$. The probability density function of $z_{r_n,d}(k)$ given the channel state information (CSI) is given by

$$p(z_{r_n,d}(k)/\text{CSI}) = \frac{1}{\pi\delta_z^2(k)}\exp\left(-\frac{1}{\delta_z^2(k)}|z_{r_n,d}(k)|^2\right). \tag{3.68}$$

The receiver applies a *Maximum Likelihood* (ML) detector to the received signal, which is given as

$$\widehat{\mathbf{s}} = \arg\min_{\mathbf{s}} \sum_{k=1}^{K} \frac{1}{\delta_z^2(k)} \left| \mathbf{y}(k) - \frac{\sqrt{P_1 P_2} H_{s,r_n}(k) H_{r_n,d}(k)}{\sqrt{P_1 |H_{s,r_n}(k)|^2 + N_0}} \mathbf{s}(k) \right|^2 , \tag{3.69}$$

where the n index (which is the index of the relay node) is adjusted according to the k index (which is the index of the subcarrier).

Now, sufficient conditions for the proposed code structure to achieve full diversity are derived. The pdf of a received vector $\mathbf{y} = [y(1), y(2), \cdots, y(K)]^T$ given that the codeword $\mathbf{s}$ was transmitted is given by

$$p(\mathbf{y}/\mathbf{s}, \text{CSI}) = \left(\prod_{k=1}^{K} \frac{1}{\pi \delta_z^2(k)} \right) \exp \left(\sum_{k=1}^{K} -\frac{1}{\delta_z^2(k)} \left| y(k) - \frac{\sqrt{P_1 P_2} H_{s,r_n}(k) H_{r_n,d}(k)}{\sqrt{P_1 |H_{s,r_n}(k)|^2 + N_0}} \mathbf{s}(k) \right|^2 \right). \tag{3.70}$$

The PEP of mistaking $\mathbf{s}$ by $\widetilde{\mathbf{s}}$ can be upper-bounded as [23]

$$PEP(\mathbf{s} \to \widetilde{\mathbf{s}}) \leq E \left\{ \exp \left(\lambda [\ln p(\mathbf{y}/\widetilde{\mathbf{s}}) - \ln p(\mathbf{y}/\mathbf{s})] \right) \right\}, \tag{3.71}$$

and the relation applies for any λ, which can selected to get the tightest bound. Any two distinct codewords $\mathbf{s}$ and $\widetilde{\mathbf{s}} = [\widetilde{\mathbf{B}}_1, \widetilde{\mathbf{B}}_2, \cdots, \widetilde{\mathbf{B}}_p]^T$ will have at least one index p_0 such that $\widetilde{\mathbf{B}}_{p_0} \neq \mathbf{B}_{p_0}$. We will assume that $\mathbf{s}$ and $\widetilde{\mathbf{s}}$ will have only one index p_0 such that $\widetilde{\mathbf{B}}_{p_0} \neq \mathbf{B}_{p_0}$, which corresponds to the worst case PEP.

Averaging the PEP expression in (3.71) over the noise distribution given in

(3.68) we get

$$PEP(\mathbf{s}\rightarrow\widetilde{\mathbf{s}}) \leq E\Bigg\{ \exp\Bigg(-\lambda(1-\lambda)\sum_{n=1}^{N}\sum_{l=1}^{L} \Bigg(\frac{P_1|H_{s,r_n}(J+(n-1)L+l)|^2 P_2|H_{r_n,d}(J+(n-1)L+l)|^2}{\Big(P_1|H_{s,r_n}(J+(n-1)L+l)|^2+P_2|H_{r_n,d}(J+(n-1)L+l)|^2+N_0\Big)N_0} \Bigg) \times \Big|\mathbf{B}_{p_0}((n-1)L+l)-\widetilde{\mathbf{B}}_{p_0}((n-1)L+l)\Big|^2 \Bigg)\Bigg\}, \tag{3.72}$$

where $J=(p_0-1)NL$. Take $\lambda=1/2$ to minimize the upper-bound in (3.72), hence, we get

$$PEP(\mathbf{s}\rightarrow\widetilde{\mathbf{s}}) \leq E\Bigg\{ \exp\Bigg(-\frac{1}{4}\sum_{n=1}^{N}\sum_{l=1}^{L} \Bigg(\frac{P_1|H_{s,r_n}(J+(n-1)L+l)|^2 P_2|H_{r_n,d}(J+(n-1)L+l)|^2}{\Big(P_1|H_{s,r_n}(J+(n-1)L+l)|^2+P_2|H_{r_n,d}(J+(n-1)L+l)|^2+N_0\Big)N_0} \Bigg) \times \Big|\mathbf{B}_{p_0}((n-1)L+l)-\widetilde{\mathbf{B}}_{p_0}((n-1)L+l)\Big|^2 \Bigg)\Bigg\}, \tag{3.73}$$

At high SNR, the term $\frac{P_1|H_{s,r_n}(k)|^2 P_2|H_{r_n,d}(k)|^2}{\big(P_1|H_{s,r_n}(k)|^2+P_2|H_{r_n,d}(k)|^2+N_0\big)N_0}$ can be approximated by $\frac{P_1|H_{s,r_n}(k)|^2 P_2|H_{r_n,d}(k)|^2}{\big(P_1|H_{s,r_n}(k)|^2+P_2|H_{r_n,d}(k)|^2\big)N_0}$ [21], which is the scaled harmonic mean of the source-relay and relay-destination SNRs on the k-th subcarrier[9]. The scaled harmonic

[9]The scaling factor is 1/2 since the harmonic mean of two number, X_1 and X_2, is defined as

mean of two nonnegative numbers, a_1 and a_2, can be upper- and lower- bounded as

$$\frac{1}{2}\min(a_1, a_2) \leq \frac{a_1 a_2}{a_1 + a_2} \leq \min(a_1, a_2). \tag{3.74}$$

Using the lower-bound in (3.74) the PEP in (3.73) can be further upper-bounded as

$$PEP(\mathbf{s} \to \widetilde{\mathbf{s}}) \leq E\Bigg\{ \exp\Bigg(-\frac{1}{8}\sum_{n=1}^{N}\sum_{l=1}^{L} \min\Bigg(\frac{P_1}{N_0}|H_{s,r_n}((p_0-1)NL + (n-1)L + l)|^2, \\ \frac{P_2}{N_0}|H_{r_n,d}((p_0-1)NL + (n-1)L + l)|^2 \Bigg) \Big|\mathbf{B}_{p_0}((n-1)L+l) - \widetilde{\mathbf{B}}_{p_0}((n-1)L+l)\Big|^2 \Bigg) \Bigg\}. \tag{3.75}$$

If $P_2 = P_1$ and SNR is defined as P_1/N_0, then the PEP is now upper-bounded as

$$PEP(\mathbf{s} \to \widetilde{\mathbf{s}}) \leq E\Bigg\{ \exp\Bigg(-\frac{1}{8}\sum_{n=1}^{N}\sum_{l=1}^{L} \min\Bigg(SNR|H_{s,r_n}((p_0-1)NL + (n-1)L + l)|^2, \\ SNR|H_{r_n,d}((p_0-1)NL + (n-1)L + l)|^2 \Bigg) \Big|\mathbf{B}_{p_0}((n-1)L+l) - \widetilde{\mathbf{B}}_{p_0}((n-1)L+l)\Big|^2 \Bigg) \Bigg\}. \tag{3.76}$$

$\frac{2X_1X_2}{X_1+X_2}$.

PEP Analysis for L=1

The case of L equal to 1 corresponds to a flat, frequency nonselective fading channel. The PEP in (3.76) is now given by

$$PEP(\mathbf{s} \to \widetilde{\mathbf{s}}) \leq E\Bigg\{ \exp\Bigg(-\frac{1}{8}\sum_{n=1}^{N} \min\Bigg(SNR|H_{s,r_n}((p_0-1)NL+(n-1)L+1)|^2, \\ SNR|H_{r_n,d}((p_0-1)NL+(n-1)L+1)|^2 \Bigg) \Big|\mathbf{B}_{p_0}((n-1)L+1) - \widetilde{\mathbf{B}}_{p_0}((n-1)L+1)\Big|^2 \Bigg) \Bigg\}. \tag{3.77}$$

It can be shown that the random variables $SNR|H_{s,r_n}(k)|^2$ and $SNR|H_{r_n,d}(k)|^2$ follow an exponential distribution with rate $1/SNR$ for all k. The minimum of two exponential random variables is an exponential random variable with rate that is the sum of the two random variables rates. Hence, $\min\left(SNR|H_{s,r_n}(k)|^2, SNR|H_{r_n,d}(k)|^2\right)$ follows an exponential distribution with rate $2/SNR$.

The PEP upper-bound is now given by

$$PEP(\mathbf{s} \to \widetilde{\mathbf{s}}) \leq \prod_{n=1}^{N} \frac{1}{1+\frac{1}{16}SNR\Big|\mathbf{B}_{p_0}((n-1)L+1) - \widetilde{\mathbf{B}}_{p_0}((n-1)L+1)\Big|^2}. \tag{3.78}$$

At high SNR, we neglect the 1 term in the denominator of (3.78). Hence, the PEP can now be upper-bounded as

$$PEP(\mathbf{s} \to \widetilde{\mathbf{s}}) \lesssim \left(\frac{1}{16}SNR\right)^{-N} \left(\prod_{n=1}^{N} \Big|\mathbf{B}_{p_0}((n-1)L+1) - \widetilde{\mathbf{B}}_{p_0}((n-1)L+1)\Big|^2\right)^{-1}. \tag{3.79}$$

The result in (3.79) is under the assumption that the product

$$\prod_{n=1}^{N} \Big|\mathbf{B}_{p_0}((n-1)L+1) - \widetilde{\mathbf{B}}_{p_0}((n-1)L+1)\Big|^2$$

is non-zero. Clearly, if that product is non-zero, then the system will achieve a diversity of order NL, where L is equal to 1 in this case. From the expression in (3.79) the coding gain of the space-frequency code is maximized when the product $\min_{\mathbf{s}\neq\widetilde{\mathbf{s}}} \prod_{n=1}^{N} \left|\mathbf{B}_{p_0}((n-1)L+1) - \widetilde{\mathbf{B}}_{p_0}((n-1)L+1)\right|^2$ is maximized. This product is known as the minimum product distance [46].

PEP Analysis for L=2

The PEP in (3.76) can now be given as

$$PEP(\mathbf{s}\rightarrow\widetilde{\mathbf{s}}) \leq E\Bigg\{ \exp\Bigg(-\frac{1}{8}\sum_{n=1}^{N}\sum_{l=1}^{2} \min\Bigg(SNR|H_{s,r_n}((p_0-1)NL+(n-1)L+l)|^2, \\ SNR|H_{r_n,d}((p_0-1)NL+(n-1)L+l)|^2 \Bigg) \left|\mathbf{B}_{p_0}((n-1)L+l) - \widetilde{\mathbf{B}}_{p_0}((n-1)L+l)\right|^2 \Bigg) \Bigg\}, \tag{3.80}$$

where $L=2$. The analysis in this case is more involved since the random variables appearing in (3.80) are correlated. Signals transmitted from the same relay node on different subcarriers will experience correlated channel attenuations. As a first step in deriving the code design criterion, we prove that the channel attenuations, $|H_{s,r_n}(k_1)|^2$ and $|H_{s,r_n}(k_2)|^2$ for any $k_1 \neq k_2$, have a bivariate Gamma distribution as their joint pdf [50]. The same applies for $|H_{r_n,d}(k_1)|^2$ and $|H_{r_n,d}(k_2)|^2$ for any $k_1 \neq k_2$. The proof of this result is given in the Appendix.

To evaluate the expectation in (3.80) we need the expression for the joint pdf of the two random variables $M_1 = \min\left(SNR|H_{s,r_n}(k_1)|^2, SNR|H_{r_n,d}(k_1)|^2\right)$ and $M_2 = \min\left(SNR|H_{s,r_n}(k_2)|^2, SNR|H_{r_n,d}(k_2)|^2\right)$ for some $k_1 \neq k_2$. Although M_1 and M_2 can be easily seen to be marginally exponential random variables, they are not

jointly Gamma distributed. Define the random variables $X_1 = SNR|H_{s,r_n}(k_1)|^2$, $X_2 = SNR|H_{s,r_n}(k_2)|^2$, $Y_1 = SNR|H_{r_n,d}(k_1)|^2$, and $Y_2 = SNR|H_{r_n,d}(k_2)|^2$. All of these random variables are marginally exponential with rate $1/SNR$. Under the assumptions of our channel model, the pairs (X_1, X_2) and (Y_1, Y_2) are independent. Hence, the joint pdf of (X_1, X_2, Y_1, Y_2), using the result in the Appendix, is given by

$$\begin{aligned}
&f_{X_1,X_2,Y_1,Y_2}(x_1, x_2, y_1, y_2) \\
=&f_{X_1,X_2}(x_1, x_2) f_{Y_1,Y_2}(y_1, y_2) \\
=&\frac{1}{SNR^2(1-\rho_{x_1x_2})(1-\rho_{y_1y_2})} \exp\left(-\frac{x_1+x_2}{SNR(1-\rho_{x_1x_2})}\right) I_0\left(\frac{2\sqrt{\rho_{x_1x_2}}}{SNR(1-\rho_{x_1x_2})}\sqrt{x_1x_2}\right) \\
&\times \exp\left(-\frac{y_1+y_2}{SNR(1-\rho_{y_1y_2})}\right) I_0\left(\frac{2\sqrt{\rho_{y_1y_2}}}{SNR(1-\rho_{y_1y_2})}\sqrt{y_1y_2}\right) U(x_1)U(x_2)U(y_1)U(y_2),
\end{aligned} \tag{3.81}$$

where $I_0(\cdot)$ is the modified Bessel function of the first kind of order zero and $U(\cdot)$ is the Heaviside unit step function [41]. $\rho_{x_1x_2}$ is the correlation coefficient between X_1 and X_2 and similarly, $\rho_{y_1y_2}$ is the correlation coefficient between Y_1 and Y_2. The joint cumulative distribution function (cdf) of the pair (M_1, M_2) can be computed as

$$\begin{aligned}
&F_{M_1,M_2}(m_1, m_2) \\
&\quad \triangleq \Pr\left[M_1 \le m_1, M_2 \le m_2\right] \\
&\quad = \Pr\left[\min\left(X_1, Y_1\right) \le m_1, \min\left(X_2, Y_2\right) \le m_2\right] \\
&\quad = 2\int_{y_1=0}^{m_1}\int_{x_1=y_1}^{\infty}\int_{y_2=0}^{m_2}\int_{x_2=y_2}^{\infty} f_{X_1,X_2}(x_1, x_2) f_{Y_1,Y_2}(y_1, y_2) dy_1 dx_1 dy_2 dx_2 \\
&\quad + 2\int_{y_1=0}^{m_1}\int_{x_1=y_1}^{\infty}\int_{x_2=0}^{m_2}\int_{y_2=x_2}^{\infty} f_{X_1,X_2}(x_1, x_2) f_{Y_1,Y_2}(y_1, y_2) dy_1 dx_1 dx_2 dy_2,
\end{aligned} \tag{3.82}$$

where we have used the symmetry assumption of the source-relay and relay-

destination channels. The joint pdf of (M_1, M_2) can now be given as

$$\begin{aligned} f_{M_1,M_2}(m_1,m_2) =& \frac{\partial^2}{\partial m_1 \partial m_2} F_{M_1,M_2}(m_1,m_2) \\ =& 2 f_{Y_1,Y_2}(m_1,m_2) \int_{x_1=m_1}^{\infty} \int_{x_2=m_2}^{\infty} f_{X_1,X_2}(x_1,x_2) dx_1 dx_2 \\ &+ 2 \int_{x_1=m_1}^{\infty} \int_{y_2=m_2}^{\infty} f_{X_1,X_2}(x_1,m_2) f_{Y_1,Y_2}(m_1,y_2) dx_1 dx_2. \end{aligned} \tag{3.83}$$

To get the PEP upper-bound in (3.80) we need to calculate the expectation

$$\begin{aligned} & E\left\{ \exp\left(-\frac{1}{8}\left(M_1 \left| \mathbf{B}(k_1) - \widetilde{\mathbf{B}}(k_1) \right|^2 + M_2 \left| \mathbf{B}(k_2) - \widetilde{\mathbf{B}}(k_2) \right|^2 \right) \right) \right\} \\ &= \int_{m_1=0}^{\infty} \int_{m_2=0}^{\infty} \exp\left(-\frac{1}{8}\left(m_1 \left| \mathbf{B}(k_1) - \widetilde{\mathbf{B}}(k_1) \right|^2 + m_2 \left| \mathbf{B}(k_2) - \widetilde{\mathbf{B}}(k_2) \right|^2 \right) \right) \\ & \quad f_{M_1,M_2}(m_1,m_2) dm_1 dm_2. \end{aligned} \tag{3.84}$$

At high enough SNR $I_0\left(\frac{2\sqrt{\rho_{x_1x_2}}}{SNR(1-\rho_{x_1x_2})} \sqrt{x_1 x_2} \right)$ can be approximated to be 1 [41]. Using this approximation, the PEP upper-bound can be approximated at high SNR as

$$PEP(\mathbf{s} \to \widetilde{\mathbf{s}}) \lesssim \left(\prod_{m=1}^{2N} \left| \mathbf{B}_{p_0}(m) - \widetilde{\mathbf{B}}_{p_0}(m) \right|^2 \right)^{-1} \left(\frac{1}{16}(1-\rho) SNR \right)^{-2N}, \tag{3.85}$$

where $\rho = \rho_{x_1x_2} = \rho_{y_1y_2}$. Again, full diversity is achieved when the product $\prod_{m=1}^{2N} \left| \mathbf{B}_{p_0}(m) - \widetilde{\mathbf{B}}_{p_0}(m) \right|^2$ is non-zero. The coding gain of the space-frequency code is maximized when the product $\min_{\mathbf{s} \neq \widetilde{\mathbf{s}}} \prod_{m=1}^{2N} \left| \mathbf{B}_{p_0}(m) - \widetilde{\mathbf{B}}_{p_0}(m) \right|^2$ is maximized.

The analysis becomes highly involved for any $L \geq 3$. It is very difficult to get closed-form expressions in this case due to the correlation among the summed terms in (3.76) for which no closed-form pdf expressions, similar to (3.81), are known [51].

3.2.3 Code Construction and Discussions

A construction method for the proposed DSFCs is presented here. This construction is the one used to do the source node and relay nodes coding for DSFCs with the DAF protocol. It is also used for designing DSFCs with the AAF protocol.

A linear mapping is used to form the transmitted subblocks, $\mathbf{D} = \mathbf{V}_{T\times T}\mathbf{s_G}$, where $\mathbf{s_G}$ is a $T \times 1$ source symbols vector transmitted in the subblock $\mathbf{D}$. $\mathbf{s_G}$ is carved from QAM or PSK constellations. We will use the transforms presented in Section 3.1.3 to design DDSTCs.

It noteworthy that the proposed DSFCs for both the DAF and AAF protocols achieve a data rate of $K/2$ symbols/OFDM block, where K is the number of subcarriers. The 1/2 factor loss is due to the two-phase nature of the DAF and AAF protocols.

3.2.4 Remarks

Here we summarize some remarks related to our proposed DSFCs

- *Remark 1*: In our problem formulation, we have considered a two-hop system model that lacks a direct link from the source node to the destination node. If such a direct link between the source node and the destination node exists, then the destination node can use its received signal from the source node to help recovering the source symbols. Assuming that the channel from the source node to the destination node has L paths, it can be shown that our proposed DSFCs, with the proposed coding at the source node and the relay nodes for both the DAF and AAF protocols, achieve a diversity of order $(N + 1)L$.

- *Remark 2*: The proposed DSFCs with the DAF protocol can be easily modified to achieve full diversity for the asymmetric case where the number of paths per fading channel is not the same for all channels. Let L_{s,r_n} denote the number of paths of the channel between the source node and n-th relay and $L_{r_n,d}$ denote the number of paths of the channel between the n-th relay node and the destination node. The proposed DSFC can be easily modified to achieve a diversity d of order

$$d = \sum_{n=1}^{N} \min(L_{s,r_n},\ L_{r_n,d}),$$

which can be easily shown to be the maximal achievable diversity order. This maximal diversity order can be achieved, for example, by designing the codes at the source node and relay nodes using $L = \max_n\ \min(L_{s,r_n},\ L_{r_n,d})$.

- *Remark 3*: The proposed construction for the design of DSFCs can be easily generalized to the case of multi-antenna nodes, where any node may have more than one antenna. Each antenna can be treated as a separate relay node and the analysis presented before directly applies.

- *Remark 4*: As mentioned before, the presence of the cyclic prefix in the OFDM transmission provides a mean for combating the relays synchronization mismatches. Hence, our proposed DSFCs, which are based on OFDM transmission, are robust against synchronization mismatches within the duration of the cyclic prefix.

3.2.5 Simulation Results for DSFCs

In this section, some simulation results for the proposed DSFCs are presented. We will compare the performance of DSFCs with the DAF protocol to DSFCs with the

AAF protocol. In all simulations, the source is assumed to have two relay nodes helping to forward its information. We use the two-hop channel model presented in the previous sections.

Fig. 3.9 shows the case of a simple two-ray, $L = 2$, channel model with a delay of $\tau = 5\mu sec$ between the two rays. The two rays have equal powers, i.e., $\sigma^2(1) = \sigma^2(2)$. The number of subcarriers is $K = 128$ with a system bandwidth of 1 MHz. We use BPSK modulation and Vandermonde based linear transformations. Fig. 3.9 shows the SER of the proposed DSFCs versus the SNR defined as $SNR = \frac{P_1+P_2}{N_0}$, and we use $P_1 = P_2$, i.e., equal power allocation between the source and relay nodes. We simulated three cases: all channel variances are ones, relays close to source, and relays close to destination. For the case of relays close to source, the variance of any source-relay channel is taken to be 10 and the variance of any relay-destination channel is taken to be 1. For the case of relays close to destination, the variance of any source-relay channel is taken to be 1 and the variance of any relay-destination channel is taken to be 10. From Fig. 3.9, it is clear that DSFCs with the DAF protocol have a better performance than DSFCs with the AAF protocol. The reason is that DSFCs with DAF protocol deliver a less noisy code to the destination node as compared to DSFCs with AAF protocol, where noise propagation results from the transmissions of the relay nodes. Decoding at the relay nodes, in the DAF protocol, has the effect of removing the noise before retransmission to the destination node. As can be seen from Fig. 3.9, a gain of about 3dB is achieved, for the case of relays close to the source, by employing DSFCs with the DAF protocol as compared to DSFCs with the AAF protocol.

Fig. 3.10 shows the case of a simple two-ray, $L = 2$, with a delay of $\tau = 20\mu sec$ between the two rays. The simulation setup is the same as that used in Fig.

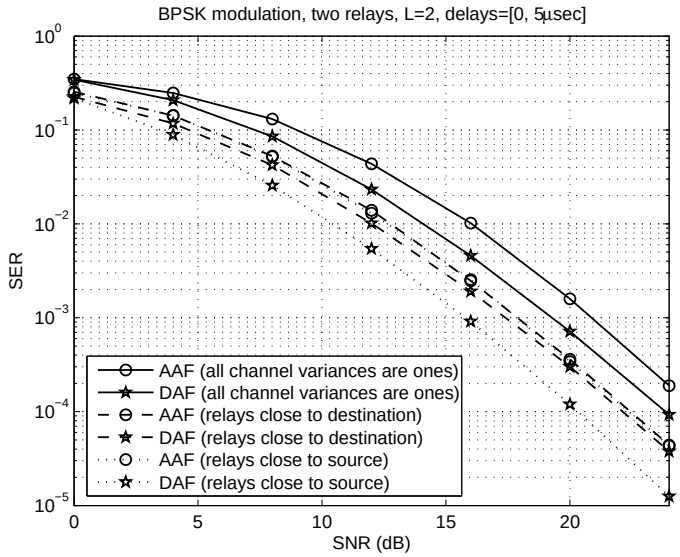

Figure 3.9: SER for DSFCs for BPSK modulation, L=2, and delay=[0, 5μsec] versus SNR.

3.9. From Fig. 3.10, it is clear that DSFCs with the DAF protocol have a better performance than DSFCs with the AAF protocol. Fig. 3.11 shows the case of $L = 4$ with a path delay vector given by $[0, 5\mu sec, 10\mu sec, 15\mu sec]$. The rays are assumed to be of equal powers, i.e., $\sigma^2(l) = \sigma^2,\ l = 1, \cdots, 4$. The number of subcarriers is $K = 128$ with a system bandwidth of 1 MHz. We use BPSK modulation and Vandermonde based linear transformations. Fig. 3.11 shows the SER of the proposed DSFCs versus the SNR defined as $SNR = \frac{P_1+P_2}{N_0}$ and again we use $P_1 = P_2$. We have simulated the same three cases as in Fig. 3.9. Fig. 3.11 shows that DSFCs with the DAF protocol have a better performance than DSFCs with the AAF protocol. We can observe a gain of about 2dB for the case of relays close to source.

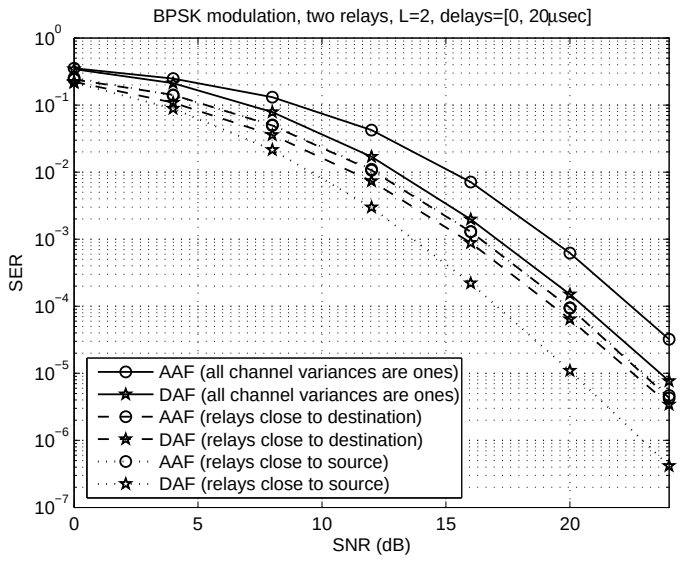

Figure 3.10: SER for DSFCs for BPSK modulation, L=2, and delay=[0, 20μsec] versus SNR.

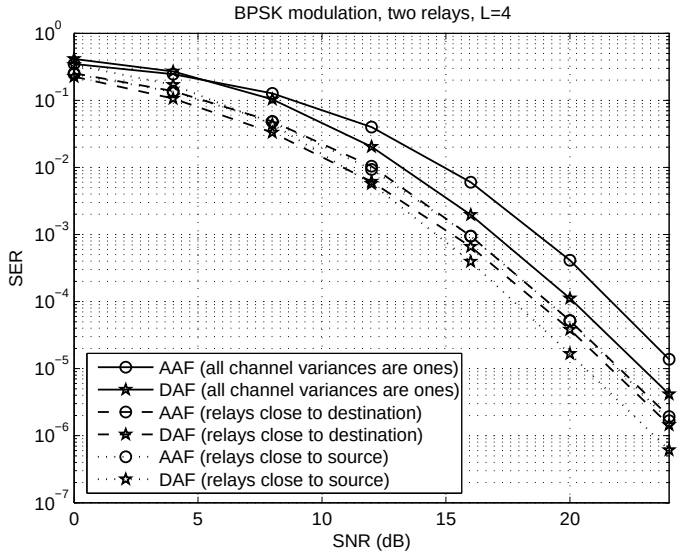

Figure 3.11: SER for DSFCs for BPSK modulation, L=4, and delay=[0, 5μsec, 10μsec, 15μsec] versus SNR.

Appendix

Consider the two random variables $H_{s,r_n}(k_1)$ and $H_{s,r_n}(k_2)$, we will assume without loss of generality that $\tau_1 = 0$, i.e., the delay of the first path is zero. $H_{s,r_n}(k_1)$ is given by

$$H_{s,r_n}(k_1) = \alpha_{s,r_n}(1) + \alpha_{s,r_n}(2)e^{-j2\pi(k_1-1)\Delta f\tau_2} = \Re\left(H_{s,r_n}(k_1)\right) + j\Im\left(H_{s,r_n}(k_1)\right), \tag{3.86}$$

where $\Re(x)$, and $\Im(x)$ are the real, and imaginary parts of x, respectively. From (3.86) we have

$$\begin{aligned}
&\Re\left(H_{s,r_n}(k_1)\right) \\
&\quad = \Re(\alpha_{s,r_n}(1)) + \Re(\alpha_{s,r_n}(2))\cos(2\pi(k_1-1)\Delta f\tau_2) + \Im(\alpha_{s,r_n}(2))\sin(2\pi(k_1-1)\Delta f\tau_2) \\
&\Im\left(H_{s,r_n}(k_1)\right) \\
&\quad = \Im(\alpha_{s,r_n}(1)) + \Im(\alpha_{s,r_n}(2))\cos(2\pi(k_1-1)\Delta f\tau_2) - \Re(\alpha_{s,r_n}(2))\sin(2\pi(k_1-1)\Delta f\tau_2).
\end{aligned} \tag{3.87}$$

Based on the channel model presented in Section 3.2.1 both $\Re\left(H_{s,r_n}(k_1)\right)$ and $\Im\left(H_{s,r_n}(k_1)\right)$ are zero-mean Gaussian random variables with variance 1/2. The correlation coefficient, ρ_{ri}, between $\Re\left(H_{s,r_n}(k_1)\right)$ and $\Im\left(H_{s,r_n}(k_1)\right)$ can be calculated as

$$\rho_{ri} = E\left\{\Re\left(H_{s,r_n}(k_1)\right)\Im\left(H_{s,r_n}(k_1)\right)\right\} = 0. \tag{3.88}$$

Hence, $H_{s,r_n}(k_1)$ is a circularly symmetric complex Gaussian random variable with variance 1/2 per dimension and the same applies for $H_{s,r_n}(k_2)$. To get the joint probability distribution of $|H_{s,r_n}(k_1)|^2$ and $|H_{s,r_n}(k_2)|^2$, we can use the standard techniques of transformation of random variables. Using transformation of random variables and the fact that both $H_{s,r_n}(k_1)$ and $H_{s,r_n}(k_2)$ are circularly symmetric

complex Gaussian random variables, it can be shown that $X_1 = |H_{s,r_n}(k_1)|^2$ and $X_2 = |H_{s,r_n}(k_2)|^2$ are jointly distributed according to a bivariate Gamma distribution with pdf [51], [50]

$$f_{X_1,X_2}(x_1,x_2) = \frac{1}{1-\rho_{x_1x_2}} \exp\left(-\frac{x_1+x_2}{1-\rho_{x_1x_2}}\right) I_0\left(\frac{2\sqrt{\rho_{x_1x_2}}}{1-\rho_{x_1x_2}}\sqrt{x_1x_2}\right) U(x_1)U(x_2), \tag{3.89}$$

where $I_0(\cdot)$ is the modified Bessel function of the first kind of order zero and $U(\cdot)$ is the Heaviside unit step function [41]. $\rho_{x_1x_2}$ is the correlation between $|H_{s,r_n}(k_1)|^2$ and $|H_{s,r_n}(k_2)|^2$ and it can calculated as

$$\rho_{x_1,x_2} = \frac{\mathrm{Cov}\left(X_1,X_2\right)}{\sqrt{\mathrm{Var}\left(X_1\right)\mathrm{Var}\left(X_2\right)}}. \tag{3.90}$$

Following tedious computations, it can be shown that

$$\rho_{x_1,x_2} = \frac{1}{2} + 2\sigma^2(1)\sigma^2(2)\cos(2\pi(k_2-k_1)\Delta f\tau_2), \tag{3.91}$$

where the last equation applies under the assumption of having $\sigma^2(1)+\sigma^2(2)=1$ and both, $\sigma^2(1)$ and $\sigma^2(2)$, are non-zeros. From (3.91) it is clear that $0 \leq \rho_{x_1,x_2} \leq 1$.

Chapter 4

Source-Channel Diversity for Multi-Hop and Relay Channels

Diversity is not exclusive to implementations at the physical layer. As studied in [52], diversity can also be formed when multiple channels are provided to the application layer, where they are exploited through multiple description source encoders. In *Multiple Description Coding* different descriptions of the source are generated with the property that they can each be individually decoded or, if possible, be jointly decoded to obtain a reconstruction of the source with lower distortion [53]. The achievable rate-distortion performance of multiple description codes was studied in [54]. Aiming at its application in communication systems, multiple description coding had been studied for error resilient source coding applications [55], for communications over networks with packet losses [56], for communications over parallel packet loss channels [57, 58] and as an alternative error control scheme for communication over single physical channel in [59].

Considering the combination of source coding and user cooperation, [60] studied the performance in terms of distortion exponent of a single description source

encoder transmitted with and without amplify-and-forward cooperation over a single-relay channel. Also, [60] presented a scheme, named "partial cooperation", which was based on a two-layer, single description source encoder. Studies on the transmission of layered source-coded sources over user-cooperation channels were presented in [61] for coded cooperation and in [62] for amplify-and-forward and a broadcast relaying strategy using broadcast code.

We focus on studying systems that exhibit diversity of three forms: source coding diversity (when using a dual description encoder), channel coding diversity, and user-cooperation diversity (implemented through either relay channels or multi-hop channels, each with amplify-and-forward or decode-and-forward user cooperation). The presented analysis derives the distortion exponent for several source-channel diversity achieving schemes. More specifically, we consider the cases where we have a single or M relays helping the source by *repeating* its information either using the amplify-and-forward or the decode-and-forward protocols. In these cases, we analyze the tradeoff between the diversity gain (number of relays) to the quality of the source encoder and find the optimum number of relays to help the source. Then, we consider source coding diversity and channel coding diversity. For multi-hop channels we find that channel coding diversity yields the best performance of all schemes, followed by source coding diversity. Furthermore, we also show that as the bandwidth expansion factor increases, the distortion exponent is improved by increasing the number of relays because user cooperation diversity becomes the dominating factor rather than the quality of the source encoder [63–65].

4.1 System Model

We will focus on systems that communicate a source signal over a wireless multi-hop or relay channel. Let the input to the system be a memoryless source. We will assume that communication is performed over a complex additive white Gaussian noise (AWGN) fading channel. Denoting by I the maximum average mutual information between the channel input and output. For the single-input single-output fading channel $I = \log(1 + |h|^2 SNR)$, where h is the fading value [24]. Because of the random nature of the fading, I and the ability of the channel to support transmission at some rate are themselves random. The probability of the channel not being able to support a rate R is called the *outage probability* and is given by $P_0 = \Pr[I < R]$. It will be convenient for us to work with the random function e^I, which has a cumulative distribution function (cdf) F_{e^I} that can be approximated at high SNR as [52]

$$F_{e^I}(t) \approx c \left(\frac{t}{SNR} \right)^p . \tag{4.1}$$

Both c and p are model-dependant parameters. For example, for the case of Rayleigh fading we have $p = 1$ and c depends on the channel variance[1].

We consider a communication system consisting of a source, a source encoder and a channel encoder. Let the input to the system be a memoryless source. The source samples are fed into the source encoder for quantization and compression. The output of the source encoder are fed into a channel encoder which outputs N channel inputs. For K source samples and N channel inputs, we denote by $\beta \triangleq N/K$, the bandwidth expansion factor or processing gain. We assume that K

[1]The value of the parameter c does not affect the analysis since we are interested in the distortion exponent which measures the exponent for the end-to-end distortion at high SNRs.

is large enough to average over the statistics of the source but N is not sufficiently large to average over the statistics of the channel, i.e., we assume block fading wireless channel. Here, we are specifically interested in systems where the source signal average end-to-end distortion is the figure of merit. Thus, performance will be measured in terms of the expected distortion $E[D] = E[d(\mathbf{s}, \widehat{\mathbf{s}})]$, where $d(\mathbf{s}, \widehat{\mathbf{s}}) = (1/K)\sum_{k=1}^{K} d(s_k, \widehat{s}_k)$ is the average distortion between a sequence $\mathbf{s}$ of K source samples and its corresponding reconstruction $\widehat{\mathbf{s}}$ and $d(s_k, \widehat{s}_k)$ is the distortion between a single sample s_k and its reconstruction $\widehat{s}_k$. We will assume $d(s_k, \widehat{s}_k)$ to be the mean-squared distortion measure.

Following the fading channels assumption, we will be interested in studying the system behavior at large channel signal-to-noise ratios (SNRs) where system performances can be compared in terms of the rate of decay of the end-to-end distortion. This figure of merit called the *distortion exponent*, [52], is defined as

$$\Delta \triangleq -\lim_{SNR\to\infty} \frac{\log E[D]}{\log SNR}. \tag{4.2}$$

We will consider two types of source encoders: a *single description* (SD) and a *dual description* source encoder, i.e. the source encoder generates either one or two coded descriptions of the source.

The performance of source encoders can be measured through its achievable rate-distortion (R-D) function, which characterizes the tradeoff between source encoding rate and distortion. The R-D function for SD source encoders is frequently considered to be of the form $R = (1/c_2)\log(c_1/D)$, where we are taking the logarithm with base e and hence, R, the source encoding rate, is measured in nats per channel use. This form of R-D function can approximate or bound a wide range of practical systems such as video coding with an MPEG codec [66], speech using a CELP-type codec [67], or when the high rate approximation holds [52].

Assuming that high resolution approximation can be applied to the source encoding operation, each of the input samples can be modeled as a memoryless Gaussian source, showing a zero-mean, unit-variance Gaussian distribution. In this case, the R-D function can be approximated without loss of generality, as [24],

$$R = \frac{1}{2\beta} \log \left(\frac{1}{D} \right). \tag{4.3}$$

For multiple description (MD) source encoders, the R-D region is only known for the dual description source encoders [54]. In dual description encoders, source samples are encoded into two descriptions. Each description can either be decoded independently of the other, when the other is unusable at the receiver, or combined to achieve a reconstruction of the source with lower distortion, when both descriptions are received correctly. This fact is reflected in the corresponding R-D function. Let R_1 and R_2 be the source encoding rates of descriptions 1 and 2, respectively, and $R_{md} = R_1 + R_2$. Let D_1 and D_2 be the reconstructed distortions associated with descriptions 1 and 2, respectively, when each is decoded alone. Let D_0 be the source distortion when both description are combined and jointly decoded. For the same source model and assumptions as in the single description case, R_1 and D_1, and R_2 and D_2 are related through,

$$\begin{aligned} R_1 &= \frac{1}{2\beta} \log \left(\frac{1}{D_1} \right), \\ R_2 &= \frac{1}{2\beta} \log \left(\frac{1}{D_2} \right). \end{aligned} \tag{4.4}$$

The R-D function when both descriptions can be combined at the source decoder differs depending on whether distortions can be considered low or high [54]. The

low distortion scenario corresponds to $D_1 + D_2 - D_0 < 1$, in which case we have

$$R_{md} = \frac{1}{2\beta}\log\left(\frac{1}{D_0}\right) + \frac{1}{2\beta}\log\left(\frac{(1-D_0)^2}{(1-D_0)^2 - \left[\sqrt{(1-D_1)(1-D_2)} - \sqrt{(D_1-D_0)(D_2-D_0)}\right]^2}\right). \tag{4.5}$$

All the schemes we will consider in this Chapter present the same communication conditions to each description. Therefore, it will be reasonable to assume $R_1 = R_2 = R_{md}/2$. Under this condition, it was shown in [52] that the following bounds can be derived from (4.5)

$$(4D_0D_1)^{-1/(2\beta)} \lessapprox e^{R_{md}} \lessapprox (2D_0D_1)^{-1/(2\beta)}, \tag{4.6}$$

where the lower-bound requires $D_0 \to 0$ and the upper-bound requires also $D_1 \to 0$.

In the case of the high distortion scenario, $D_1 + D_2 - D_0 > 1$, the R-D function equals

$$R_{md} = \frac{1}{2\beta}\log\left(\frac{1}{D_0}\right). \tag{4.7}$$

The channel-encoded message is then sent from the source node to a destination node with or without user cooperation. In a setup with user cooperation, the relay nodes are associated with the source node to achieve user-cooperation diversity. Communication in a cooperative setup with one relay node takes place in two phases. In phase 1, the source node sends information to its destination node. The source node's transmission can be overheard by the relay because of the broadcast nature of wireless communications. In phase 2, the relay node cooperates by forwarding to the destination the information received from its associated source node. At the destination node, both signals received from the source and the relay

are combined and detected, thus creating a virtual spatial diversity setup. For each additional relay used during transmission, a new phase, similar to phase 2, needs to be added to allow transmission of the new relay. Because of this multi-phase transmission, we need for fair comparison of the different schemes considered in this Chapter to fix the total number of channel uses for a source block of size K and change the bandwidth expansion factor accordingly to each scheme, as will be seen in the sequel. We will consider two techniques that implement user cooperation, amplify-and-forward and decode-and-forward, each differing in the processing done at the relay.

4.2 Multi-Hop Channels

In this section, we consider the distortion exponents of multi-hop networks using amplify-and-forward and decode-and-forward user-cooperation protocols. The multi-hop channel is a channel where there is no direct path between the source and destination; i.e. the information path between source and destination contains one or more relaying nodes. Without loss of generality we consider the two-hop case. The analysis can be easily extended to scenarios with larger number of hops.

4.2.1 Multi-Hop Amplify-and-Forward Protocol

In this section, we will consider the analysis for multi-hop amplify-and-forward schemes with different channel and source coding diversity achieving schemes. We derive the distortion exponent for the two-hop single relay channel with a SD source encoder and extend the result to the case of M relays with repetition channel coding diversity. The result shows a tradeoff between the number of relays (user

cooperation diversity) and the quality of the source encoder. We also derive the distortion exponent when using the multiple description coding. Since we consider the case of dual description source encoders we derive the distortion exponent for the case of two relays helping the source. In addition, we consider channel coding diversity with two relay nodes so as to be able to compare the results with the source coding diversity scheme.

Single Relay

The system under consideration consists of a source, a relay and a destination as shown in Fig. 4.1. Transmission of a message is done in two phases. In phase 1, the source sends its information to the relay node. The received signal at the relay node is given by

$$y_{r_1} = h_{s,r_1}\sqrt{P}x_s + n_{s,r_1}, \tag{4.8}$$

where h_{s,r_1} is the channel gain between the source and the relay node, x_s is the transmitted source symbol with $E\{||x_s||^2\} = 1$, P is the source transmit power, and n_{s,r_1} is the noise at the relay node modeled as zero-mean circularly symmetric complex Gaussian noise with variance $N_0/2$ per dimension.

In phase 2, the relay normalizes the received signal by the factor $\alpha_1 \leq \sqrt{\frac{P}{P|h_{s,r_1}|^2+N_0}}$ [11] and retransmits to the destination. The received signal at the destination is given by

$$y_d = h_{r_1,d}\alpha_1 y_{r_1} + n_{r_1,d} = h_{r_1,d}\alpha_1 h_{s,r_1}\sqrt{P}x_s + h_{r_1,d}\alpha_1 n_{s,r_1} + n_{r_1,d}, \tag{4.9}$$

where $n_{r_1,d}$ is the noise at the destination node and is modeled as zero-mean circularly symmetric complex Gaussian noise with variance $N_0/2$ per dimension. Mutual information is maximized when x_s, the transmitted source symbol, is distributed as

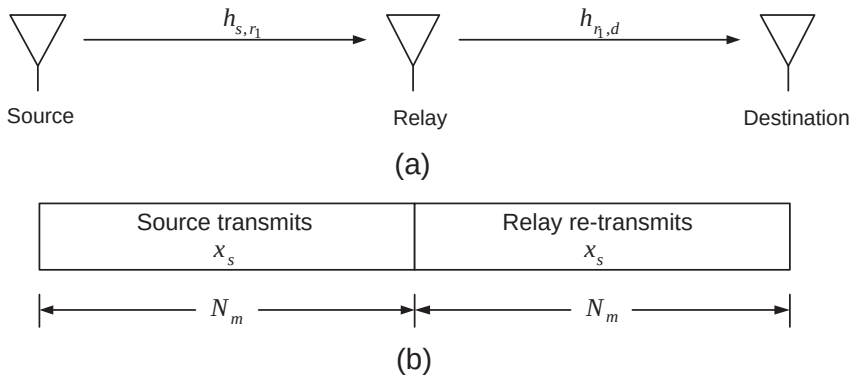

Figure 4.1: Two-hop single relay system (a) system model (b) time frame structure.

a circularly symmetric complex Gaussian random variable with zero-mean and variance 1/2 per dimension [24]. Consequently, the mutual information is maximized when $\alpha_1 = \sqrt{\frac{P}{P|h_{s,r_1}|^2+N_0}}$, i.e., satisfying the power constraint with equality [11]. The mutual information in this case was found to be [11]

$$I(x_s, y_d) = \log\left(1 + \frac{|h_{s,r_1}|^2 SNR |h_{r_1,d}|^2 SNR}{|h_{s,r_1}|^2 SNR + |h_{r_1,d}|^2 SNR + 1}\right), \tag{4.10}$$

where $SNR = P/N_0$. At high SNR, we have

$$\begin{aligned} I(x_s, y_d) &\approx \log\left(1 + \frac{|h_{s,r_1}|^2 SNR |h_{r_1,d}|^2 SNR}{|h_{s,r_1}|^2 SNR + |h_{r_1,d}|^2 SNR}\right) \\ &\approx \log\left(\frac{|h_{s,r_1}|^2 SNR |h_{r_1,d}|^2 SNR}{|h_{s,r_1}|^2 SNR + |h_{r_1,d}|^2 SNR}\right). \end{aligned} \tag{4.11}$$

Equation (4.11) indicates that the two-hop amplify-and-forward channel appears as a link with signal-to-noise ratio that is a scaled harmonic mean of the source-relay and relay-destination channels signal-to-noise ratios. To calculate the distortion exponent let $Z_1 = |h_{s,r_1}|^2 SNR$ and $Z_2 = |h_{r_1,d}|^2 SNR$. Assuming symmetry be-

tween the source-relay and relay-destination channels, we have

$$\begin{aligned} F_{Z_1}(t) &\approx c\left(\frac{t}{SNR}\right)^p \\ F_{Z_2}(t) &\approx c\left(\frac{t}{SNR}\right)^p, \end{aligned} \tag{4.12}$$

where $F_{Z_1}(.)$ and $F_{Z_2}(.)$ are the cdf of Z_1 and Z_2, respectively. The scaled harmonic mean of two nonnegative random variables can be upper- and lower-bounded as

$$\frac{1}{2}\min(Z_1, Z_2) \leq \frac{Z_1 Z_2}{Z_1 + Z_2} \leq \min(Z_1, Z_2). \tag{4.13}$$

While the lower-bound is achieved if and only if $Z_1 = Z_2$, $Z_1 = 0$, or $Z_2 = 0$ and the upper-bound is achieved if and only if $Z_1 = 0$ or $Z_2 = 0$.

Define the random variable $Z = \frac{Z_1 Z_2}{Z_1 + Z_2}$. From (4.13) we have

$$\Pr\left[\min(Z_1, Z_2) < t\right] \leq \Pr\left[Z < t\right] \leq \Pr\left[\min(Z_1, Z_2) < 2t\right]. \tag{4.14}$$

Then we have

$$\begin{aligned} \Pr\left[\min(Z_1, Z_2) < t\right] &= 2F_{Z_1}(t) - \left(F_{Z_1}(t)\right)^2 \\ &\approx 2c\left(\frac{t}{SNR}\right)^p - c^2\left(\frac{t}{SNR}\right)^{2p} \\ &\approx c_1\left(\frac{t}{SNR}\right)^p, \end{aligned} \tag{4.15}$$

where $c_1 = 2c$. Similarly, we have

$$\Pr\left[\min(Z_1, Z_2) < 2t\right] \approx c_2\left(\frac{t}{SNR}\right)^p, \tag{4.16}$$

where $c_2 = 2^{p+1}c$. From (4.15) and (4.16) we get

$$c_1\left(\frac{t}{SNR}\right)^p \lessapprox F_Z(t) \lessapprox c_2\left(\frac{t}{SNR}\right)^p, \tag{4.17}$$

where $F_Z(t)$ is the cdf of the random variable Z. The minimum expected end-to-end distortion can now be computed as

$$E\left[D\right] = \min_D \left\{\Pr\left[I(x_s, y_d) < R(D)\right] + D\ \Pr\left[I(x_s, y_d) \geq R(D)\right]\right\}, \tag{4.18}$$

where D is the source encoder distortion and R is the source encoding rate. Note that (4.18) implicitly assumes that in the case of an outage the missing source data is concealed by replacing the missing source samples with their expected value (equal to zero). Using the bounds in (4.17) the minimum expected distortion can be upper- and lower-bounded as

$$\begin{aligned}\min_D \left\{ c_1 \left(\frac{\exp(R(D))}{SNR} \right)^p + \left[1 - c_2 \left(\frac{\exp(R(D))}{SNR} \right)^p \right] \ D \right\} \\ \lessapprox E[D] \lessapprox \min_D \left\{ c_2 \left(\frac{\exp(R(D))}{SNR} \right)^p + \left[1 - c_1 \left(\frac{\exp(R(D))}{SNR} \right)^p \right] \ D \right\}.\end{aligned} \tag{4.19}$$

For sufficiently large SNRs, we have

$$\min_D \left\{ c_1 \left(\frac{\exp(R(D))}{SNR} \right)^p + D \right\} \lessapprox E[D] \lessapprox \min_D \left\{ c_2 \left(\frac{\exp(R(D))}{SNR} \right)^p + D \right\}. \tag{4.20}$$

From (4.3), $\exp(R(D)) = D^{\frac{-1}{2\beta_m}}$, where $\beta_m = N_m/K$ as illustrated in Fig. 4.1, which leads to

$$\min_D c_1 \frac{D^{\frac{-p}{2\beta_m}}}{SNR^p} + D \lessapprox E[D] \lessapprox \min_D c_2 \frac{D^{\frac{-p}{2\beta_m}}}{SNR^p} + D. \tag{4.21}$$

Differentiating the lower-bound and setting equal to zero we get the optimizing distortion

$$D^* = \left(\frac{2\beta_m}{c_1 p} \right)^{\frac{-2\beta_m}{2\beta_m + p}} SNR^{\frac{-2\beta_m p}{2\beta_m + p}}. \tag{4.22}$$

Substituting from (4.22) into (4.21) we get

$$C_{LB}\ SNR^{\frac{-2\beta_m p}{2\beta_m + p}} \lessapprox E[D] \lessapprox C_{UB}\ SNR^{\frac{-2\beta_m p}{2\beta_m + p}}, \tag{4.23}$$

where C_{LB} and C_{UB} are terms that are independent of the SNR.

The distortion exponent is now given by the following theorem.

Theorem 2 *The distortion exponent of the two-hop single relay amplify-and-forward protocol is*

$$\Delta_{SH-1R-AMP} = \frac{2p\beta_m}{p + 2\beta_m}, \tag{4.24}$$

where $\beta_m = N_m/K$, and N_m is the number of the source channel uses. (refer to Fig. 4.1)

In the sequel, we will use

$$F_Z(t) \approx \acute{c} \left(\frac{t}{SNR}\right)^p, \tag{4.25}$$

where Z is the scaled harmonic mean of the source-relay and relay-destination signal-to-noise ratios and $\acute{c}$ is a constant. Although the last relation does not follow directly from (4.17) we use it for simplicity of presentation. The analysis is not affected by this substitution as we can always apply the analysis presented here by forming upper- and lower-bound on the expected distortion and this will yield the same distortion exponent.

We consider now a system consisting of a source, M relay nodes and a destination as shown in Fig. 4.2. The M relay nodes amplify the received signals from the source and then retransmit to the destination. The destination selects the signal of the highest quality (highest SNR) to recover the source signal[2]. The distortion exponent of this system is given by the following theorem.

Theorem 3 *The distortion exponent of the two-hop M relays selection channel coding diversity with the amplify-and-forward protocol is*

$$\Delta_{SH-MR-AMP} = \frac{4Mp\beta_m}{M(M+1)p + 4\beta_m}. \tag{4.26}$$

[2]The system where the destination selects the signal with the highest quality will have the same distortion exponent as the system where the destination applies maximum ratio combiner (MRC) to the received signals from the relay nodes.

Proof Let y_{d_i} be the signal received at the destination due to the ith relay transmission. At sufficiently high SNR, the mutual information between x_s and y_{d_i} is given by

$$I(x_s, y_{d_i}) \approx \log\left(\frac{|h_{s,r_i}|^2 SNR |h_{r_i,d}|^2 SNR}{|h_{s,r_i}|^2 SNR + |h_{r_i,d}|^2 SNR}\right),\ i = 1, 2, ..., M.$$

Define the random variables $W_i = \frac{|h_{s,r_i}|^2 SNR |h_{r_i,d}|^2 SNR}{|h_{s,r_i}|^2 SNR + |h_{r_i,d}|^2 SNR},\ i = 1, 2, ..., M$. The cdf of W_i can be approximated at high SNR as

$$F_{W_i}(t) \approx \acute{c}\left(\frac{t}{SNR}\right)^p. \tag{4.27}$$

The minimum end-to-end expected distortion can be computed as

$$\begin{aligned}
E[D] = &\min_D \Bigg\{ \Pr[\max(I(x_s, y_{d_1}), I(x_s, y_{d_2}), ..., I(x_s, y_{d_M})) < R(D)] \\
&\quad + \Pr[\max(I(x_s, y_{d_1}), I(x_s, y_{d_2}), ..., I(x_s, y_{d_M})) \geq R(D)]\ D \Bigg\} \\
= &\min_D \left\{ \prod_{i=1}^{M} F_{W_i}(\exp(R(D))) + \left[1 - \prod_{i=1}^{M} F_{W_i}(\exp(R(D)))\right]\ D \right\} \qquad (4.28) \\
\approx &\min_D \left\{ \acute{c}^M \frac{D^{\frac{-Mp}{2\beta'_m}}}{SNR^{Mp}} + \left[1 - \acute{c}^M \frac{D^{\frac{-Mp}{2\beta'_m}}}{SNR^{Mp}}\right]\ D \right\} \\
\approx &\min_D \left\{ \acute{c}^M \frac{D^{\frac{-Mp}{2\beta'_m}}}{SNR^{Mp}} + D \right\},
\end{aligned}$$

where D is the source encoding distortion and $\beta'_m = N'_m/K$, where N'_m is the number of the source channel uses (refer to Fig. 4.2). Differentiating and setting equal to zero we get the optimizing distortion

$$D^* = \left(\acute{c}^M \frac{Mp}{2\beta'_m}\right)^{\frac{2\beta'_m}{Mp+2\beta'_m}} SNR^{\frac{-2M\beta'_m p}{2\beta'_m + Mp}}. \tag{4.29}$$

Substituting we get

$$E[D] \approx C_{MR}\ SNR^{\frac{-2M\beta'_m p}{2\beta'_m + Mp}}, \tag{4.30}$$

where C_{MR} is a term that does not depend on the SNR. Hence, the distortion exponent is given as

$$\Delta_{SH-MR-AMP} = \frac{2M\beta'_m p}{2\beta'_m + Mp}. \tag{4.31}$$

For fair comparison with the single relay case, we should compare the different systems under the same number of channel uses. So that we have $2N_m = (M+1)N'_m$ (refer to Fig. 4.1 and Fig. 4.2), from which we have $\beta'_m = \frac{2}{M+1}\beta_m$. Substituting in (4.31) we get

$$\Delta_{SH-MR-AMP} = \frac{4Mp\beta_m}{M(M+1)p + 4\beta_m}. \tag{4.32}$$

□

The distortion exponent shows a tradeoff between the number of relay nodes and the source encoder performance. Increasing the number of relay nodes increases the diversity of the system at the expense of using a lower rate source encoder (higher distortion under no outage). To get the optimal number of relays M_{opt} note that the distortion exponent in (4.26) can be easily shown to be concave in the number of relays (if we think of M as a continuous variable). Differentiating and setting equal to zero, we get

$$\frac{\partial}{\partial M}\Delta_{SH-MR-AMP} = 0 \longrightarrow M_{opt} = 2\sqrt{\frac{\beta_m}{p}}. \tag{4.33}$$

If M_{opt} in (4.33) is an integer number then it is the optimal number of relays. If M_{opt} in (4.33) is not an integer, substitute in (4.26) with the largest integer that is less than M_{opt} and the smallest integer that is greater than M_{opt} and choose the one that yields the higher distortion exponent as the optimum number of relay nodes. From the result in (4.33) it is clear that the number of relays decreases, for a fixed β_m, as p increases. For higher channel quality (higher p) the system performance is limited by the distortion introduced by the source encoder in the absence of

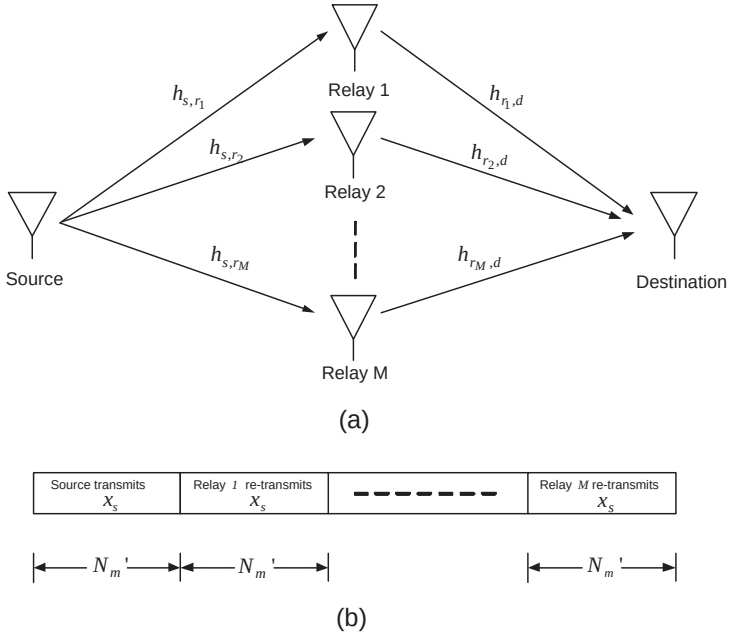

Figure 4.2: Two-hop M relays system (a) system model (b) time frame structure.

outage. Then, as p increases, the optimum number of relays decreases to allow for the use of a better source encoder with a lower source encoding distortion. In this scenario, the system is said to be a quality limited system because the dominant phenomenon in the end-to-end distortion is source encoding distortion and not outage. Similarly as β_m increases (higher bandwidth), for a fixed p, the performance will be limited by the outage event rather than the source encoding distortion. As β_m increases, the optimum number of relays increases to achieve better outage performance. In this case, the system is said to be an outage limited system.

Channel Coding Diversity with 2 Relays

We consider now a system as shown in Fig. 4.3 comprising a source, two relays and a destination. After channel encoding, the resulting block is split into two blocks: x_{s_1} and x_{s_2}, which are transmitted to the relay nodes. The first relay will only forward the block x_{s_1} and the second relay will only forward x_{s_2} as shown in Fig. 4.3. From (4.11), it can be shown that the mutual information is given by

$$I \approx \log\left(1+\frac{|h_{s,r_1}|^2 SNR|h_{r_1,d}|^2 SNR}{|h_{s,r_1}|^2 SNR+|h_{r_1,d}|^2 SNR}\right)+\log\left(1+\frac{|h_{s,r_2}|^2 SNR|h_{r_2,d}|^2 SNR}{|h_{s,r_2}|^2 SNR+|h_{r_2,d}|^2 SNR}\right), \tag{4.34}$$

where x_{s_1} and x_{s_2} are independent zero-mean circularly symmetric complex Gaussian random variables each with variance 1/2 per dimension. We can show that the distortion exponent of this system is given by the following theorem.

Theorem 4 *The distortion exponent of the two-hop two-relay channel coding diversity amplify-and-forward system is*

$$\Delta_{SH-2R-OPTCH-AMP} = \frac{2p\beta_m}{p+\beta_m}. \tag{4.35}$$

Proof From [52], the distortion exponent for the channel coding diversity over two parallel channels can be written as

$$\Delta_{SH-2R-OPTCH-AMP} = \frac{4p\beta''_m}{p+2\beta''_m}, \tag{4.36}$$

Using (4.25) and (4.34) and considering $\beta''_m = N''_m/K$ where N''_m is the number of source channel uses for the x_{s_1} (x_{s_2}) block (refer to Fig. 4.3) we get for our system the same distortion exponent as (4.36). For fair comparison with the previous schemes we should have $2N_m = 4N''_m$, which means that $\beta''_m = \frac{1}{2}\beta_m$. Finally, substituting this relation in (4.36) yields (4.35).□

In the context of parallel channels, the notion of multiplexed channel coding diversity was presented in [52]. The gain in the distortion exponent for the multiplexed channel coding diversity scheme (compared to the direct transmission) is a result of the increase of the bandwidth due to the simultaneous use of parallel channels. In the multiplexed channel coding diversity scheme discussed in [52], the two blocks, x_{s_1} and x_{s_2}, represent a split of a channel-coded message from a SD source encoder over two parallel channels, which will be the two source-relay-destination links in our system. In our system, there is no gain in using multiplexed channel coding diversity because, for fair comparison, using either one relay or two relays does not increase the bandwidth of the channel. This is because only one node, either the source or a relay, is transmitting at a given time slot. The multiplexed channel coding diversity in this case is equivalent to allowing one relay helping the source to forward an SD source-coded message during one block and using the other relay for the next block. Hence, in our system, the multiplexed channel coding diversity is equivalent to the two-hop single relay system with the same distortion exponent.

Source Coding Diversity with 2 Relays

We consider again a system with one source, two relays and one destination nodes as shown in Fig. 4.3. The source transmits two blocks x_{s_1} and x_{s_2} to the relay nodes. Each block represents one of the two descriptions generated by the dual descriptions source encoder. In this case, the two blocks are broken up before the channel encoder, that is each description is fed to a different channel encoder. The first relay will only forward the block x_{s_1} and the second relay will only forward x_{s_2} as shown in Fig. 4.3. The distortion exponent of this system is given by the

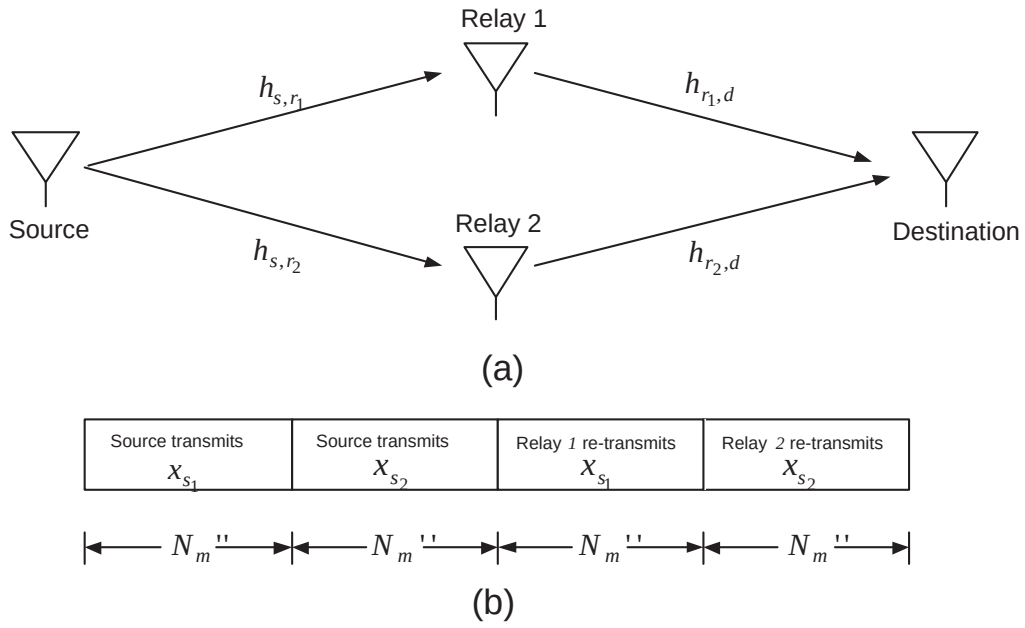

Figure 4.3: Two-hop 2 relays channel coding diversity (source coding diversity) system (a) system model (b) time frame structure.

following theorem.

Theorem 5 *The distortion exponent of the two-hop 2 relays source coding diversity amplify-and-forward protocol is*

$$\Delta_{SH-2R-SRC-AMP} = \max\left[\frac{4p\beta_m}{3p+2\beta_m}, \frac{2p\beta_m}{p+2\beta_m}\right]. \tag{4.37}$$

Proof From [52], the distortion exponent for the source coding diversity over two parallel channels can be written as

$$\Delta_{SH-2R-SRC-AMP} = \max\left[\frac{8p\beta''_m}{3p+4\beta''_m}, \frac{4p\beta''_m}{p+4\beta''_m}\right], \tag{4.38}$$

Using (4.25) and (4.34) and considering $\beta''_m = N''_m/K$ (refer to Fig. 4.3) we get for our system the same distortion exponent as (4.38). For fair comparison with the previous schemes, $2N_m = 4N''_m$; which leads to $\beta''_m = \frac{1}{2}\beta_m$. Substituting this equality in (4.38) completes the proof.□

4.2.2 Multi-Hop Decode-and-Forward Protocol

In this section, we will analyze schemes using multi-hop decode-and-forward user cooperation under different channel and source coding diversity schemes. In these cases, the relay nodes decode the received source symbols. Only those relay nodes that had correctly decoded the source symbols will proceed to retransmit them to the destination node. When a relay fails in decoding the source symbols we say that an outage has occurred. Furthermore, an outage occurs when either the source-relay or the relay-destination channel are in outage, as discussed in Section 4.1. That is, the quality of the source-relay-destination link is limited by the minimum of the source-relay and relay-destination channels. For the single relay case we can formulate the outage as

$$P_{outage} = \Pr\left[\min(I(x_s, y_{r_1}), I(x_{r_1}, y_d)) < R(D)\right], \tag{4.39}$$

where x_{r_1} is the transmitted signal from the relay node. Note that in those schemes using decode-and-forward the quality (mutual information) of any source-relay-destination link is limited by the minimum of the source-relay and relay-destination links SNRs. On the other hand, for two-hop amplify-and-forward schemes, the performance is limited by the scaled harmonic mean of the source-relay and the relay-destination links SNRs which is strictly less than the minimum of the two links SNRs. Hence, the multi-hop amplify-and-forward protocol has a higher outage probability (lower quality) than the multi-hop decode-and-forward protocol. That is, in terms of outage probability, the multi-hop decode-and-forward protocol outperforms the multi-hop amplify-and-forward protocol. The above argument is also applicable under different performance measures (for example, if the performance measure was symbol error rate). From our presentation so far it is clear that the distortion exponents for multi-hop decode-and-forward schemes are the same

as their corresponding multi-hop amplify-and-forward schemes for the repetition channel coding diversity and source coding diversity cases. For example, for the two-hop single relay decode-and-forward scheme, the minimum expected distortion is given by the lower-bound in (4.23), which has the same distortion exponent as the two-hop single relay amplify-and-forward scheme. We collect these results in the following theorem.

Theorem 6 *The distortion exponent of the multi-hop decode-and-forward schemes are:*

- *for the two-hop single relay*

$$\Delta_{SH-1R-DEC} = \frac{2p\beta_m}{p+2\beta_m}, \tag{4.40}$$

- *for the two-hop M relays selection channel coding diversity*

$$\Delta_{SH-MR-DEC} = \frac{4Mp\beta_m}{M(M+1)p+4\beta_m}, \tag{4.41}$$

- *for the two-hop 2 relays source coding diversity*

$$\Delta_{SH-2R-SRCDEC} = \max\left[\frac{4p\beta_m}{3p+2\beta_m}, \frac{2p\beta_m}{p+2\beta_m}\right]. \tag{4.42}$$

Channel Coding Diversity with 2 Relays

We consider now the use of channel coding with two-relay decode-and-forward protocols. In this case, the relay will perform joint decoding of the two blocks x_{s_1} and x_{s_2} as illustrated in Fig. 4.4, which means that when any relay decodes correctly it could forward both x_{s_1} and x_{s_2}. Allowing the first relay to forward only x_{s_1} if it has decoded correctly will cause a degradation in the performance if the second relay decoded erroneously. Hence, if the first relay decoded correctly

and the second did not, it is better (in terms of outage probability) for the first relay to forward both x_{s_1} and x_{s_2}. Clearly, a similar argument could be applied to the operation of the second relay. Also, when both relays decode correctly, allowing the second relay to transmit also x_{s_1} and x_{s_2} will cause a loss of diversity. To gain both advantages (lower outage probability when only one relay decodes correctly and diversity when both correctly decode) we propose to use a space-time transmission scheme. In our case we choose the Alamouti scheme [40], with the time frame structure as shown in Fig. 4.4. Then, the distortion exponent of this system is given by the following theorem

Theorem 7 *The distortion exponent of the two-hop 2 relays channel coding diversity decode-and-forward protocol is*

$$\Delta_{SH-2R-OPTCH-DEC} = \frac{2p\beta_m}{p+\beta_m}. \tag{4.43}$$

Proof The outage probability is given by (proof in Appendix I)

$$P_{outage} = c_o \left(\frac{\exp(pR(D))}{SNR^{2p}} \right). \tag{4.44}$$

The minimum expected distortion can now be computed as

$$\begin{aligned} E[D] &= \min_D \left\{ P_{outage} + D\left(1 - P_{outage}\right) \right\} \\ &\approx \min_D \left\{ c_o \left(\frac{\exp(pR(D))}{SNR^{2p}} \right) + D\left[1 - c_o \left(\frac{\exp(pR(D))}{SNR^{2p}} \right) \right] \right\} \\ &\approx \min_D \left\{ c_o \left(\frac{\exp(pR(D))}{SNR^{2p}} \right) + D \right\} \qquad (4.45) \\ &\approx \min_D \left\{ c_o \frac{D^{-\frac{p}{2\beta_m'}}}{SNR^{2p}} + D \right\}, \qquad (4.46) \end{aligned}$$

where D is the source encoder distortion, (4.45) follows from high SNR approximation and (4.46) follows from (4.3). Differentiating and setting equal to zero we

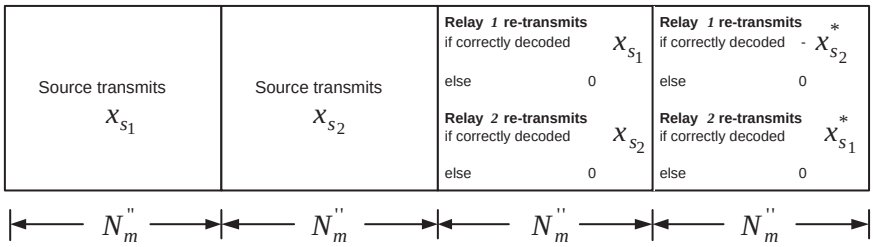

Figure 4.4: Two-hop 2 relays decode-and-forward channel coding diversity system' time frame structure.

get the optimizing distortion

$$D^* = \left(\frac{2\beta''_m}{c_o p}\right)^{\frac{-2\beta''_m}{2\beta''_m+p}} SNR^{\frac{-4\beta''_m p}{2\beta''_m+p}}. \tag{4.47}$$

Hence, the distortion exponent is given as

$$\Delta_{RC-1R-AMP} = \frac{4\beta''_m p}{2\beta''_m + p}. \tag{4.48}$$

For fair comparison, the total number of channel uses should be kept fixed for all schemes. Thus, we have $N_m = 2N''_m$, from which we have $\beta''_m = \frac{1}{2}\beta_m$. Substituting in (4.48) we get

$$\Delta_{SH-2R-OPTCH-DEC} = \frac{2p\beta_m}{p + \beta_m}. \tag{4.49}$$

□

4.3 Relay Channels

We now extend our study on distortion exponents to the case of a relay channel when using either amplify-and-forward or decode-and-forward user cooperation. Thus, we now consider that in addition to the source-relay-destination channels there is also a communication channel between the source and destination nodes.

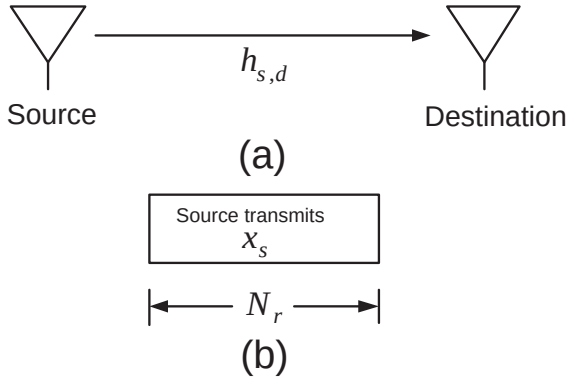

Figure 4.5: No diversity (direct transmission) system (a) system model (b) time frame structure.

For comparison purposes, we consider the case when the source transmits a single description source coded message over the source-destination channel without the help of any relay node. The system is shown in Fig. 4.5. In this case, the distortion exponent is given by [52] as

$$\Delta_{NO-DIV} = \frac{2p\beta_r}{p + 2\beta_r}, \tag{4.50}$$

where $\beta_r = N_r/K$ and N_r is the number of channel uses for the source block (refer to Fig. 4.5).

4.3.1 Amplify-and-Forward Protocol

In this section, we analyze the same schemes presented for the multi-hop channels when now they are used over the amplify-and-forward relay channel. We will consider the single and M relays repetition channel coding diversity and the 2 relays channel coding diversity and source coding diversity.

Single Relay

Consider a system comprising a source, a relay and a destination as shown in Fig. 4.6. We consider that the relay operates following an amplify-and-forward user-cooperation scheme. We also assume that the destination applies a Maximum Ratio Combiner (MRC) to detect the transmitted signal from those received in each phase [11]. The mutual information of this system is given by [11]

$$I(x_s, y_d) = \log\left(1 + |h_{s,d}|^2 SNR + \frac{|h_{s,r_1}|^2 SNR |h_{r_1,d}|^2 SNR}{|h_{s,r_1}|^2 SNR + |h_{r_1,d}|^2 SNR + 1}\right), \tag{4.51}$$

where $SNR = P/N_0$ and $h_{s,d}$ is the channel between the source and the destination. At high SNR, we have

$$\begin{aligned} I(x_s, y_d) &\approx \log\left(1 + |h_{s,d}|^2 SNR + \frac{|h_{s,r_1}|^2 SNR |h_{r_1,d}|^2 SNR}{|h_{s,r_1}|^2 SNR + |h_{r_1,d}|^2 SNR}\right) \\ &\approx \log\left(|h_{s,d}|^2 SNR + \frac{|h_{s,r_1}|^2 SNR |h_{r_1,d}|^2 SNR}{|h_{s,r_1}|^2 SNR + |h_{r_1,d}|^2 SNR}\right). \end{aligned} \tag{4.52}$$

The distortion exponent of this system is given by the following theorem.

Theorem 8 *The distortion exponent of the single relay amplify-and-forward scheme is*

$$\Delta_{RC-1R-AMP} = \frac{2p\beta_r}{2p + \beta_r}. \tag{4.53}$$

Proof Let $W_1 = |h_{s,d}|^2 SNR$ and $W_2 = \frac{|h_{s,r_1}|^2 SNR |h_{r_1,d}|^2 SNR}{|h_{s,r_1}|^2 SNR + |h_{r_1,d}|^2 SNR}$. The outage probability can be calculated as

$$\begin{aligned} P_{outage} &= \Pr\left[\log(1 + W_1 + W_2) < R(D)\right] \\ &\approx \Pr\left[W_1 + W_2 < \exp(R(D))\right]. \end{aligned} \tag{4.54}$$

From Appendix I the cdf of $W_1 + W_2$ is given by

$$F_{W_1+W_2}(w) \approx c_{33}\left(\frac{w}{SNR}\right)^{2p}. \tag{4.55}$$

The minimum expected distortion can now be computed as

$$\begin{aligned}
E[D] &\approx \min_{D} \{\Pr[W_1 + W_2 < \exp(R(D))] + \Pr[W_1 + W_2 \geq \exp(R(D))]\ D\} \\
&= \min_{D} \{F_{W_1+W_2}(\exp(R(D))) + \Pr[1 - F_{W_1+W_2}(\exp(R(D)))]\ D\} \\
&\approx \min_{D} \left\{ c_{33} \left(\frac{\exp(2pR(D))}{SNR^{2p}} \right) + \left[1 - c_{33} \left(\frac{\exp(2pR(D))}{SNR^{2p}} \right) \right]\ D \right\} \\
&\approx \min_{D} \left\{ c_{33} \left(\frac{D^{\frac{-p}{\beta_r'}}}{SNR^{2p}} \right) + D \right\},
\end{aligned} \tag{4.56}$$

where $\beta_r' = N_r'/K$ and N_r' is the number of source channel uses (refer to Fig. 4.6). Differentiating and setting equal to zero we get the optimizing distortion

$$D^* = \left(\frac{\beta_r}{c_{33}p} \right)^{\frac{-\beta_r'}{\beta_r'+p}} SNR^{\frac{-2\beta_r'p}{\beta_r'+p}}. \tag{4.57}$$

Hence, the distortion exponent is given as

$$\Delta_{RC-1R-AMP} = \frac{2\beta_r'p}{\beta_r' + p}. \tag{4.58}$$

For fair comparison we should have $N_r = 2N_r'$ from which we have $\beta_r' = \frac{1}{2}\beta_r$. Substituting in (4.58) we get

$$\Delta_{RC-1R-AMP} = \frac{2\beta_r p}{\beta_r + 2p}. \tag{4.59}$$

□

Asymptotically comparing the distortion exponents for case of no diversity and a single relay we have

$$\begin{aligned}
\lim_{\beta_r/p \to \infty} \frac{\Delta_{RC-1R-AMP}}{\Delta_{NO-DIV}} &= 2, \\
\lim_{\beta_r/p \to 0} \frac{\Delta_{RC-1R-AMP}}{\Delta_{NO-DIV}} &= \frac{1}{2}.
\end{aligned} \tag{4.60}$$

Note that as β_r/p increases (bandwidth increases) the system becomes outage limited because the performance is limited by the outage event. In this case, the

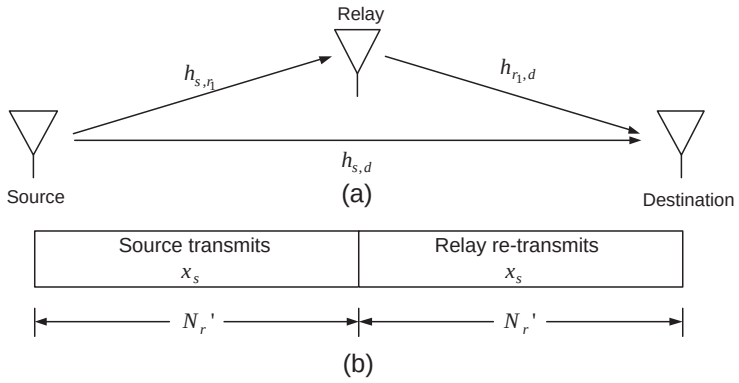

Figure 4.6: Single relay system (a) system model (b) time frame structure.

single relay amplify-and-forward system will achieve a higher distortion exponent since it achieves higher diversity order. Conversely, as β_r/p tends to zero (higher channel quality) the performance is not limited by the outage event, but is limited by the source encoder quality performance. A similar observation was made in [52] in comparing the performance for parallel channels of selection and multiplexed channel diversities. In the case of the multiplexed channel diversity from [52], we can think of the two parallel channels as a single channel with no diversity but with twice the bandwidth. When regarding the multiplexed channel diversity as a single channel, the performance of selection and multiplexed channel diversities for parallel channels can be compared in the same way as (4.60).

The ongoing analysis can be extended to the case of M amplify-and-forward relay nodes. The distortion exponent in this case is given by the following theorem.

Theorem 9 *The distortion exponent of M relay nodes amplify-and-forward protocol is*

$$\Delta_{RC-MR-AMP} = \frac{2(M+1)p\beta_r}{2\beta_r + (M+1)^2 p}. \tag{4.61}$$

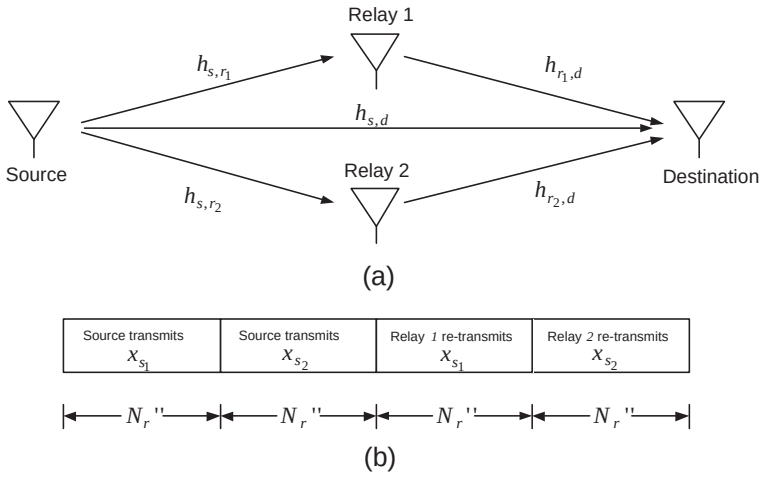

Figure 4.7: Two relays system (a) system model (b) time frame structure.

Again we can think of selecting the optimum number of relays to maximize the distortion exponent. This is again a tradeoff between the diversity and the quality of the source encoder.

Channel Coding Diversity with 2 Relays

We consider a system consisting of a source, two relays and a destination as shown in Fig. 4.7. The source transmits two channel-coded blocks x_{s_1} and x_{s_2} to the destination and the relay nodes. The first relay will only forward the block x_{s_1} and the second relay will only forward x_{s_2} as shown in Fig. 4.7. First, we will calculate the mutual information for the channel coding scheme.

The system model can be described as follows. In phase 1, the source broadcasts its information to the destination and two relay nodes. The received signals are

$$y_{s,d_m} = \sqrt{P} h_{s,d} x_{s_m} + n_{s,d}, \tag{4.62}$$

$$y_{s,r_i} = \sqrt{P} h_{s,r_i} x_{s_m} + n_{s,r_i}, \quad i = 1, 2, \ m = 1, 2. \tag{4.63}$$

Relay 1 will only forward x_{s_1} and relay 2 will only forward x_{s_2}. The received signals at the destination due to relay 1 and relay 2 transmissions are given by

$$y_{r_i,d} = h_{r_i,d}\zeta_i y_{s,r_i} + n_{r_i,d},\ i = 1, 2, \tag{4.64}$$

where ζ_i is the signal amplification performed at the relay which satisfies the power constraint with equality, that is

$$\zeta_i = \sqrt{\frac{P}{P|h_{s,r_i}|^2 + N_0}}, \tag{4.65}$$

and where all the noise components are modeled as independent, zero-mean complex Gaussian random variables with variance $N_0/2$ per dimension.

Define the 4×1 vector, $\mathbf{y} = [y_{s,d_1}, y_{s,d_2}, y_{r_1,d}, y_{r_2,d}]^T$. To get the mutual information between $\mathbf{x} = [x_{s_1}, x_{s_2}]$ and $\mathbf{y}$ we consider that an MRC detector is applied on $y_{s,d_1}, y_{r_1,d}$ and another MRC detector is applied on $y_{s,d_2}, y_{r_2,d}$. The output of the first MRC detector is given by

$$r_1 = \alpha_s y_{s,d_1} + \alpha_1 y_{r_1,d}, \tag{4.66}$$

where $\alpha_s = \sqrt{P}h^*_{s,d}/N_0$ and

$$\alpha_1 = \frac{\sqrt{P}\zeta_1 h^*_{r_1,d} h^*_{s,r_1}}{(\zeta_1^2|h_{r_1,d}|^2 + 1)N_0}.$$

We can write r_1 in terms of x_{s_1} as

$$r_1 = \left(|h_{s,d}|^2 SNR + \frac{|h_{r_1,d}|^2 SNR|h_{s,r_1}|^2 SNR}{|h_{s,r_1}|^2 SNR + |h_{r_1,d}|^2 SNR + 1}\right) x_{s_1} + n_1, \tag{4.67}$$

where n_1 is a zero-mean circularly symmetric complex Gaussian random noise with variance $|h_{s,d}|^2 SNR + \frac{|h_{r_1,d}|^2 SNR|h_{s,r_1}|^2 SNR}{|h_{s,r_1}|^2 SNR + |h_{r_1,d}|^2 SNR + 1}$. Similarly we can have r_2, representing the output of the second MRC detector, given by

$$r_2 = \left(|h_{s,d}|^2 SNR + \frac{|h_{r_2,d}|^2 SNR|h_{s,r_2}|^2 SNR}{|h_{s,r_2}|^2 SNR + |h_{r_2,d}|^2 SNR + 1}\right) x_{s_2} + n_2, \tag{4.68}$$

where n_2 is a zero-mean circularly symmetric complex Gaussian random noise with variance $|h_{s,d}|^2 SNR + \frac{|h_{r_2,d}|^2 SNR |h_{s,r_2}|^2 SNR}{|h_{s,r_2}|^2 SNR + |h_{r_2,d}|^2 SNR + 1}$. Next, the conditional pdf of $\mathbf{y}$ given $\mathbf{x}$ and the channel coefficients is given by

$$p(\mathbf{y}/\mathbf{x}) = p(y_{s,d_1}, y_{r_1,d}/x_{s_1}) p(y_{s,d_2}, y_{r_2,d}/x_{s_2}). \tag{4.69}$$

The conditional pdf of $\mathbf{y}$ given $\mathbf{x}$ and the channel coefficients represents an exponential family of distributions [23]. Therefore, it can be easily shown that r_1 and r_2, given the channel coefficients, are sufficient statistics for $\mathbf{x}$, that is

$$p(\mathbf{y}/\mathbf{x}, r_1, r_2) = p(\mathbf{y}/r_1, r_2) = p(y_{s,d_1}, y_{r_1,d}/r_1) p(y_{s,d_2}, y_{r_2,d}/r_2), \tag{4.70}$$

Since r_1 and r_2 are sufficient statistics for $\mathbf{x}$, then the mutual information between $\mathbf{x}$ and $\mathbf{y}$ equals the mutual information between $\mathbf{x}$ and $\mathbf{r} = [r_1, r_2]$ [24], that is

$$I(\mathbf{x}; \mathbf{r}) = I(\mathbf{x}; \mathbf{y}). \tag{4.71}$$

For any covariance matrix of $\mathbf{x}$ the mutual information is maximized when $\mathbf{x}$ is zero-mean circularly symmetric complex Gaussian random vector [24]. Define

$$\gamma_1 = |h_{s,d}|^2 SNR + \frac{|h_{r_1,d}|^2 SNR |h_{s,r_1}|^2 SNR}{|h_{s,r_1}|^2 SNR + |h_{r_1,d}|^2 SNR + 1}$$
$$\gamma_2 = |h_{s,d}|^2 SNR + \frac{|h_{r_2,d}|^2 SNR |h_{s,r_2}|^2 SNR}{|h_{s,r_2}|^2 SNR + |h_{r_2,d}|^2 SNR + 1}.$$

The mutual information can be computed as

$$I(\mathbf{x}, \mathbf{y}) = I(\mathbf{x}, \mathbf{r}) = \log \left(\mathbf{I}_2 + \begin{bmatrix} \gamma_1 & \alpha\gamma' \\ \alpha^*\gamma'' & \gamma_2 \end{bmatrix} \right), \tag{4.72}$$

where $\mathbf{I}_2$ is the 2×2 identity matrix, γ' and γ'' are functions of the channel coefficients and the noise variance and $\alpha = E\left[x_{s_1} x_{s_2}^*\right]$. From (4.72) it is clear that both α and $-\alpha$ will give the same mutual information. From the concavity of the

log-function we can see that the mutual information maximizing α is $\alpha = 0$, that is x_{s_1} and x_{s_2} are independent (since both x_{s_1} and x_{s_2} are Gaussian). The maximum mutual information can now be given as

$$\begin{aligned} I \approx \log\left(1 + |h_{s,d}|^2 SNR + \frac{|h_{s,r_1}|^2 SNR |h_{r_1,d}|^2 SNR}{|h_{s,r_1}|^2 SNR + |h_{r_1,d}|^2 SNR}\right) + \\ \log\left(1 + |h_{s,d}|^2 SNR + \frac{|h_{s,r_2}|^2 SNR |h_{r_2,d}|^2 SNR}{|h_{s,r_2}|^2 SNR + |h_{r_2,d}|^2 SNR}\right). \end{aligned} \tag{4.73}$$

The distortion exponent of this system is given by the following theorem.

Theorem 10 *The distortion exponent of the 2 relays channel coding diversity amplify-and-forward protocol is*

$$\Delta_{RC-2R-OPTCH-AMP} = \frac{3p\beta_r}{3p + \beta_r}. \tag{4.74}$$

Proof To compute the distortion exponent of that system we start with the analysis of a suboptimal system at the destination node. This suboptimal system will give a lower-bound on the distortion exponent. In the suboptimal system, the detector (suboptimal detector) selects the paths with the highest SNR and does not apply an MRC detector (the optimal detector is the one that applies MRC to the received signals). For example, for x_{s_1}, it either selects the source-destination link or the source-relay-destination link based on which one has higher SNR. The mutual information for the suboptimal system can be proved to be

$$\begin{aligned} I_{sub} \approx \log\left(1 + \max\left(|h_{s,d}|^2 SNR, \frac{|h_{s,r_1}|^2 SNR |h_{r_1,d}|^2 SNR}{|h_{s,r_1}|^2 SNR + |h_{r_1,d}|^2 SNR}\right)\right) + \\ \log\left(1 + \max\left(|h_{s,d}|^2 SNR, \frac{|h_{s,r_2}|^2 SNR |h_{r_2,d}|^2 SNR}{|h_{s,r_2}|^2 SNR + |h_{r_2,d}|^2 SNR}\right)\right). \end{aligned} \tag{4.75}$$

The distortion exponent of the suboptimal system is given by (proof in Appendix II)

$$\Delta_{SUBOPTIMAL} = \frac{3\beta_r p}{\beta_r + 3p}. \tag{4.76}$$

For the optimal detector (the one using an MRC detector), the distortion exponent satisfies

$$\Delta_{RC-2R-OPTCH-AMP} \geq \Delta_{SUBOPTIMAL} = \frac{3\beta_r p}{\beta_r + 3p}. \tag{4.77}$$

Next, we find an upper-bound on the distortion exponent for the optimal system. In this case, the mutual information in (4.73) can be upper- and lower-bounded as

$$\begin{aligned}\log(1 + 2W_1 + W_2 + W_3) &\leq \log(1 + W_1 + W_2) + \log(1 + W_1 + W_3) \\ &\leq 2\log(1 + W_1 + \frac{1}{2}W_2 + \frac{1}{2}W_3),\end{aligned}$$

where $W_1 = |h_{s,d}|^2 SNR$, $W_2 = \frac{|h_{s,r_1}|^2 SNR |h_{r_1,d}|^2 SNR}{|h_{s,r_1}|^2 SNR + |h_{r_1,d}|^2 SNR}$ and $W_3 = \frac{|h_{s,r_2}|^2 SNR |h_{r_2,d}|^2 SNR}{|h_{s,r_2}|^2 SNR + |h_{r_2,d}|^2 SNR}$ are nonnegative numbers. The upper-bound follows from the concavity of the log-function. Therefore, the outage probability P_o of the optimal system can be upper- and lower-bounded as

$$\Pr\left[2\log(1 + W_1 + \frac{1}{2}W_2 + \frac{1}{2}W_3) < R\right] \leq P_o \leq \Pr\left[\log(1 + 2W_1 + W_2 + W_3) < R\right]. \tag{4.78}$$

From (4.78) we can easily show that

$$C_L \frac{\exp\left(\frac{3pR}{2}\right)}{SNR^{3p}} \lessapprox P_o \lessapprox C_U \frac{\exp(3pR)}{SNR^{3p}}, \tag{4.79}$$

where C_L and C_U are two constants that do not depend on the SNR. Similar to the suboptimal system, and using (4.79), the minimum expected end-to-end distortion for the optimal system can be lower-bounded as

$$\begin{aligned}E[D] &\gtrapprox \min_D \left\{ C_L \frac{\exp\left(\frac{3pR}{2}\right)}{SNR^{3p}} + \left(1 - C_U \frac{\exp(3pR)}{SNR^{3p}}\right) D \right\} \\ &\approx \min_D \left\{ \frac{C_L D^{\frac{-3p}{4\beta_r''}}}{SNR^{3p}} + \left(1 - \frac{C_U D^{\frac{-3p}{2\beta_r''}}}{SNR^{3p}}\right) D \right\} \\ &\approx \min_D \left\{ \frac{C_L D^{\frac{-3p}{4\beta_r''}}}{SNR^{3p}} + D \right\}.\end{aligned} \tag{4.80}$$

Differentiating the lower-bound and setting equal to zero we get the optimizing distortion as

$$D^* = \left(\frac{4\beta_r''}{3pC_L}\right)^{\frac{-4\beta_r''}{4\beta_r''+3p}} SNR^{\frac{-12\beta_r''p}{4\beta_r''+3p}}. \tag{4.81}$$

substituting we get

$$E[D] \gtrapprox C_{LO} SNR^{\frac{-12\beta_r''p}{4\beta_r''+3p}}, \tag{4.82}$$

from which we can upper-bound the distortion exponent of the optimal system as

$$\Delta_{RC-2R-OPTCH-AMP} \leq \frac{12\beta_r''p}{4\beta_r''+3p} = \frac{3\beta_r p}{\beta_r+3p}. \tag{4.83}$$

Finally, from (4.77) and (4.83) we get

$$\Delta_{RC-2R-OPTCH-AMP} = \frac{3\beta_r p}{\beta_r+3p}. \tag{4.84}$$

□

Source Coding Diversity with 2 Relays

We continue analyzing a system as in Fig. 4.7 but now we assume that each of the two blocks sent from the source, x_{s_1} and x_{s_2}, represents one description generated from a dual descriptions source encoder. The first relay will only forward the block x_{s_1} and the second relay will only forward x_{s_2} as shown in Fig. 4.7. The distortion exponent of this system is given by the following theorem .

Theorem 11 *The distortion exponent of the 2 relays source coding diversity amplify-and-forward protocol is*

$$\Delta_{RC-2R-SRC-AMP} = \max\left[\frac{2p\beta_r}{2p+\beta_r}, \frac{3p\beta_r}{4p+\beta_r}\right], \tag{4.85}$$

Proof The minimum expected end-to-end distortion can be upper- and lower-bounded as (proof in Appendix III)

$$\begin{aligned} E\left[D\right] &\gtrapprox \min_{D_0,D_1} \frac{c_{s1}}{SNR^{3p}} \left(\frac{1}{4D_0D_1}\right)^{\frac{3p}{4\beta_r''}} + \frac{c_{s2}}{SNR^{2p}} \left(\frac{1}{4D_0D_1}\right)^{\frac{p}{2\beta_r''}} .D_1 + D_0 \\ E\left[D\right] &\lessapprox \min_{D_0,D_1} \frac{c_{s1}}{SNR^{3p}} \left(\frac{1}{2D_0D_1}\right)^{\frac{3p}{4\beta_r''}} + \frac{c_{s2}}{SNR^{2p}} \left(\frac{1}{2D_0D_1}\right)^{\frac{p}{2\beta_r''}} .D_1 + D_0. \end{aligned} \tag{4.86}$$

Note that for $p \geq 2\beta_r''$ the minimum expected distortion increases as D_1 decreases. Hence, the optimal choice of D_1 approaches a constant that is bounded away from zero [52]. For $D_1 \geq 1/2$ the source coding rate is given by (4.7) and not (4.6). The optimal system in this case degenerates to the channel multiplexed scheme which is equivalent, in our system, to the single relay system (the argument is the same as for the multi-hop channel). Thus, the distortion exponent is given by

$$\Delta_{RC-2R-SRC-AMP} = \frac{2p\beta_r}{2p+\beta_r}, \quad p \geq \frac{1}{2}\beta_r = 2\beta_r''. \tag{4.87}$$

For $p < 2\beta_r''$, we can find the optimal value of D_1 by differentiating the lower-bound in (4.120) and setting equal to zero. We get

$$D_1^* = \left(\frac{c_{s_1}}{c_{s_2}}\left(\frac{3p}{(\beta_r - 2p)}\right)\right)^{\frac{\beta_r}{p+\beta_r}} SNR^{-\frac{p\beta_r}{p+\beta_r}} (4D_0)^{-\frac{p}{p+\beta_r}}, \quad p < \frac{1}{2}\beta_r, \tag{4.88}$$

where, for fair comparison, we fix the total number of channel uses and get $\beta_r'' = \frac{1}{4}\beta_r$. For the case when $p < \frac{1}{2}\beta_r$, substituting (4.88) in the lower-bound in (4.120) we get

$$E\left[D\right] \gtrapprox \min_{D_0} C.D_0^{-\frac{3p}{p+\beta_r}}.SNR^{-\frac{3p\beta_r}{p+\beta_r}} + D_0, \quad p < \frac{1}{2}\beta_r, \tag{4.89}$$

where C is a constant that does not depend on D_0 and the SNR. Differentiating and setting equal to zero we can get the expression for the optimizing D_0 as

$$D_0^* = C'.SNR^{-\frac{3p\beta_r}{4p+\beta_r}}, \quad p < \frac{1}{2}\beta_r. \tag{4.90}$$

Hence, from (4.90) we have

$$C'_{LB} SNR^{-\frac{3p\beta_r}{4p+\beta_r}} \lessapprox E\left[D\right] \lessapprox C'_{UB} SNR^{-\frac{3p\beta_r}{4p+\beta_r}}, \quad p < \frac{1}{2}\beta_r. \tag{4.91}$$

From (4.87) and (4.91) we conclude that the distortion exponent for the source diversity system is given by

$$\Delta_{RC-2R-SRC-AMP} = \max\left[\frac{2p\beta_r}{2p+\beta_r}, \frac{3p\beta_r}{4p+\beta_r}\right], \tag{4.92}$$

where the second term in (4.92) is the maximum for the case $p < \frac{1}{2}\beta_r$.□

4.3.2 Decode-and-Forward Relay Channel

We now analyze the decode-and-forward relay channel. The distortion exponents for the different schemes can be derived from the analysis presented in the previous sections. We collect the corresponding results in the following theorem

Theorem 12 *The distortion exponents of the decode-and-forward relay channel are*

- *For the single relay channel*

$$\Delta_{RC-1R-DEC} = \frac{2p\beta_r}{2p+\beta_r}. \tag{4.93}$$

- *For the M relays selection channel coding diversity*

$$\Delta_{RC-MR-DEC} = \frac{2(M+1)p\beta_r}{2\beta_r + (M+1)^2 p}. \tag{4.94}$$

- *For the channel coding with 2 relays, with the same time frame structure as in Fig. 4.4,*

$$\Delta_{RC-2R-OPTCH-AMP} = \frac{3p\beta_r}{3p+\beta_r}. \tag{4.95}$$

- *For the source coding diversity with 2 relays*

$$\Delta_{RC-2R-SRC-DEC} = \max\left[\frac{2p\beta_r}{2p+\beta_r}, \frac{3p\beta_r}{4p+\beta_r}\right]. \tag{4.96}$$

In summary, the distortion exponents for the decode-and-forward relay channel are the same as the amplify-and-forward relay channel.

4.4 Discussion

The distortion exponent for the various schemes analyzed in this Chapter are given in Table 4.1. From the results in Table 4.1 we can see that the channel coding diversity scheme always results in a higher distortion exponent than the source coding diversity scheme at any bandwidth expansion factor (the result is valid over both the multi-hop and relay channels). This means that, between source and channel coding, it is better to exploit diversity at the channel encoder level. Comparing the expressions for the distortion exponents for the single relay and M relay nodes we can see that increasing the number of relays does not always result in an increase in the distortion exponent, showing that there is a tradeoff between the quality (resolution) of the source encoder and the amount of cooperation (number of relays).

Figure 4.8 compares the distortion exponent for the various systems as a function of β_m for the multi-hop channel. The results in Figure 4.8 confirms that the channel coding diversity gives better distortion exponent than the source coding diversity. A similar observation was made in [52] for the case of parallel channels. Note that as β_m increases, the factor that limits the distortion exponent performance is the diversity (number of relays nodes). In this case (high β_m), the system is said to be an outage limited system as the outage probability, rather than the

Table 4.1: Distortion Exponents for the Amplify-and-Forward (Decode-and-Forward) Multi-Hop and Relay Channels.

	Multi-Hop Channels	Relay Channel
Single relay	$\frac{2p\beta_m}{p+2\beta_m}$	$\frac{2p\beta_r}{2p+\beta_r}$
Selective channel coding diversity with M relays	$\frac{4Mp\beta_m}{M(M+1)p+4\beta_m}$	$\frac{2(M+1)p\beta_r}{2\beta_r+(M+1)^2p}$
Channel coding diversity with 2 relays	$\frac{2p\beta_m}{p+\beta_m}$	$\frac{3p\beta_r}{3p+\beta_r}$
Source coding diversity with 2 relays	$\max\left[\frac{4p\beta_m}{3p+2\beta_m}, \frac{2p\beta_m}{p+2\beta_m}\right]$	$\max\left[\frac{2p\beta_r}{2p+\beta_r}, \frac{3p\beta_r}{4p+\beta_r}\right]$

quality of the source encoder, is the main limiting factor in the end-to-end distortion. Figure 4.8 shows that in this scenario, the distortion exponent performance is improved by increasing the number of relays so as to increase diversity. At low β_m the system is said to be quality limited as the quality of the source encoder (distortion under no outage), rather than the outage probability, is the main limiting factor in the end-to-end distortion. In this case, the gain from using a better source encoder, that has a higher resolution, is more significant than the gain from increasing the number of relay nodes. Figure 4.8 shows that in this scenario, the distortion exponent performance is improved by using only a single relay node allowing for the use of a higher resolution source encoder.

Figure 4.9 shows the distortion exponent versus β_r for the various relay channel schemes. Figure 4.9 confirms that the scheme with channel coding diversity yields better distortion exponent than the one with source coding diversity. As was the case for multi-hop schemes, as β_r increases, diversity becomes the limiting factor for the distortion exponent, in which case, Figure 4.9 shows that increasing the number of relays improves the distortion exponent results. Again, at low β_r, direct transmission (no-diversity) results in a lower end-to-end distortion which can be

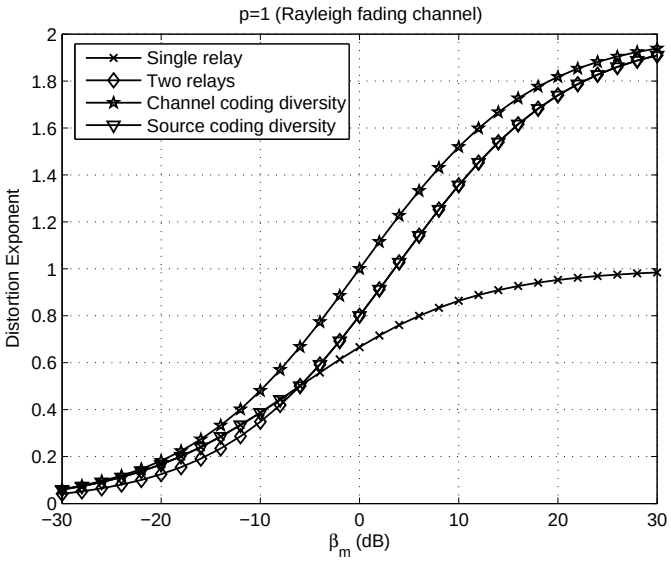

Figure 4.8: Distortion exponents for two-hop amplify-and-forward (decode-and-forward) protocol.

interpreted in the same way as for the multi-hop channel.

Appendix I Outage Analysis for Channel Coding diversity with 2 relays Multi-Hop Decode-and-Forward Scheme

Let $S \longrightarrow R_i$ and $R_i \longrightarrow D$ denote the channel between the source and the ith relay and the channel between the ith relay and the destination, respectively. Let $R_1, R_2 \longrightarrow D$ denote the channel between the two relays and the destination when both relays decode correctly. We calculate the outage probability by splitting the

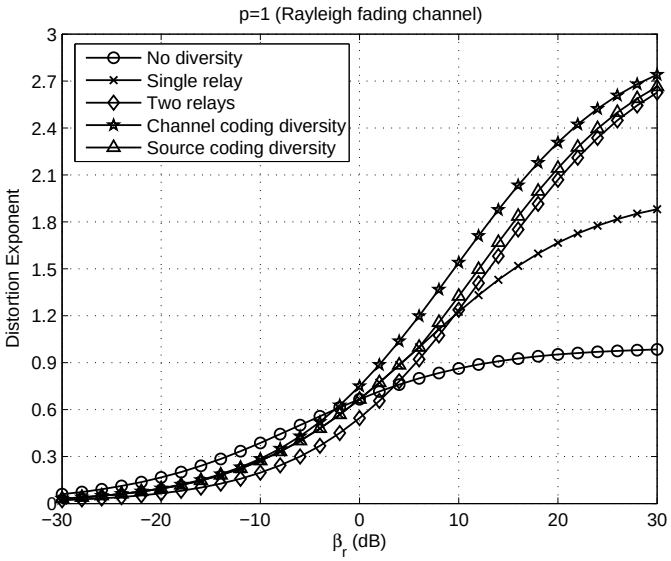

Figure 4.9: Distortion exponents for amplify-and-forward (decode-and-forward) relay channel.

outage event into disjoint events, i.e. $P_{outage} = P_{o_1} + P_{o_2} + P_{o_3} + P_{o_4}$, where

$$\begin{aligned} P_{o_1} &= \Pr\left[S \longrightarrow R_1 \text{ in outage},\ S \longrightarrow R_2 \text{ in outage}\right] \\ &= \Pr\left[S \longrightarrow R_1 \text{ in outage}\right].\Pr\left[S \longrightarrow R_2 \text{ in outage}\right] \\ &= \Pr\left[2\log(1+|h_{s,r_1}|^2 SNR) < R(D)\right].\Pr\left[2\log(1+|h_{s,r_2}|^2 SNR) < R(D)\right] \\ &\approx c_{o_1}\left(\frac{\exp(pR(D))}{SNR^{2p}}\right). \end{aligned} \tag{4.97}$$

$$\begin{aligned} &P_{o_2} \\ &= \Pr\left[S \longrightarrow R_1 \text{ in outage},\ S \longrightarrow R_2 \text{ not in outage},\ R_2 \longrightarrow D \text{ in outage}\right] \\ &= \Pr\left[S \longrightarrow R_1 \text{ in outage}\right].\Pr\left[S \longrightarrow R_2 \text{ not in outage}\right].\Pr\left[R_2 \longrightarrow D \text{ in outage}\right] \\ &\approx c_{o_2}\left(\frac{\exp(pR(D))}{SNR^{2p}}\right). \end{aligned} \tag{4.98}$$

$$
\begin{aligned}
&P_{o_3} \\
&= \Pr\left[S \longrightarrow R_2 \text{ in outage},\ S \longrightarrow R_1 \text{ not in outage},\ R_1 \longrightarrow D \text{ in outage}\right] \quad (4.99)\\
&\approx c_{o_3}\left(\frac{\exp(pR(D))}{SNR^{2p}}\right).
\end{aligned}
$$

$$
\begin{aligned}
&P_{o_4} \\
&= \Pr\left[S \longrightarrow R_1 \text{ not in outage},\ S \longrightarrow R_2 \text{ not in outage},\ R_1, R_2 \longrightarrow D \text{ in outage}\right] \\
&= \Pr\left[S \longrightarrow R_1 \text{ not in outage}\right].\Pr\left[S \longrightarrow R_2 \text{ not in outage}\right].\Pr\left[R_1, R_2 \longrightarrow D \text{ in outage}\right] \\
&\approx \Pr\left[2\log(1+\frac{1}{2}(|h_{r_1,d}|^2 SNR + |h_{r_2,d}|^2 SNR)) < R(D)\right], \qquad (4.100)
\end{aligned}
$$

where the factor $1/2$ in (4.100) is due to the loss in SNR because of the use of transmit diversity [40]. To calculate P_{o_4} in (4.100) we need to calculate the cdf of the random variable $|h_{r_1,d}|^2 SNR + |h_{r_2,d}|^2 SNR$. Let $W_1 = |h_{r_1,d}|^2 SNR$ and $W_2 = |h_{r_2,d}|^2 SNR$. The pdf of $W_1 + W_2$ can be computed as

$$
\begin{aligned}
f_{W_1+W_2}(w) &= \int_0^w f_{W_1}(\tau) f_{W_2}(w-\tau) d\tau \\
&\approx \frac{c_{11}c_{22}p^2}{SNR^{2p}} \int_0^w \tau^{p-1}(w-\tau)^{p-1} d\tau \qquad (4.101)\\
&= c_{11}c_{22}p^2 \frac{w^{2p-1}}{SNR^{2p}} B(p,p),
\end{aligned}
$$

where $B(.,.)$ is the Beta function [41]. The cdf of $W_1 + W_2$ can be computed as

$$
F_{W_1+W_2}(w) = \int_0^w f_{W_1+W_2}(\tau) d\tau = c_{33}\left(\frac{w}{SNR}\right)^{2p}, \qquad (4.102)
$$

from which we have

$$
P_{o_4} \approx c_{o_4}\left(\frac{\exp(pR(D))}{SNR^{2p}}\right). \qquad (4.103)
$$

Then, the outage probability is

$$P_{outage} = P_{o_1} + P_{o_2} + P_{o_3} + P_{o_4} = c_o \left(\frac{\exp(pR(D))}{SNR^{2p}} \right). \tag{4.104}$$

In the proof, we have assumed that x_{s_1} and x_{s_2} are independent zero-mean complex Gaussian with variance 1/2 per dimension. We can easily show that this choice of x_{s_1} and x_{s_2} is the optimal choice for maximizing the mutual information (minimizing the outage probability) by inspection of the individual outage events in (4.104).

Appendix II Distortion Exponent of the Suboptimal Detector for the Channel Coding Diversity Scheme

Let $W_1 = |h_{s,d}|^2 SNR$, $W_2 = \frac{|h_{s,r_1}|^2 SNR |h_{r_1,d}|^2 SNR}{|h_{s,r_1}|^2 SNR + |h_{r_1,d}|^2 SNR}$ and $W_3 = \frac{|h_{s,r_2}|^2 SNR |h_{r_2,d}|^2 SNR}{|h_{s,r_2}|^2 SNR + |h_{r_2,d}|^2 SNR}$. The outage probability of the suboptimal system is given by

$$
\begin{aligned}
&P_{outage} \\
&= \Pr\left[I_{sub} < R\right] \\
&= \Pr\left[\log(1+\max(W_1,W_2)) + \log(1+\max(W_1,W_3)) < R\right] \\
&= \Pr\Big[\{2\log(1+W_1) < R, W_1 > W_2, W_1 > W_3\} \bigcup \{\log(1+W_1) + \log(1+W_3) < R \\
&, W_1 > W_2, W_3 > W_1\} \bigcup \{\log(1+W_2) + \log(1+W_1) < R, W_2 > W_1, W_1 > W_3\} \\
&\bigcup \{\log(1+W_2) + \log(1+W_3) < R, W_2 > W_1, W_3 > W_1\}\Big] \\
&= \Pr\left[2\log(1+W_1) < R, W_1 > W_2, W_1 > W_3\right] + \Pr\Big[\log(1+W_1) + \log(1+W_3) < R \\
&, W_1 > W_2, W_3 > W_1\Big] + \Pr\left[\log(1+W_2) + \log(1+W_1) < R, W_2 > W_1, W_1 > W_3\right] \\
&+ \Pr\left[\log(1+W_2) + \log(1+W_3) < R, W_2 > W_1, W_3 > W_1\right],
\end{aligned}
\tag{4.105}
$$

where the last equality follows from the events being disjoint. In the last equation we used R instead of $R(D)$ for simplicity of presentation. The joint pdf of W_1, W_2 and W_3, which are independent random variables, is given by

$$
f(w_1, w_2, w_3) \approx c_j p^3 \left(\frac{w_1^{p-1} w_2^{p-1} w_3^{p-1}}{SNR^{3p}}\right), \tag{4.106}
$$

where c_j is a constant. To find the outage probability, we calculate the probability of the individual outage events in (4.105),

$$\begin{aligned}
P_1 =& \Pr[2\log(1+W_1) < R, W_1 > W_2, W_1 > W_3] \\
=& \int_{w_1=0}^{\exp(R/2)} \int_{w_3=0}^{w_1} \int_{w_2=0}^{w_1} f(w_1, w_2, w_3) dw_2 dw_3 dw_1 \\
\approx& \int_{w_1=0}^{\exp(R/2)} \int_{w_3=0}^{w_1} \int_{w_2=0}^{w_1} c_j p^3 \left(\frac{w_1^{p-1} w_2^{p-1} w_3^{p-1}}{SNR^{3p}} \right) dw_2 dw_3 dw_1 \\
=& \frac{c_j \exp\left(\frac{3pR}{2}\right)}{3SNR^{3p}}.
\end{aligned} \tag{4.107}$$

$$\begin{aligned}
P_2 =& \Pr[\log(1+W_1) + \log(1+W_3) < R, W_1 > W_2, W_3 > W_1] \\
\approx& \Pr[\log(W_1) + \log(W_3) < R, W_1 > W_2, W_3 > W_1] \\
=& \int_{w_1=0}^{\exp(R/2)} \int_{w_3=w_1}^{\frac{\exp(R)}{w_1}} \int_{w_2=0}^{w_1} f(w_1, w_2, w_3) dw_2 dw_3 dw_1 \\
\approx& \int_{w_1=0}^{\exp(R/2)} \int_{w_3=w_1}^{\frac{\exp(R)}{w_1}} \int_{w_2=0}^{w_1} c_j p^3 \left(\frac{w_1^{p-1} w_2^{p-1} w_3^{p-1}}{SNR^{3p}} \right) dw_2 dw_3 dw_1 \\
=& \frac{c_j p^2}{SNR^{3p}} \int_{w_1=0}^{\exp(R/2)} \int_{w_3=w_1}^{\frac{\exp(R)}{w_1}} w_1^{2p-1} w_3^{p-1} dw_3 dw_1 \\
=& \frac{2c_j \exp\left(\frac{3pR}{2}\right)}{3SNR^{3p}}.
\end{aligned} \tag{4.108}$$

$$\begin{aligned}
P_3 =& \Pr[\log(1+W_2) + \log(1+W_1) < R, W_2 > W_1, W_1 > W_3] \\
\approx& \Pr[\log(W_1) + \log(W_3) < R, W_1 > W_2, W_3 > W_1] \\
\approx& \frac{2c_j \exp\left(\frac{3pR}{2}\right)}{3SNR^{3p}}.
\end{aligned} \tag{4.109}$$

$$
\begin{aligned}
P_4 =& \Pr[\log(1+W_2)+\log(1+W_3)<R, W_2>W_1, W_3>W_1] \\
\approx& \Pr[\log(W_2)+\log(W_3)<R, W_2>W_1, W_3>W_1] \\
=& \int_{w_1=0}^{\exp(R/2)} \int_{w_2=w_1}^{\frac{\exp(R)}{w_1}} \int_{w_3=w_1}^{\frac{\exp(R)}{w_2}} f(w_1,w_2,w_3) dw_3 dw_2 dw_1 \\
\approx& \int_{w_1=0}^{\exp(R/2)} \int_{w_2=w_1}^{\frac{\exp(R)}{w_1}} \int_{w_3=w_1}^{\frac{\exp(R)}{w_2}} c_j p^3 \left(\frac{w_1^{p-1} w_2^{p-1} w_3^{p-1}}{SNR^{3p}} \right) dw_3 dw_2 dw_1 \\
=& \frac{4 c_j \exp\left(\frac{3pR}{2}\right)}{3 SNR^{3p}},
\end{aligned}
\tag{4.110}
$$

where we have $\lim_{w_1 \to 0^+} w_1^p \log w_1 = 0$ for $p \geq 1$. The outage probability for the suboptimal system is

$$
P_{outage} = P_1 + P_2 + P_3 + P_4 \approx \frac{c_m \exp\left(\frac{3pR}{2}\right)}{SNR^{3p}}, \tag{4.111}
$$

where c_m is a constant. The minimum expected end-to-end distortion can now be computed as

$$
\begin{aligned}
E[D] =& \min_D \{ P_{outage} + (1 - P_{outage}) \ D \} \\
\approx& \min_D \left\{ \frac{c_m \exp\left(\frac{3pR}{2}\right)}{SNR^{3p}} + \left(1 - \frac{c_m \exp\left(\frac{3pR}{2}\right)}{SNR^{3p}} \right) \ D \right\} \\
\approx& \min_D \left\{ \frac{c_m D^{\frac{-3p}{4\beta_r''}}}{SNR^{3p}} + \left(1 - \frac{c_m D^{\frac{-3p}{4\beta_r''}}}{SNR^{3p}} \right) \ D \right\} \\
\approx& \min_D \left\{ \frac{c_m D^{\frac{-3p}{4\beta_r''}}}{SNR^{3p}} + D \right\},
\end{aligned}
\tag{4.112}
$$

where $\beta_r'' = N_r''/K$ (refer to Fig. 4.7), D is the source encoder distortion and we have used both high SNR approximations and (4.3). Differentiating and setting equal to zero we get the optimizing distortion

$$
D^* = \left(\frac{4\beta_r''}{3 c_m p} \right)^{\frac{-4\beta_r''}{4\beta_r''+3p}} SNR^{\frac{-12\beta_r'' p}{4\beta_r''+3p}}. \tag{4.113}
$$

Substituting we get the distortion exponent for this suboptimal system as

$$
\Delta_{SUBOPTIMAL} = \frac{12\beta_r'' p}{4\beta_r'' + 3p}. \tag{4.114}
$$

For fair comparison the total number of channel uses is fixed and, thus, $\beta_r'' = \frac{1}{4}\beta_r$.

Appendix III Outage Analysis for Source Coding diversity with 2 relays Decode-and-Forward Relay Channel

The receiver applies an MRC detector on the received data to detect x_{s_1} and x_{s_2}. Let $W_1 = |h_{s,d}|^2 SNR$, $W_2 = \frac{|h_{s,r_1}|^2 SNR |h_{r_1,d}|^2 SNR}{|h_{s,r_1}|^2 SNR + |h_{r_1,d}|^2 SNR}$ and $W_3 = \frac{|h_{s,r_2}|^2 SNR |h_{r_2,d}|^2 SNR}{|h_{s,r_2}|^2 SNR + |h_{r_2,d}|^2 SNR}$. The minimum expected end-to-end distortion is given by

$$
\begin{aligned}
&E[D] \approx \\
&\min_{D_0,D_1} \Pr\left[\, \log(1+W_1+W_2) < R_{md}(D_0,D_1)/2, \log(1+W_1+W_3) < R_{md}(D_0,D_1)/2\right] \\
&+ \Bigg(\Pr\left[\, \log(1+W_1+W_2) < R_{md}(D_0,D_1)/2, \log(1+W_1+W_3) > R_{md}(D_0,D_1)/2\right] \\
&+ \Pr\left[\, \log(1+W_1+W_2) > R_{md}(D_0,D_1)/2, \log(1+W_1+W_3) < R_{md}(D_0,D_1)/2\right] \Bigg) D_1 \\
&+ \Pr\left[\, \log(1+W_1+W_2) > R_{md}(D_0,D_1)/2, \log(1+W_1+W_3) > R_{md}(D_0,D_1)/2\right] D_0,
\end{aligned}
\tag{4.115}
$$

where R_{md}, D_0 and D_1 are as introduced in Section 4.1. To calculate the minimum expected distortion we need to calculate the following probabilities in (4.115)

$$
\begin{aligned}
P_1' =& \Pr\left[\, \log(1+W_1+W_2) < R_{md}(D_0,D_1)/2, \log(1+W_1+W_3) < R_{md}(D_0,D_1)/2\right] \\
=& \Pr\left[\, \log(1+W_1+\max(W_2,W_3)) < R_{md}(D_0,D_1)/2\right] \\
\approx& c_{s1} \frac{1}{SNR^{3p}} \exp\left(\frac{3p}{2} R_{md}(D_0,D_1)\right).
\end{aligned}
\tag{4.116}
$$

$$
\begin{aligned}
P_2' =& \Pr\left[\ \log(1+W_1+W_2) > R_{md}(D_0,D_1)/2, \log(1+W_1+W_3) > R_{md}(D_0,D_1)/2\right] \\
=& \Pr\left[\ \log(1+W_1+\min(W_2,W_3)) > R_{md}(D_0,D_1)/2\right] \\
=& 1 - \Pr\left[\ \log(1+W_1+\min(W_2,W_3)) < R_{md}(D_0,D_1)/2\right] \\
\approx& 1 - c_{s2}\frac{1}{SNR^{2p}}\exp\left(pR_{md}(D_0,D_1)\right).
\end{aligned}
\tag{4.117}
$$

$$
\begin{aligned}
P_3' =& \Pr\left[\ \log(1+W_1+W_2) < R_{md}(D_0,D_1)/2, \log(1+W_1+W_3) > R_{md}(D_0,D_1)/2\right] \\
&+ \Pr\left[\ \log(1+W_1+W_2) > R_{md}(D_0,D_1)/2, \log(1+W_1+W_3) < R_{md}(D_0,D_1)/2\right] \\
=& 1 - P_1' - P_2' \\
\approx& c_{s2}\frac{1}{SNR^{2p}}\exp\left(pR_{md}(D_0,D_1)\right) - c_{s1}\frac{1}{SNR^{3p}}\exp\left(\frac{3p}{2}R_{md}(D_0,D_1)\right) \\
\approx& c_{s2}\frac{1}{SNR^{2p}}\exp\left(pR_{md}(D_0,D_1)\right).
\end{aligned}
\tag{4.118}
$$

The minimum expected distortion in (4.115) can now be calculated as

$$
\begin{aligned}
E[D] \approx& \min_{D_0,D_1}\Bigg\{c_{s1}\frac{1}{SNR^{3p}}\exp\left(\frac{3p}{2}R_{md}(D_0,D_1)\right) + c_{s2}\frac{1}{SNR^{2p}}\exp\left(pR_{md}(D_0,D_1)\right)\ D_1 \\
&+ \left(1 - c_{s2}\frac{1}{SNR^{2p}}\exp\left(pR_{md}(D_0,D_1)\right)\right)\ D_0\Bigg\} \\
\approx& \min_{D_0,D_1}\Bigg\{c_{s1}\frac{1}{SNR^{3p}}\exp\left(\frac{3p}{2}R_{md}(D_0,D_1)\right) + \\
&\qquad c_{s2}\frac{1}{SNR^{2p}}\exp\left(pR_{md}(D_0,D_1)\right)\ D_1 + D_0\Bigg\}.
\end{aligned}
\tag{4.119}
$$

Substituting from (4.6) yields upper- and lower-bound for the minimum expected end-to-end distortion as

$$
\begin{aligned}
E[D] &\gtrapprox \min_{D_0,D_1}\frac{c_{s1}}{SNR^{3p}}\left(\frac{1}{4D_0D_1}\right)^{\frac{3p}{4\beta_r''}} + \frac{c_{s2}}{SNR^{2p}}\left(\frac{1}{4D_0D_1}\right)^{\frac{p}{2\beta_r''}}.D_1 + D_0 \\
E[D] &\lessapprox \min_{D_0,D_1}\frac{c_{s1}}{SNR^{3p}}\left(\frac{1}{2D_0D_1}\right)^{\frac{3p}{4\beta_r''}} + \frac{c_{s2}}{SNR^{2p}}\left(\frac{1}{2D_0D_1}\right)^{\frac{p}{2\beta_r''}}.D_1 + D_0.
\end{aligned}
\tag{4.120}
$$

Chapter 5

Distributed Detection in Wireless Networks: A Sensor or a Relay?

Lately, sensor networks have gained a lot of interest due to their wide range of applications and this has increased the thrill toward the study of sensor networks. The applications of sensor networks include monitoring environmental conditions such as temperature, military applications such as battlefield surveillance, health monitoring, and many other applications.

Our interest in this Chapter will be focused on how to deploy relay nodes in the sensor networks. We assume dumb sensor nodes, which means that the sensor nodes do not have processing capabilities of the sensed measurements, which can be due to lack of knowledge of the measurement data models under each hypothesis or due to limited processing capabilities of the nodes [68]. Based on our model assumption, some sensor nodes measurements will be provide more information to the fusion center. So some sensors are assumed to be "more-informative" and some sensors are assumed to be "less-informative" to the fusion center. The use of relay nodes, instead of some of the sensor nodes that are less-informative to the

fusion center, to relay measurement for the more-informative sensor nodes will be considered.

The problem of distributed detection in the wireless sensor networks is considered. There exists a plethora of works on distributed detection in sensor network. In [69], the authors considered the problem of how to determine the density of sensor nodes in a linear network where nodes are placed on a line. They study the problem of whether to employ many low-cost, low-power sensors or few high-cost, high-power sensors. The work in [69] considered the cases of deterministic signals and correlated Gaussian processes both corrupted by Gaussian noise. For the case of deterministic signals corrupted by Gaussian noise it was proved that the performance, measured in terms of the *error exponent*, improved by increasing the density of the sensor nodes. For the other case of correlated Gaussian process corrupted by Gaussian noise, it was proved that there exists an optimal density that maximizes the error exponent. In [70], closed-form expressions for the error exponents of the Neyman-Pearson detector are derived for the detection of Gauss-Markov signals corrupted by noise. The work in [71] considered the problem of distributed detection with a rate constraint. The authors proved that the use of more sensors, each signaling a binary signal, can be optimal under certain conditions compared to the case of having less sensor nodes each sending at a higher rate to the fusion center.

Some works on distributed detection focused on the problem of energy-efficiency in the sensor networks by allowing some sensor nodes to censor their transmission [72, 73]. These works considered the tradeoff between the performance of the detector at the fusion center to the energy consumption of the sensor network. Other works have considered the problem of distributed detection with correlated

sensor nodes signals [74–78]. These works mostly focused on the study of deriving optimal fusion rules at the fusion center or the conditions under which some detectors turn to be optimal. The work in [68] studied the type-based distributed (decentralized) detection in the sensor networks over parallel access channels (PAC) and multiple access channels (MAC).

Considering the application of relaying schemes for distributed detection, [79] has considered the use of relaying to improve the energy-efficiency of the sensor network. The work in [79] also proposed a consensus protocol and analyzes its energy consumption if cooperation is present to improve the energy-efficiency of the sensor network.

In this Chapter we the performance of two protocols will be compared. In Protocol I, each node directly transmits its measurement to the fusion center. In Protocol II, we allocate the resources of some of the less-informative sensor nodes to relay nodes, which relay the measurements of the more-informative sensor nodes. We will compare the performance of the two protocols in terms of the probability of detection error and characterize the regions in terms of the measurement noise and the communication noise variances where one protocol performs better than the other protocol [80, 81].

5.1 System Model

In this section, the system model for the wireless sensor network is presented. The sensor network is assumed to have N sensor nodes that are used to monitor a certain phenomenon. The sensor nodes send their sensed measurements to a fusion center to make decisions about the state of nature observed by the sensor network. The sensor nodes are assumed to be dumb, i.e., they can not apply any precessing

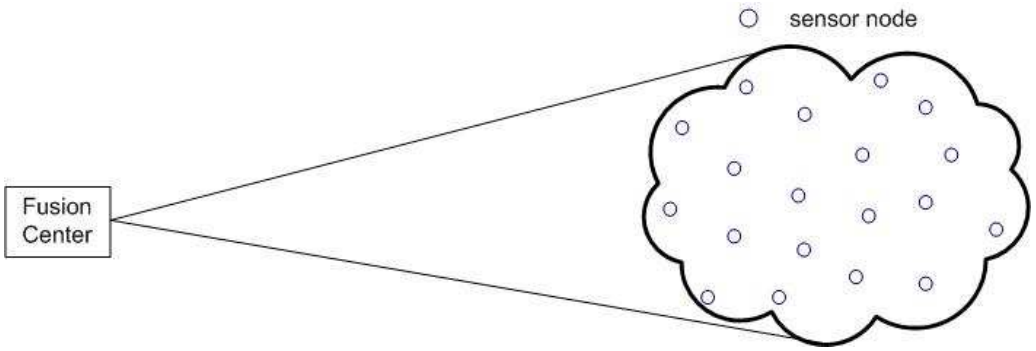

Figure 5.1: A Schematic Diagram for the Wireless Sensor Network.

to the sensed measurement. In other words, the sensor nodes sense the medium and directly transmit their measurements to the fusion center where decisions are made. The wireless sensor networks is as depicted in Fig. 5.1. We assume a binary hypotheses detection problem, i.e., the fusion center makes decisions between two hypotheses, namely, H_0 and H_1.

The i-th sensor node measurement is x_i, $i = 1, \cdots, N$. The x_i's are assumed to be mutually independent under each hypothesis. The data model under each hypothesis is given by

$$\begin{aligned} H_0 &: \; x_i \sim \mathcal{CN}\left(0, \sigma^2\right) \\ H_1 &: \; x_i \sim \mathcal{CN}\left(m_i, \sigma^2\right), \end{aligned} \tag{5.1}$$

where σ^2 can be thought of as the measurement noise variance at any sensor node. The notation $x \sim \mathcal{CN}\left(m, \sigma^2\right)$ is used to denote that x is a complex Gaussian random variable with mean m and variance $\sigma^2/2$ per dimension.

In the sequel, the performance of two transmission protocols from the sensor nodes to the fusion center will be compared. In the first protocol, which is denoted by Protocol I, each sensor node directly transmits its measurement to the fusion center without the help of any other node in the network. In the second protocol,

which is denoted by Protocol II, relay nodes are used instead of some of the less-informative sensor nodes to forward information of the more-informative sensor nodes. We will derive expressions of the probability of detection error P_e for the previous two protocols. Based on the derived expressions, it can be decide which of the two protocols will result in a better performance in terms of P_e.

5.1.1 Protocol I System Model

In Protocol I, each sensor node directly transmits its measurement to the fusion center. Let h_{s_iF} denote the channel gain from the i-th sensor node to the fusion center, which is modeled as zero-mean circularly symmetric complex Gaussian random variable with variance $1/2$ per dimension, i.e., Rayleigh flat-fading is assumed. The channel gains from the sensor nodes to the fusion center are assumed to be independent. The received data at the fusion center due to the i-th sensor node transmission is given by

$$y_{s_iF} = h_{s_iF}\sqrt{P_i}x_i + n_{s_iF}, \tag{5.2}$$

where P_i is selected to satisfy a power constraint at the sensor node and n_{s_iF} is a receiver additive white Gaussian noise. The term n_{s_iF} is modeled as zero-mean circularly symmetric complex Gaussian random variable with variance $N_0/2$ per dimension.

5.1.2 Protocol II System Model

In Protocol II, relay nodes will be deployed in the network, which will be used instead of the sensor nodes that their measurements do not provide the fusion center with a lot of information about the observed phenomenon. Again, dumb

sensor nodes are assumed, which means that a sensor node is not able to process the sensed measurement.

If node j works as a relay for sensor i, then the received signal at the fusion center due to node j transmission is given by

$$y_{jF} = h_{jF}\sqrt{P_i}x_i + n_{jF}, \quad j \in \mathcal{R} \tag{5.3}$$

where for simplicity of analysis the noise from node i to node j is neglected. Hence, node j transmits a clean version of the measurement of node i to the fusion center[1]. h_{jF} denotes the channel gain from the j-th relay node to the fusion center and is modeled as zero-mean circularly symmetric complex Gaussian random variable with variance 1/2 per dimension and $\mathcal{R}$ denotes the subset of relay nodes.

5.2 Performance Analysis

In this section, performance analysis of the two protocols presented in Section 5.1 will be provided. The probability of detection error P_e will be used as the performance measure. Comparing the P_e expressions for the two previously presented protocols will enable the selection of the better protocol in terms of the

[1]If the amplify-and-forward protocol is used at the sensor nodes and assuming that the distance between the sensor node and the node that relays its measurement is much less than the distance between any sensor node and the fusion center then the noise coming from the sensor node to relay node communication link can be neglected compared to the noise coming from the sensor (relay) node to fusion center link. In the case of amplify-and-forward protocol, the signal to noise ratio (SNR) of sensor-relay-fusion center link will be a scaled harmonic mean of the sensor-relay and relay-fusion center links SNRs, which can be tightly approximated to be the SNR of the relay-fusion center link for the case of relay node very close to the sensor node as presented in Chapter 2. This enables us to neglect the noise coming from the sensor-relay communication link.

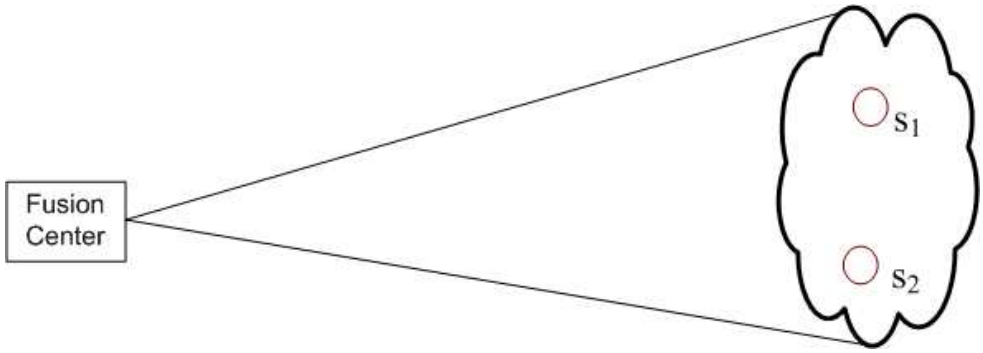

Figure 5.2: A Two-Sensor Network.

performance measure used. To illustrate the idea, we will start with the analysis of a two-sensor network over additive white Gaussian noise (AWGN) channel. Then, the analysis will be extended to the multi-node wireless sensor network over Rayleigh flat-fading channel model.

5.2.1 Performance Analysis over AWGN Channels

In this section, a two-sensor network as shown in Fig. 5.2 will be considered. The analysis is easily extendable to the multi-node sensor network over AWGN channels. Through this example, more insights into the problem of the multi-node wireless sensor network can be gained. For the case of AWGN, the same model as in (5.1), (5.2), and (5.3) will be used with $h_{s_iF} = 1$ for all i. Without loss of generality, all the random variables in (5.1), (5.2), and (5.3) are assumed to be real with the same means and variances as described before, i.e., the m_i's are now assumed to be real and n_{s_iF} is a zero-mean Gaussian random variable with variance N_0 for all i's.

In Fig. 5.2, the signal from sensor 1 is assumed to have a mean of m_1 and the signal from sensor 2 is assumed to have a mean of m_2 both under hypothesis

H_1. Without loss of generality we assume that $m_1 > m_2$. Therefore, we assume that the measurement coming from sensor 1 is more-informative about the state of nature than the measurement coming from sensor 2.

We will consider comparing the two protocols presented in Section 5.1. To gain more insights into the problem, consider two extreme cases as follows. The first extreme case is $m_2 = 0$. In this case, the measurement from sensor 2 does not provide any information to the fusion center about the state of nature because the data model at sensor 2 is the same under both hypotheses. In this case, Protocol II will have a better performance as compared to Protocol I. The second extreme case is when $m_2 = m_1$. In this case, the measurements from both sensors are of equal importance to the fusion center. Therefore, Protocol I will have a better performance if compared to Protocol II. These statements will be rigorously proved in the following subsections.

Protocol I Probability of Detection Error

Let $P_{e,I}^{AWGN}$ denote the probability of detection error of Protocol I over AWGN channels. The probability of detection error is defined as $P_{e,I}^{AWGN} = \Pr\{\widehat{H} \neq H\}$, where H is the true state of nature and $\widehat{H}$ is the estimated state of nature at the fusion center.

Let $\pi_0 = \Pr\{H = H_0\}$ and $\pi_1 = \Pr\{H = H_1\}$ denote the prior probabilities. Without loss of generality, we assume that $\pi_0 = \pi_1 = 1/2$. The variable P_i in (5.2) is selected such that the average power of each sensor node equals a power constraint P. Therefore, we have

$$P = \pi_0 P_i \sigma^2 + \pi_1 P_i \left(m_i^2 + \sigma^2\right) \rightarrow P_i = \frac{P}{\sigma^2 + \frac{1}{2} m_i^2}. \tag{5.4}$$

The data model for the received data under each hypothesis is given by

$$\begin{aligned} H_0 :\ & y_{s_iF} \sim \mathcal{N}\left(0, P_i\sigma^2 + N_0\right) \\ H_1 :\ & y_{s_iF} \sim \mathcal{N}\left(\sqrt{P_i}m_i, P_i\sigma^2 + N_0\right). \end{aligned} \tag{5.5}$$

Define $\sigma_i^2 = P_i\sigma^2 + N_0$, $i = 1, 2$. Using $P_{e,I}^{AWGN}$ as the performance measure, the optimal decision rule is the likelihood ratio (LR) test, which is given by

$$\frac{e^{-\sum_{i=1}^{2}\frac{1}{2\sigma_i^2}\left(y_{s_iF}-\sqrt{P_i}m_i\right)^2}}{e^{-\sum_{i=1}^{2}\frac{1}{2\sigma_i^2}y_{s_iF}^2}} \underset{\widehat{H}=H_0}{\overset{\widehat{H}=H_1}{\gtrless}} 1. \tag{5.6}$$

The decision rule can be further simplified to

$$q_1 \underset{\widehat{H}=H_0}{\overset{\widehat{H}=H_1}{\gtrless}} \frac{1}{2}\left(\frac{P_1m_1^2}{\sigma_1^2} + \frac{P_2m_2^2}{\sigma_2^2}\right), \tag{5.7}$$

where

$$q_1 = \frac{1}{\sigma_1^2}\sqrt{P_1}m_1y_{s_1F} + \frac{1}{\sigma_2^2}\sqrt{P_2}m_2y_{s_2F}.$$

The probability density functions of the random variable q_1 under each hypothesis are given by

$$\begin{aligned} P_{H_0}(q_1) &\sim \mathcal{N}\left(0, \frac{P_1m_1^2}{\sigma_1^2} + \frac{P_2m_2^2}{\sigma_2^2}\right) \\ P_{H_1}(q_1) &\sim \mathcal{N}\left(\frac{P_1m_1^2}{\sigma_1^2} + \frac{P_2m_2^2}{\sigma_2^2}, \frac{P_1m_1^2}{\sigma_1^2} + \frac{P_2m_2^2}{\sigma_2^2}\right), \end{aligned} \tag{5.8}$$

where $P_{H_k}(q_1)$ is the probability density function of q_1 under hypothesis H_k, $k = 0, 1$.

The probability of detection error can be calculated as

$$\begin{aligned} P_{e,I}^{AWGN} &= \pi_0 \Pr\{\widehat{H} = H_1 | H = H_0\} + \pi_1 \Pr\{\widehat{H} = H_0 | H = H_1\} \\ &= Q\left(\frac{1}{2}\sqrt{\frac{P_1m_1^2}{\sigma_1^2} + \frac{P_2m_2^2}{\sigma_2^2}}\right), \end{aligned} \tag{5.9}$$

where $Q(u) = \frac{1}{\sqrt{2\pi}} \int_u^\infty \exp\left(-\frac{t^2}{2}\right) dt$ is the Gaussian Q-function [41]. Substituting for the P_i's from (5.4) we get

$$P_{e,I}^{AWGN} = Q\left(\frac{1}{2}\sqrt{\frac{Pm_1^2}{P\sigma^2 + \left(\sigma^2 + \frac{1}{2}m_1^2\right)N_0} + \frac{Pm_2^2}{P\sigma^2 + \left(\sigma^2 + \frac{1}{2}m_2^2\right)N_0}}\right). \tag{5.10}$$

Protocol II Probability of Detection Error

In this case, a relay is used instead of sensor 2 to forward the signal from sensor 1. Let $P_{e,II}^{AWGN}$ denote the probability of detection error of Protocol II over AWGN channels. Define a 2×1 received data vector $\mathbf{y} = [y_{s_1F}, y_{s_2F}]^T$. The fusion center should decide between the two hypotheses based on the received vector $\mathbf{y}$. In Protocol II, the components of the vector $\mathbf{y}$ are no longer independent since the measurement of sensor 1 will be forwarded by the relay node. In this case, the probability density functions of the vector $\mathbf{y}$ under both hypothesis are given by

$$\begin{aligned} H_0 &: \ \mathbf{y} \sim \mathcal{N}(\mathbf{0}, \mathbf{C}) \\ H_1 &: \ \mathbf{y} \sim \mathcal{N}(\mathbf{m}, \mathbf{C}), \end{aligned} \tag{5.11}$$

where

$$\mathbf{C} = \begin{pmatrix} \sigma_1^2 & P_1\sigma^2 \\ P_1\sigma^2 & \sigma_1^2 \end{pmatrix} \tag{5.12}$$

is the auto-covariance matrix of the vector $\mathbf{y}$ and is the same under both hypotheses, $\sigma_i^2 = P_i\sigma^2 N_0$, $i = 1, 2$, $\mathbf{0} = [0, 0]^T$ and $\mathbf{m} = \left[\sqrt{P_1}m_1, \sqrt{P_1}m_1\right]^T$.

Using the probability of detection error as a performance measure, the optimal decision rule is the LR test given by

$$\frac{e^{-\frac{1}{2}(\mathbf{y}-\mathbf{m})^T\mathbf{C}^{-1}(\mathbf{y}-\mathbf{m})}}{e^{-\frac{1}{2}\mathbf{y}^T\mathbf{C}^{-1}\mathbf{y}}} \underset{\widehat{H}=H_0}{\overset{\widehat{H}=H_1}{\gtrless}} 1. \tag{5.13}$$

Simplifying, we get

$$\mathbf{m}^T\mathbf{C}^{-1}\mathbf{y} \underset{\widehat{H}=H_0}{\overset{\widehat{H}=H_1}{\gtrless}} \frac{1}{2}\mathbf{m}^T\mathbf{C}^{-1}\mathbf{m}. \tag{5.14}$$

The probability of detection error of Protocol II can now be given as

$$\begin{aligned} P_{e,II}^{AWGN} &= Q\left(\frac{1}{2}\sqrt{\mathbf{m}^T\mathbf{C}^{-1}\mathbf{m}}\right) \\ &= Q\left(\frac{1}{2}\sqrt{\frac{2Pm_1^2}{2P\sigma^2 + \left(\sigma^2 + \frac{1}{2}m_1^2\right)N_0}}\right). \end{aligned} \tag{5.15}$$

Now, we will consider comparing the probability of detection error expressions in (5.10) and (5.15). Note that the $Q(\cdot)$ is a monotonically decreasing function of its argument. Hence, the protocol that has a higher argument inside the Q-function will have a better performance. Therefore, to compare the performance of the two protocols, it is sufficient to compare the arguments of the Q-functions in (5.10) and (5.15).

A first thing to note is that the following inequality holds

$$\frac{2Pm_1^2}{P\sigma^2 + \left(\sigma^2 + \frac{1}{2}m_1^2\right)N_0} > \frac{2Pm_1^2}{2P\sigma^2 + \left(\sigma^2 + \frac{1}{2}m_1^2\right)N_0} > \frac{Pm_1^2}{P\sigma^2 + \left(\sigma^2 + \frac{1}{2}m_1^2\right)N_0}, \tag{5.16}$$

from which it is clear that Protocol II is better than Protocol I if $m_2 = 0$, which corresponds to the lower-bound in (5.16). Also, Protocol I is better than Protocol II if $m_2 = m_1$, which corresponds to the upper-bound in (5.16). For a general value of m_2, Protocol II is better than Protocol I if

$$\frac{2Pm_1^2}{2P\sigma^2 + \left(\sigma^2 + \frac{1}{2}m_1^2\right)N_0} > \frac{Pm_1^2}{P\sigma^2 + \left(\sigma^2 + \frac{1}{2}m_1^2\right)N_0} + \frac{Pm_2^2}{P\sigma^2 + \left(\sigma^2 + \frac{1}{2}m_2^2\right)N_0} \tag{5.17}$$

and vice versa.

With our assumption of having $m_1 > m_2$, the measurement of the first sensor node is more-informative to the fusion center than the measurement of the second

sensor node. Protocol I, in which each sensor node sends its measurement, delivers measurements from more sensor nodes to the fusion center than Protocol II. However, Protocol II guarantees higher reliability for the more-informative measurement coming from sensor 1. The extreme case of having $m_2 = 0$, is the case where the measurement from sensor 2 contains no information (in this case, we have the same data model at the second sensor under both hypotheses), in which case Protocol II results in a better performance. In this case, the reliability of the measurement from sensor 1 is increased by transmitting the measurement twice to the fusion center. The other extreme case of having $m_2 = m_1$ is a case where the measurements from both sensors are of equal importance. In this case, it is better for sensor 2 to send its measurement than to use a relay to forward the measurement of sensor 1, and in this case Protocol I results in a better performance.

An N-Sensor Network

The analysis presented above can be extended to the case of sensor network with N sensor nodes communicating over AWGN channels each with mean m_i, $i = 1, \cdots, N$. In this case we will have three different subsets of nodes. Let $\mathcal{T}$ denote the subset of sensor nodes that are not helped by relay nodes, $\mathcal{H}$ denote the subset of sensor nodes that are helped by relay nodes, and $\mathcal{L}$ denote the subset of relay nodes. If each sensor node is restricted to have at most one node to relay its information then $|\mathcal{H}| = |\mathcal{L}|$. In this case, the probability of detection error expression can be given by

$$P_e^{AWGN} = Q\left(\frac{1}{2}\sqrt{\sum_{i\in\mathcal{H}} \frac{2Pm_i^2}{2P\sigma^2 + \left(\sigma^2 + \frac{1}{2}m_i^2\right)N_0} + \sum_{i\in\mathcal{T}} \frac{Pm_i^2}{P\sigma^2 + \left(\sigma^2 + \frac{1}{2}m_i^2\right)N_0}}\right). \tag{5.18}$$

The question now is how to partition the set of sensor nodes for an N-sensor network communicating over AWGN channel to minimize the probability of detection error at the fusion center. An algorithm for partition the set of sensor nodes under the restriction of having at most one relay node to help any sensor node is given in Table 5.1. The algorithm given in Table 5.1 can be proved to yield the optimal partitioning by proving that moving any node from one subset to another subset will always result in a system performance degradation in terms of the probability of detection error.

5.2.2 Performance Analysis over Rayleigh Flat-Fading Channels

In this section the performances of Protocol I and Protocol II over wireless Rayleigh flat-fading channels are considered. In the case of Rayleigh flat-fading channel model, it is very difficult to get closed-form expressions for the probability of detection error similar to those derived in Section 5.2.1. Therefore, we consider a large sensor network where the number of sensor nodes N is very large, which enables the derivation of asymptotic approximations for the probability of detection error expressions. For simplicity of presentation, the sensor network is assumed to be divided into two subsets of sensor nodes of equal cardinality, namely, $\mathcal{S}$ and $\mathcal{R}$, each has $N/2$ sensor nodes. Sensor nodes in subset $\mathcal{S}$ have a mean of m_S and sensor nodes in subset $\mathcal{R}$ have a mean of m_R. We consider that model of having two subsets of sensor nodes of equal size for sake of simplicity of presentation. However, the analysis presented here can be generalized if we have a different partitioning of the sensor nodes.

Table 5.1: An algorithm for partitioning the set of N sensor nodes communicating over AWGN channel if each sensor node is restricted to have at most one relay node.

1. Initialization: assign all of the sensor nodes to the subset $\mathcal{T}$, which is the subset of sensor nodes that are not helped by any relay node. The subsets $\mathcal{H}$ and $\mathcal{L}$ are empty at the beginning.
2. Arrange the sensor nodes in the subset $\mathcal{T}$ in a descending order according to their means such that $m_i \geq m_j$ for all $i < j$, $i = 1, \cdots, \lvert\mathcal{T}\rvert$, where $\lvert\mathcal{T}\rvert$ is the cardinality of the subset $\mathcal{T}$.
3. For the sensor nodes with the maximum mean m_1 and minimum mean $m_{\lvert\mathcal{T}\rvert}$ in the subset $\mathcal{T}$, use equation (5.17) with $m_2 = m_{\lvert\mathcal{T}\rvert}$ to determine whether it is better to use a relay node for helping the sensor node with mean m_1 or use the sensor node with mean $m_{\lvert\mathcal{T}\rvert}$ to send its measurement. If the use of a relay node is better, then remove the sensor node with mean $m_{\lvert\mathcal{T}\rvert}$ from the subset $\mathcal{T}$. Then, remove the sensor node with mean m_1 from the subset $\mathcal{T}$, put it in the subset $\mathcal{H}$ and put a relay in the subset $\mathcal{L}$ for helping in forwarding its information. If it is better to have the sensor node with mean $m_{\lvert\mathcal{T}\rvert}$ sending its measurement then exist the partitioning algorithm.
4. Repeat Step 2 if the subset $\mathcal{T}$ is nonempty.

Protocol I Probability of Detection Error

Let $P_{e,I}^{Ray}$ denote the probability of detection error of Protocol I over Rayleigh flat-fading channels. The data model for the received data under each hypothesis is given by

$$\begin{aligned} H_0 &: \; y_{s_iF} \sim \mathcal{CN}\left(0, P_i|h_{s_iF}|^2\sigma^2 + N_0\right) \\ H_1 &: \; y_{s_iF} \sim \mathcal{CN}\left(\sqrt{P_i}h_{s_iF}m_i, P_i|h_{s_iF}|^2\sigma^2 + N_0\right), \end{aligned} \tag{5.19}$$

where each m_i is either m_S or m_R.

With the probability of detection error as a performance measure and assuming perfect channel state information (CSI) at the fusion center, the optimal decision rule is the LR test given by

$$\frac{e^{-\sum_{i=1}^{N}\frac{1}{P_i|h_{s_iF}|^2\sigma^2+N_0}\left|y_{s_iF}-\sqrt{P_i}h_{s_iF}m_i\right|^2}}{e^{-\sum_{i=1}^{N}\frac{1}{P_i|h_{s_iF}|^2\sigma^2+N_0}\left|y_{s_iF}\right|^2}} \underset{\widehat{H}=H_0}{\overset{\widehat{H}=H_1}{\gtrless}} 1, \tag{5.20}$$

where we assumed equal priors, i.e., $\pi_0 = \pi_1 = 1/2$. The decision rule in (5.20) can be simplified to

$$\begin{aligned} \sum_{i=1}^{N}\frac{1}{P_i|h_{s_iF}|^2\sigma^2+N_0}\left(\sqrt{P_i}y_{s_iF}h_{s_iF}^*m_i^* + \sqrt{P_i}y_{s_iF}^*h_{s_iF}m_i\right) \\ \underset{\widehat{H}=H_0}{\overset{\widehat{H}=H_1}{\gtrless}} \sum_{i=1}^{N}\frac{1}{P_i|h_{s_iF}|^2\sigma^2+N_0}P_i\left|m_i\right|^2\left|h_{s_iF}\right|^2. \end{aligned} \tag{5.21}$$

The probability of detection error expression can be found to be given by

$$\begin{aligned} P_{e,I}^{Ray} &= E\left\{Q\left(\frac{1}{2}\sqrt{\sum_{i=1}^{N}\frac{P_i\left|h_{s_iF}\right|^2\left|m_i\right|^2}{P_i\left|h_{s_iF}\right|^2\sigma^2+N_0}}\right)\right\} \\ &= E\left\{Q\left(\frac{1}{2}\sqrt{\sum_{i\in\mathcal{S}}\frac{P_S\left|h_{s_iF}\right|^2\left|m_S\right|^2}{P_S\left|h_{s_iF}\right|^2\sigma^2+N_0}+\sum_{i\in\mathcal{R}}\frac{P_R\left|h_{s_iF}\right|^2\left|m_R\right|^2}{P_R\left|h_{s_iF}\right|^2\sigma^2+N_0}}\right)\right\}, \end{aligned} \tag{5.22}$$

where

$$P_S = \frac{P}{\sigma^2 + \frac{1}{2}m_S^2}$$

and

$$P_R = \frac{P}{\sigma^2 + \frac{1}{2}m_R^2}.$$

The expectation in (5.22) is taken over the channel statistics. Finding a closed-form expression for the expectation in (5.22) is very difficult even for the simple case of having $N = 2$. This motivates us to consider a large sensor network in which the number of sensor nodes is very large which enables the calculation of asymptotic approximation for the probability of detection error. For such a large network, define the random variable u as

$$u = \sum_{i=1}^{N} \frac{P_i \left|h_{s_iF}\right|^2 \left|m_i\right|^2}{P_i \left|h_{s_iF}\right|^2 \sigma^2 + N_0}, \tag{5.23}$$

which is the summation inside the argument of the Q-function of (5.22). The random variable u is the summation of $N/2$ i.i.d. random variables[2], which can be approximated to be a Gaussian random variable. This results from using the central limit theory (CLT) [82]. The probability of detection error is now given by

$$P_{e,I}^{Ray} = E\left\{Q\left(\frac{1}{2}\sqrt{u}\right)\right\}. \tag{5.24}$$

To get the approximation for the expression in (5.24), we need to calculate the mean and the variance of the random variable u. The mean of u can be found as

[2]The expression in (5.23) is the summation of $N/2$ i.i.d., where each random variable is the sum of an element from the subset $\mathcal{S}$ and an element from the subset $\mathcal{R}$.

follows

$$\begin{aligned} m_u =& E\{u\} \\ =& E\left\{\sum_{i=1}^{N} \frac{P_i \left|h_{s_iF}\right|^2 |m_i|^2}{P_i \left|h_{s_iF}\right|^2 \sigma^2 + N_0}\right\} \\ =& \frac{N}{2} \cdot E\left\{\frac{P_S \left|h_{s_iF}\right|^2 |m_S|^2}{P_S \left|h_{s_iF}\right|^2 \sigma^2 + N_0} + \frac{P_R \left|h_{s_jF}\right|^2 |m_R|^2}{P_R \left|h_{s_jF}\right|^2 \sigma^2 + N_0}\right\}, \text{ for some } i \in \mathcal{S},\ j \in \mathcal{R}. \end{aligned} \tag{5.25}$$

Define the random variable $h = \left|h_{s_iF}\right|^2$ for some i. Under our model assumptions, h follows, for any i, an exponential distribution with a probability density function (pdf) given by

$$P(h) = e^{-h},\ h \geq 0. \tag{5.26}$$

The mean of the random variable u can be found as follows.

$$\begin{aligned} & m_u \\ &= \frac{N}{2} \cdot E\left\{\frac{P_S \left|h_{s_iF}\right|^2 |m_S|^2}{P_S \left|h_{s_iF}\right|^2 \sigma^2 + N_0} + \frac{P_R \left|h_{s_jF}\right|^2 |m_R|^2}{P_R \left|h_{s_jF}\right|^2 \sigma^2 + N_0}\right\} \\ &= \frac{N}{2\sigma^2}\left(|m_S|^2 + |m_R|^2 - \frac{N_0 |m_S|^2}{P_S\sigma^2} e^{\frac{N_0}{P_S\sigma^2}} \mathbf{\Gamma}\left(0, \frac{N_0}{P_S\sigma^2}\right) - \frac{N_0 |m_R|^2}{P_R\sigma^2} e^{\frac{N_0}{P_R\sigma^2}} \mathbf{\Gamma}\left(0, \frac{N_0}{P_R\sigma^2}\right)\right), \end{aligned} \tag{5.27}$$

where $\mathbf{\Gamma}(.,.)$ is the incomplete Gamma function defined as [41]

$$\mathbf{\Gamma}(a, \mu) = \int_{\mu}^{\infty} t^{a-1} e^{-t} dt, \quad \mu > 0. \tag{5.28}$$

Let δ_u^2 denote the variance of the random variable u. The variance of u can be

calculated as

$$\begin{aligned}\delta_u^2 =&\frac{N}{2}\Bigg(E\left\{\left(\frac{P_S\left|h_{s_iF}\right|^2|m_S|^2}{P_S\left|h_{s_iF}\right|^2\sigma^2+N_0}\right)^2\right\}-\left(E\left\{\frac{P_S\left|h_{s_iF}\right|^2|m_S|^2}{P_S\left|h_{s_iF}\right|^2\sigma^2+N_0}\right\}\right)^2\\&+E\left\{\left(\frac{P_R\left|h_{s_jF}\right|^2|m_R|^2}{P_R\left|h_{s_jF}\right|^2\sigma^2+N_0}\right)^2\right\}-\left(E\left\{\frac{P_R\left|h_{s_jF}\right|^2|m_R|^2}{P_R\left|h_{s_jF}\right|^2\sigma^2+N_0}\right\}\right)^2\Bigg)\end{aligned} \tag{5.29}$$

for some $i \in \mathcal{S}$ and $j \in \mathcal{R}$. Evaluating the expectations in (5.29), we get

$$\begin{aligned}\delta_u^2 =&\frac{N}{2}\Bigg(\frac{|m_S|^4}{\sigma^4}\left[\frac{N_0}{P_S\sigma^2}-\frac{N_0^2}{P_S^2\sigma^4}e^{\frac{N_0}{P_S\sigma^2}}\mathbf{\Gamma}\left(0,\frac{N_0}{P_S\sigma^2}\right)-\frac{N_0^2}{P_S^2\sigma^4}e^{\frac{2N_0}{P_S\sigma^2}}\left(\mathbf{\Gamma}\left(0,\frac{N_0}{P_S\sigma^2}\right)\right)^2\right]\\&+\frac{|m_R|^4}{\sigma^4}\left[\frac{N_0}{P_R\sigma^2}-\frac{N_0^2}{P_R^2\sigma^4}e^{\frac{N_0}{P_R\sigma^2}}\mathbf{\Gamma}\left(0,\frac{N_0}{P_R\sigma^2}\right)-\frac{N_0^2}{P_R^2\sigma^4}e^{\frac{2N_0}{P_R\sigma^2}}\left(\mathbf{\Gamma}\left(0,\frac{N_0}{P_R\sigma^2}\right)\right)^2\right]\Bigg).\end{aligned} \tag{5.30}$$

Using the Gaussian approximation for the random variable u, the probability of detection error for large N can be approximated as

$$\begin{aligned}P_{e,I}^{Ray} &= E\left\{Q\left(\frac{1}{2}\sqrt{u}\right)\right\}\\&\approx \frac{1}{\pi}\int_{\theta=0}^{\frac{\pi}{2}} e^{-\left(\frac{m_u}{8\sin^2\theta}+\frac{\delta_u^2}{128\sin^4\theta}\right)}\,d\theta,\end{aligned} \tag{5.31}$$

where we have used the special property of the Q-function as $Q(u)=\frac{1}{\pi}\int_0^{\pi/2} e^{-\frac{u^2}{2\sin^2\theta}}d\theta$ [22]. The integration in the last equation can be easily computed using any numerical integration algorithm. Equation (5.31) provides an approximation for the probability of detection error of Protocol I over Rayleigh flat-fading channels. Next, we will consider the performance analysis for Protocol II over Rayleigh flat-fading channels.

Protocol II Probability of Detection Error

In this section, we will compute an approximate expression for the probability of detection error of Protocol II over Rayleigh flat-fading channels.

In Protocol II, each sensor from the subset $\mathcal{S}$ will be assigned a relay node to forward its measurement. In this case, sensor nodes from the subset $\mathcal{R}$ are not used and their resources are assigned to relay nodes. Let $\mathcal{L}$ denote the subset of relay nodes where $|\mathcal{L}| = N/2$. This enables the definition of the set $\mathcal{O}$ of size $N/2$ such that

$$\mathcal{O} = \{(i,j) : \ i \in \mathcal{S}, \ j \in \mathcal{L}, \text{ node } j \text{ works as a relay for sensor } i\}. \tag{5.32}$$

Now, we start the probability of detection error analysis at the fusion center. Define the 2×1 received data vector $\mathbf{y}_{(i,j)} = [y_{s_iF}, y_{jF}]^T$ and the mean vector $\mathbf{m}_{(i,j)} = [\sqrt{P_i}h_{s_iF}m_i, \sqrt{P_i}h_{jF}m_i]^T, \ (i,j) \in \mathcal{O}$. In Protocol II, the components of the vector $\mathbf{y}_{(i,j)}$ are correlated since the measurement of sensor i will be transmitted by relay node j. Therefore, the probability density function of the vector $\mathbf{y}_{(i,j)}$ under each hypothesis is given by

$$\begin{aligned} H_0 : \ \mathbf{y}_{(i,j)} &\sim \mathcal{N}\left(\mathbf{0}, \mathbf{C}_{(i,j)}\right) \\ H_1 : \ \mathbf{y}_{(i,j)} &\sim \mathcal{N}\left(\mathbf{m}_{(i,j)}, \mathbf{C}_{(i,j)}\right), \end{aligned} \tag{5.33}$$

where

$$\mathbf{C}_{(i,j)} = \begin{pmatrix} P_i \left|h_{s_iF}\right|^2 \sigma^2 + N_0 & P_i h_{s_iF} h_{jF}^* \sigma^2 \\ P_i h_{s_iF}^* h_{jF} \sigma^2 & P_i \left|h_{jF}\right|^2 \sigma^2 + N_0 \end{pmatrix} \tag{5.34}$$

is the auto-covariance matrix of the vector $\mathbf{y}_{(i,j)}$ and is the same under both hypotheses. Note that under our data model assumption of having independent measurements at the sensor nodes the vectors $\mathbf{y}_{(i,j)}$ and $\mathbf{y}_{(k,l)}$, for (i,j) and (k,l) $\in \mathcal{O}$, are mutually independent for $(i,j) \neq (k,l)$.

Using the probability of detection error as a performance measure, the optimal decision rule is the LR test given by

$$\frac{e^{-\sum_{(i,j)\in\mathcal{O}}\left(\mathbf{y}_{(i,j)}-\mathbf{m}_{(i,j)}\right)^{\mathcal{H}}\mathbf{C}_{(i,j)}^{-1}\left(\mathbf{y}_{(i,j)}-\mathbf{m}_{(i,j)}\right)}}{e^{-\sum_{(i,j)\in\mathcal{O}}\mathbf{y}_{(i,j)}^{\mathcal{H}}\mathbf{C}_{(i,j)}^{-1}\mathbf{y}_{(i,j)}}} \underset{\widehat{H}=H_0}{\overset{\widehat{H}=H_1}{\gtrless}} 1, \tag{5.35}$$

where $(\cdot)^{\mathcal{H}}$ denotes the Hermitian transpose. Simplifying, we get

$$\sum_{(i,j)\in\mathcal{O}}\left(\mathbf{m}_{(i,j)}^{\mathcal{H}}\mathbf{C}_{(i,j)}^{-1}\mathbf{y}_{(i,j)}+\mathbf{y}_{(i,j)}^{\mathcal{H}}\mathbf{C}_{(i,j)}^{-1}\mathbf{m}_{(i,j)}\right) \underset{\widehat{H}=H_0}{\overset{\widehat{H}=H_1}{\gtrless}} \sum_{(i,j)\in\mathcal{O}}\mathbf{m}_{(i,j)}^{\mathcal{H}}\mathbf{C}_{(i,j)}^{-1}\mathbf{m}_{(i,j)}. \tag{5.36}$$

The probability of detection error of Protocol II can now be given as

$$\begin{aligned} P_{e,II}^{Ray} &= E\left\{Q\left(\frac{1}{2}\sqrt{\sum_{(i,j)\in\mathcal{O}}\mathbf{m}_{(i,j)}^{\mathcal{H}}\mathbf{C}_{(i,j)}^{-1}\mathbf{m}_{(i,j)}}\right)\right\} \\ &= E\left\{Q\left(\frac{1}{2}\sqrt{\sum_{(i,j)\in\mathcal{O}}\frac{P_S\left|h_{s_iF}\right|^2\left|m_S\right|^2+P_S\left|h_{jF}\right|^2\left|m_S\right|^2}{P_S\left|h_{s_iF}\right|^2\sigma^2+P_S\left|h_{jF}\right|^2\sigma^2+N_0}}\right)\right\}, \end{aligned} \tag{5.37}$$

where $P_i = P_S$ for all i since $i \in \mathcal{S}$.

It is very difficult to get a closed-form expression for $P_{e,II}^{Ray}$ in (5.37). Again, we make the assumption of large sensor network to get an approximate expression for the probability of detection error in this case. To get that expression, define the random variable w as

$$w = \sum_{(i,j)\in\mathcal{O}}\frac{P_S\left|h_{s_iF}\right|^2\left|m_S\right|^2+P_S\left|h_{jF}\right|^2\left|m_S\right|^2}{P_S\left|h_{s_iF}\right|^2\sigma^2+P_S\left|h_{jF}\right|^2\sigma^2+N_0}, \tag{5.38}$$

which is the summation in the argument of the Q-function in (5.37). The probability of detection error is now given by

$$P_{e,II}^{Ray} = Q\left(\frac{1}{2}\sqrt{w}\right). \tag{5.39}$$

The random variable w is the summation of $N/2$ i.i.d. random variables that can be approximated for large N to be a Gaussian random variable by applying

the CLT. To get the approximate expression for the probability of detection error we need to calculate the mean and the variance of w. The mean m_w of w is given by

$$\begin{aligned} m_w &= E\left\{\sum_{(i,j)\in\mathcal{O}} \frac{P_S\left|h_{s_iF}\right|^2\left|m_S\right|^2 + P_S\left|h_{jF}\right|^2\left|m_S\right|^2}{P_S\left|h_{s_iF}\right|^2\sigma^2 + P_S\left|h_{jF}\right|^2\sigma^2 + N_0}\right\} \\ &= \frac{N}{2}\cdot E\left\{\frac{P_S\left|h_{s_iF}\right|^2\left|m_S\right|^2 + P_S\left|h_{jF}\right|^2\left|m_S\right|^2}{P_S\left|h_{s_iF}\right|^2\sigma^2 + P_S\left|h_{jF}\right|^2\sigma^2 + N_0}\right\}, \text{ for some } (i,j)\in\mathcal{O}. \end{aligned} \tag{5.40}$$

Define $h = \left|h_{s_iF}\right|^2$ and $t = \left|h_{jF}\right|^2$. The random variables h and t are independent, exponential random variables. Hence, m_w can be found as

$$\begin{aligned} m_w &= \frac{N}{2}\int_{h=0}^{\infty}\int_{t=o}^{\infty} \frac{P_S\left|m_S\right|^2 h + P_S\left|m_S\right|^2 t}{P_S\sigma^2 h + P_S\sigma^2 t + N_0} e^{-(h+t)}\, dh\, dt \\ &= \frac{N\left|m_S\right|^2}{2\sigma^2}\left(1 - \frac{N_0}{P_S\sigma^2}e^{\frac{N_0}{P_S\sigma^2}}\int_{t=o}^{\infty}\mathbf{\Gamma}\left(0, t+\frac{N_0}{P_S\sigma^2}\right)\, dt\right), \end{aligned} \tag{5.41}$$

where the last integral can be efficiently evaluated using any numerical integration algorithm.

The variance δ_w^2 of the random variable w can be calculated as

$$\begin{aligned} \delta_w^2 =& \frac{N}{2}\Bigg[E\left\{\left(\frac{P_S\left|h_{s_iF}\right|^2\left|m_S\right|^2 + P_S\left|h_{jF}\right|^2\left|m_S\right|^2}{P_S\left|h_{s_iF}\right|^2\sigma^2 + P_S\left|h_{jF}\right|^2\sigma^2 + N_0}\right)^2\right\} \\ &- \left(E\left\{\frac{P_S\left|h_{s_iF}\right|^2\left|m_S\right|^2 + P_S\left|h_{jF}\right|^2\left|m_S\right|^2}{P_S\left|h_{s_iF}\right|^2\sigma^2 + P_S\left|h_{jF}\right|^2\sigma^2 + N_0}\right\}\right)^2\Bigg] \text{ for some } (i,j)\in\mathcal{O}. \end{aligned} \tag{5.42}$$

To evaluate the expectations in (5.42), we need to calculate the expectation

$$\begin{aligned} &E\left\{\left(\frac{P_S\left|h_{s_iF}\right|^2\left|m_S\right|^2 + P_S\left|h_{jF}\right|^2\left|m_S\right|^2}{P_S\left|h_{s_iF}\right|^2\sigma^2 + P_S\left|h_{jF}\right|^2\sigma^2 + N_0}\right)^2\right\} \\ &= \frac{\left|m_S\right|^2}{\sigma^2}\Bigg(1 - \left(\frac{N_0}{P_S\sigma^2}\right)^2 e^{\frac{N_0}{P_S\sigma^2}}\mathbf{\Gamma}\left(0, \frac{N_0}{P_S\sigma^2}\right) - \frac{N_0}{P_S\sigma^2}\left(2+\frac{N_0}{P_S\sigma^2}\right) \\ &\quad\times e^{\frac{N_0}{P_S\sigma^2}}\int_0^{\infty}\mathbf{\Gamma}\left(0, t+\frac{N_0}{P_S\sigma^2}\right)\, dt\Bigg). \end{aligned} \tag{5.43}$$

From (5.41) and (5.43) the value of δ_w^2 can be calculated.

Following a similar analysis to the one presented in the previous section, we can get an approximate expression for the probability of detection error as

$$P_{e,II}^{Ray} \approx \frac{1}{\pi} \int_{\theta=0}^{\frac{\pi}{2}} e^{-\left(\frac{m_w}{8\sin^2\theta}+\frac{\delta_w^2}{128\sin^4\theta}\right)} d\theta. \tag{5.44}$$

To compare the performances of the two protocols, the values of the approximate expressions for the probability of detection error given in (5.31) and (5.44) are used to decide which of the two protocols performs better in terms of P_e.

Returning back to the exact error expressions given in (5.22) and (5.37), we have the following inequality

$$\begin{aligned}\frac{P_S\left|h_{s_iF}\right|^2\left|m_S\right|^2}{P_S\left|h_{s_iF}\right|^2\sigma^2+N_0}+\frac{P_S\left|h_{jF}\right|^2\left|m_S\right|^2}{P_S\left|h_{jF}\right|^2\sigma^2+N_0} &> \frac{P_S\left|h_{s_iF}\right|^2\left|m_S\right|^2+P_S\left|h_{jF}\right|^2\left|m_S\right|^2}{P_S\left|h_{s_iF}\right|^2\sigma^2+P_S\left|h_{jF}\right|^2\sigma^2+N_0} \\ &> \frac{P_S\left|h_{s_iF}\right|^2\left|m_S\right|^2}{P_S\left|h_{s_iF}\right|^2\sigma^2+N_0},\end{aligned} \tag{5.45}$$

from which we have

$$\begin{aligned}&E\left\{Q\left(\frac{1}{2}\sqrt{\sum_{i=1}^{N}\frac{P_S\left|h_{s_iF}\right|^2\left|m_S\right|^2}{P_S\left|h_{s_iF}\right|^2\sigma^2+N_0}}\right)\right\} < \\ &E\left\{Q\left(\frac{1}{2}\sqrt{\sum_{(i,j)\in\mathcal{O}}\frac{P_S\left|h_{s_iF}\right|^2\left|m_S\right|^2+P_S\left|h_{jF}\right|^2\left|m_S\right|^2}{P_S\left|h_{s_iF}\right|^2\sigma^2+P_S\left|h_{jF}\right|^2\sigma^2+N_0}}\right)\right\} \\ &< E\left\{Q\left(\frac{1}{2}\sqrt{\sum_{i\in\mathcal{S}}\frac{P_S\left|h_{s_iF}\right|^2\left|m_S\right|^2}{P_S\left|h_{s_iF}\right|^2\sigma^2+N_0}}\right)\right\},\end{aligned} \tag{5.46}$$

which means that

$$P_{e,I}^{Ray}\left(|m_R|=|m_S|\right) < P_{e,II}^{Ray} < P_{e,I}^{Ray}\left(m_R=0\right). \tag{5.47}$$

Equation (5.47) tells the story. For the extreme case of having $m_R = 0$, Protocol II results in a better performance if compared to Protocol I. In this case, the

measurements from sensors that have a zero-mean measurement convey no information to the fusion center. Therefore, in this case it is better to use relay nodes, instead of sensor nodes with zero-mean measurements, to forward information for the other more-informative sensor nodes. For the other case of having $|m_R| = |m_S|$, the measurements coming from the different sensor nodes are of equal importance to the fusion sensors. As such, Protocol I performs better than Protocol II as what can be seen from (5.47). Between these two extremes, and depending on the value of $|m_R|$ and other system parameters, Protocol I may preform better than Protocol II and vice versa.

5.3 Performance Analysis for Two Special Cases

In this section we present the analysis for Protocol I and Protocol II over wireless fading channels for two special cases to gain more insights into the problem of allocating the system resources to a relay node or a sensor node. One case is having $N_0 = 0$, i.e., no communication noise in the system, and the other case is having $\sigma^2 = 0$, i.e., no measurement noise. In this section, we will assume that $|m_S| > |m_R| > 0$ (so the system is not operating at any of the extreme cases of $m_R = 0$ or $|m_R| = |m_S|$).

5.3.1 Case 1: $N_0 = 0$

In this case, there exists no communication noise in the system. Following the analysis presented in the previous sections, we can get the probability of detection error for Protocol I as

$$P_{e,I}^{Ray}\left(N_0 = 0\right) = Q\left(\frac{1}{2}\sqrt{\frac{N}{2}\left(\frac{|m_S|^2}{\sigma^2} + \frac{|m_R|^2}{\sigma^2}\right)}\right), \tag{5.48}$$

which is the probability of detection error of the optimal centralized detector that have access to all of the local measurements at the sensor nodes. For the case of $N_0 = 0$, the probability of detection error for Protocol II is given by

$$P_{e,I}^{Ray}\left(N_0 = 0\right) = Q\left(\frac{1}{2}\sqrt{\frac{N}{2} \cdot \frac{\left|m_S\right|^2}{\sigma^2}}\right). \tag{5.49}$$

Comparing (5.48) and (5.49) we can easily see that Protocol I performs better than Protocol II for the case of having $N_0 = 0$. Clearly, in the case of having $N_0 = 0$, the detector performance at the fusion center is not limited by the communication noise but limited by the measurement noise. In this case, each sensor node can reliably communicate its measurement to the fusion center. Therefore, there will be no gain of having some sensors forwarding other sensors measurement. In this case, it is better for each sensor node to send its measurement to the fusion center directly, which means that Protocol I is superior to protocol II in this case.

5.3.2 Case 2: $\sigma^2 = 0$

In this case, we assume that there is no measurement noise at the sensor nodes, i.e., $\sigma^2 = 0$. Following the analysis presented in the previous section, the probability of detection error of Protocol I can be proved to be given by

$$\begin{aligned} P_{e,I}^{Ray} &= E\left\{Q\left(\frac{1}{2}\sqrt{\sum_{i=1}^{N}\frac{P_i\left|h_{s_iF}\right|^2\left|m_i\right|^2}{N_0}}\right)\right\} \\ &= E\left\{Q\left(\frac{1}{2}\sqrt{\left|m_S\right|^2\sum_{i\in\mathcal{S}}\frac{P_S\left|h_{s_iF}\right|^2}{N_0} + \left|m_R\right|^2\sum_{i\in\mathcal{R}}\frac{P_R\left|h_{s_iF}\right|^2}{N_0}}\right)\right\} \\ &= E\left\{Q\left(\frac{1}{2}\sqrt{\frac{2P}{N_o}\sum_{i=1}^{N}\left|h_{s_iF}\right|^2}\right)\right\}. \end{aligned} \tag{5.50}$$

The probability of detection error of Protocol II can be proved to be given by

$$P_{e,II}^{Ray} = E\left\{Q\left(\frac{1}{2}\sqrt{|m_S|^2\sum_{i=1}^{N}\frac{P_S\,|h_{s_iF}|^2}{N_0}}\right)\right\} = E\left\{Q\left(\frac{1}{2}\sqrt{\frac{2P}{N_o}\sum_{i=1}^{N}|h_{s_iF}|^2}\right)\right\}. \tag{5.51}$$

Comparing the expressions in (5.50) and (5.51), and under our assumption of having $|m_R| > 0$, we can see that both protocols achieve the same performance when $\sigma^2 = 0$. Clearly, in this case power scaling at the sensor nodes of mean m_R will result in the same transmitted measurement as that of sensor nodes of mean m_S since there is no measurement noise.

For any operating signal power, communication noise variance, and measurement noise variance there will be a tradeoff between the number of measurements sent to the fusion center and the reliability of the more-informative measurements. The question is whether to send more measurements from the less-informative sensor nodes or increase the reliability of the more-informative measurements, i.e., is it better to assign the system resources to a sensor node or a relay node? As clear from the analysis presented in the previous sections, the answer to that question is not that clear. The extreme cases considered give more insights into that tradeoff. The two special cases considered in this section serves that goal of having more insight to the problem.

For the case of having $N_0 = 0$, there is no communication noise and to send more measurements to the fusion center is better than increasing the reliability of the more-informative measurements, since the communication system is already reliable, hence Protocol I performs better. For the other case of having $\sigma^2 = 0$, there is no measurement noise in the system. In this case, both protocols will have the same performance for any $|m_R| > 0$. Between these two special cases, we need to compare the performances of the two protocols based on the derived expressions

for the probability of detection error to decide which protocol performs better at a given system parameters.

5.4 Simulation Results

In this section, we present some simulation results. In all simulations we will normalize the power at each sensor node to be $P = 1$ and $m_S = 1$, which is the mean of the more-informative sensor nodes under hypothesis H_1.

We start by simulating a two-sensor network over AWGN channels as presented in Section 5.2.1. Fig. 5.3 shows the probability of detection error versus P/N_0 for the case of having a measurement noise of variance $\sigma^2 = 0.01$. From Fig. 5.3, it is clear that Protocol I always performs better than Protocol II for the case of having $m_R = 1$ as explained before. From Fig. 5.3, we can see that Protocol II is always better than Protocol I for the case of having $m_R = 0$. For any value of m_R that is between 0 and 1, deciding which protocol will perform better depends on other system parameters such as the measurement noise and communication noise variances. In Fig. 5.3 and as P/N_0 increases we can see that Protocol II saturates to a probability of detection error level that equals the error level of Protocol I for the case $m_R = 0$. As P/N_0 increases the system performance will be limited by the measurement noise and hence, having a relay instead of the second sensor to forward the measurement of the first sensor will not improve the system performance (in this case, the received signals from the two sensors will be almost the same and hence, there will no gain for Protocol II over the case of having $m_R = 0$). In this case of very high P/N_0, it is better to have the second sensor sending its measurement to the fusion center instead of using a relay to forward the measurement of the first sensor.

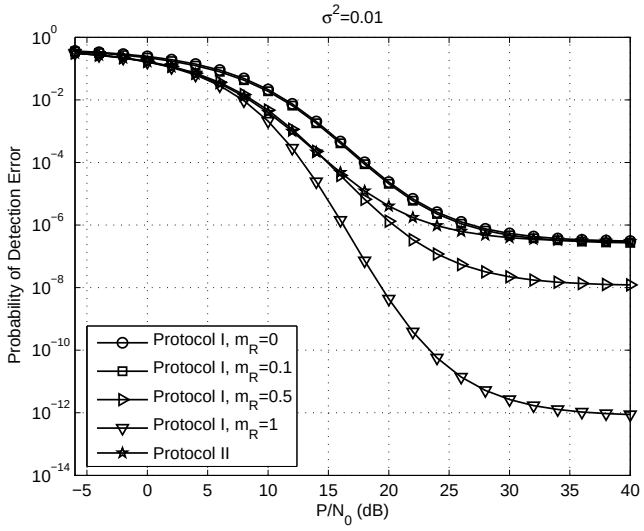

Figure 5.3: The probability of detection error versus P/N_0 (dB) for a two-sensor network over AWGN channels for the case of having a measurement noise of variance $\sigma^2 = 0.01$.

Fig. 5.4 shows the probability of detection error versus P/N_0 for the case of having a measurement noise of variance $\sigma^2 = 0.1$. Again, we can see that Protocol I always performs better than Protocol II for the case of having $m_R = 1$ and Protocol II always performs better than Protocol I for the case of having $m_R = 0$. Also, as P/N_0 becomes very large there will no gain for Protocol II over the case of having $m_R = 0$.

Fig. 5.5 shows the probability of detection error versus P/σ^2 for the case of having $P/N_0 = 10$ dB. In Fig. 5.5, Protocol II is always better than Protocol I for the case of having $m_R = 0$ as expected. Also, Protocol I is better than Protocol II for the case of having $m_R = 1$. As P/σ^2 becomes very large the performance of Protocol II approaches that of Protocol I with $m_R = 1$. In this case of very high P/σ^2 the system performance will be limited by the communication noise rather than the measurement noise. In this case the signal from the relay node will

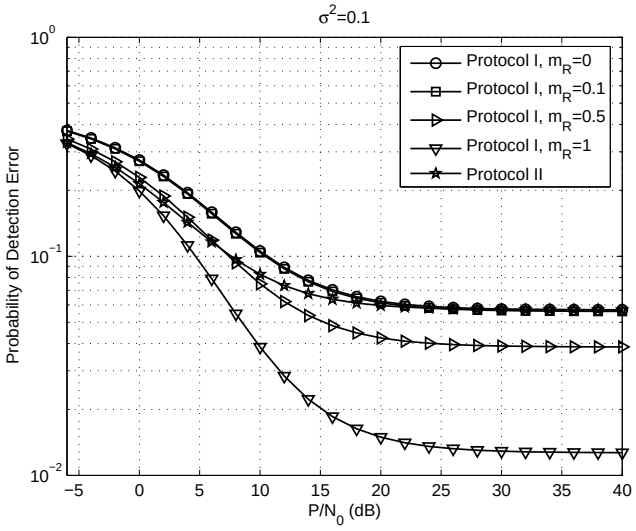

Figure 5.4: The probability of detection error versus P/N_0 (dB) for a two-sensor network over AWGN channels for the case of having a measurement noise of variance $\sigma^2 = 0.1$.

appear as a new measurement with mean equals 1 under hypothesis H_1 and this is why the performance of Protocol II approaches the performance of Protocol I with $m_R = 1$. Note that As P/σ^2 becomes very large the performance of Protocol I with any $m_R > 0$ approaches the same error value as that of Protocol I with $m_R = 1$. The reason for that is because we assume all nodes to have the same power for transmission. At very high P/σ^2, scaling the measurement by a factor to meet the power constraint, and because we have a very low level of measurement noise, will make the signals transmitted from all of the sensor nodes to be almost the same. This can be seen from Equation (5.10) by substituting $\sigma^2 = 0$; we can see that the contribution of both sensors to the error expression will be the same independent of the value of m_R.

Next, we consider the simulations for a two-sensor network over wireless fading channels. Fig. 5.6 shows the probability of detection error versus P/N_0 for the

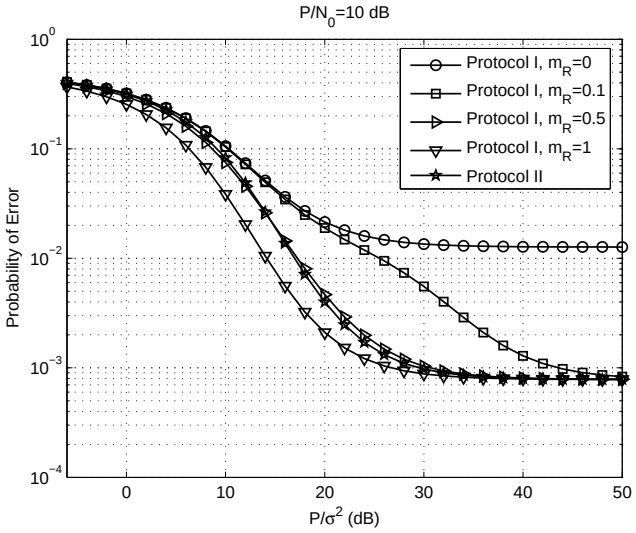

Figure 5.5: The probability of detection error versus P/σ^2 (dB) for a two-sensor network over AWGN channels for the case of having a communication signal-to-noise ratio of variance $P/N_0 = 10$ dB.

case of having a measurement noise of variance $\sigma^2 = 0.01$. From Fig. 5.6, it is clear that Protocol I always performs better than Protocol II for the case of having $m_R = 1$ as explained before. Also, we can see that Protocol II is always better than Protocol I for the case of having $m_R = 0$. Fig. 5.7 shows the probability of detection error versus P/N_0 for the case of having a measurement noise of variance $\sigma^2 = 0.1$. The same observations that were made for the case of AWGN channels can be made here.

Finally, Figs. 5.8 and 5.9 shows the probability of detection error versus P/σ^2 for the case of having $P/N_0 = 0$ dB and $P/N_0 = 10$ dB, respectively. Again, the observations that were made for Fig. 5.5 for the case of AWGN channel also applies for Figs. 5.8 and 5.9. As P/σ^2 tends to infinity, the performance of Protocol II approaches that of Protocol I with $m_R = 1$ for the same reason as explained for

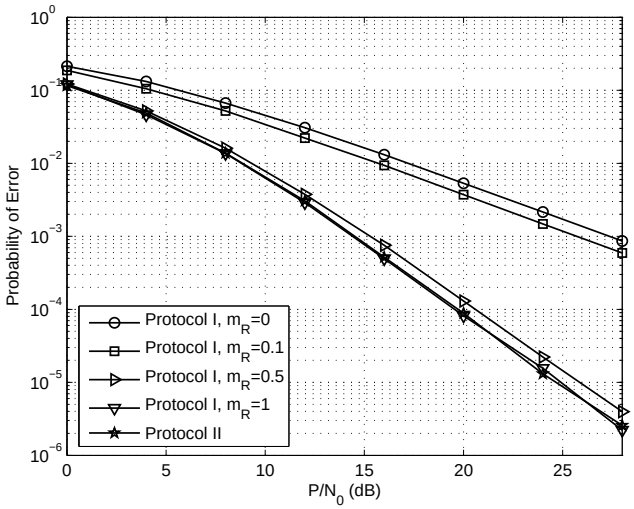

Figure 5.6: The probability of detection error versus P/N_0 (dB) for a two-sensor network over wireless fading channels for the case of having a measurement noise of variance $\sigma^2 = 0.01$.

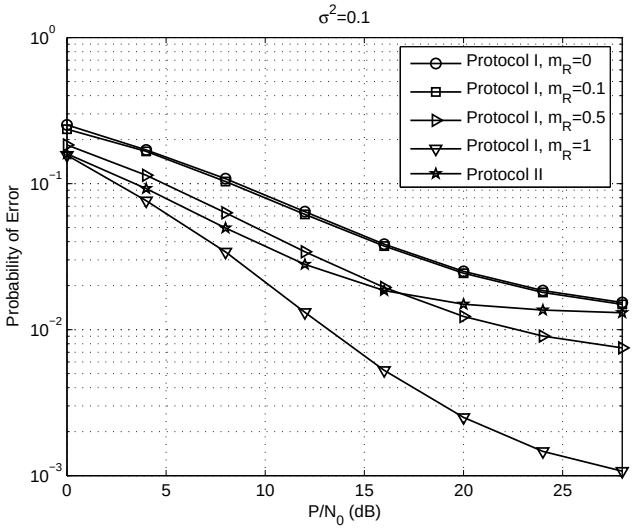

Figure 5.7: The probability of detection error versus P/N_0 (dB) for a two-sensor network over wireless fading channels for the case of having a measurement noise of variance $\sigma^2 = 0.1$.

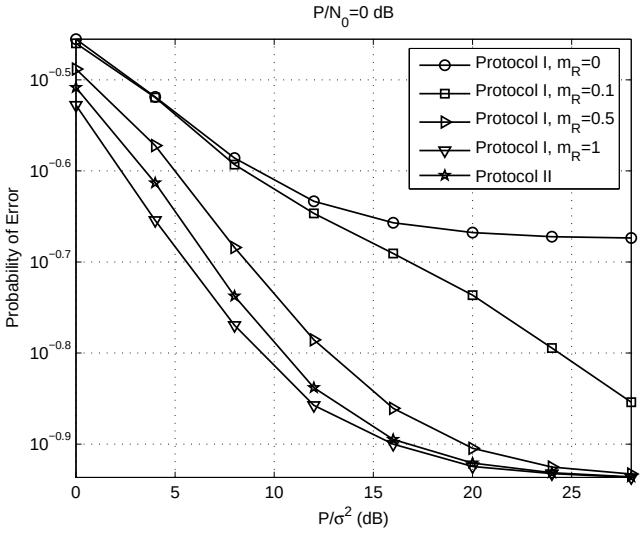

Figure 5.8: The probability of detection error versus P/σ^2 (dB) for a two-sensor network over wireless fading channels for the case of having a communication signal-to-noise ratio of variance $P/N_0 = 0$ dB.

the AWGN channels.

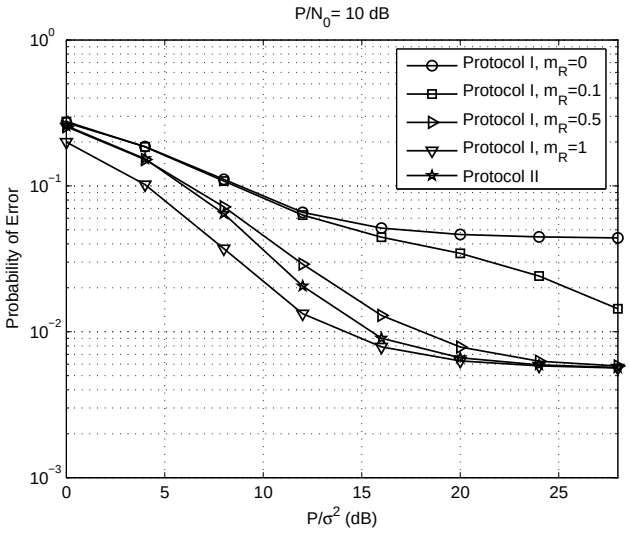

Figure 5.9: The probability of detection error versus P/σ^2 (dB) for a two-sensor network over wireless fading channels for the case of having a communication signal-to-noise ratio of variance $P/N_0 = 10$ dB.

Chapter 6

Conclusions and Future Work

6.1 Conclusions

In this thesis we have developed and analyzed cooperative communications protocols for wireless networks. Nodes Cooperation as a new communication paradigm provides a new dimension over which diversity can be exploited to mitigate the fading nature of wireless channels. We have tried to answer the question of how to achieve and where to exploit diversity in cooperative networks. More specifically, we have addressed the following problems.

First, we studied the multi-node amplify-and-forward cooperation protocol. We considered the performance analysis for a system in which each relay only amplifies the source signal. We derive an SER bound for the multi-node amplify-and-forward protocol that proves to be tight at high SNR. Furthermore, by forming an upper-bound on any amplify-and-forward protocol SER performance, we prove that the multi-node amplify-and-forward protocol, in which each relay only amplifies the source signal, achieves this SER upper-bound if the relay node are close to the source; therefore, if the relays are close to the source they need not to combine

the signals from the source and the previous relays. Then, we provided the outage probability analysis of the multi-node amplify-and-forward protocol. Based on the derived SER and outage probability bounds, we determined the optimal power allocation between the source and the relays that minimizes the system SER.

Then, the design of distributed space-time codes in wireless relay networks was considered for different user cooperation schemes, which vary in the processing performed at the relay nodes. For the decode-and-forward distributed space-time codes, any space-time code that is designed to achieve full diversity over MIMO channels can achieve full diversity under the assumption that the relay nodes can decide whether they have decoded correctly or not. A code that maximizes the coding gain over MIMO channels is not guaranteed to maximize the coding gain in the decode-and-forward distributed space-time coding. This is due to the fact that not all of the relays will always transmit their code columns in the second phase. Then, the code design criteria for the amplify-and-forward distributed space-time codes were considered. In this case, a code designed to achieve full diversity over MIMO channels will also achieve full diversity. Furthermore, a code that maximizes the coding gain over MIMO channels will also maximize the coding gain in the amplify-and-forward distributed space-time scheme.

The design of DDSTC for wireless relay networks was investigated. In DDSTC, the diagonal structure of the code was imposed to simplify the synchronization between randomly located relay nodes. Synchronization mismatches between the relay nodes causes inter-symbol interference, which can highly degrade the system performance. DDSTC relaxes the stringent synchronization requirement by allowing only one relay to transmit at any time slot. The code design criterion for the DDSTC based on minimizing the PEP was derived and the design criterion is

found to be maximizing the minimum product distance.

Then, the design of distributed space-frequency codes (DSFCs) was considered for the wireless multipath relay channels. The use of DSFCs can greatly improve system performance by achieving higher diversity orders by exploiting the multipath diversity of the channel as well as the cooperative diversity. We have considered the design of DSFCs with the DAF and AAF cooperation protocols. For the case of DSFCs with the DAF protocol, we have proposed a two-stage coding scheme: source node coding and relay nodes coding. We have derived sufficient conditions for the proposed code structure to achieve full diversity of order NL where N is the number of relay nodes and L is the number of multipaths per channel. For the case of DSFCs with the AAF protocol, we have derived sufficient conditions for the proposed code structure to achieve full diversity of order NL for the special cases of $L = 1$ and $L = 2$.

The proposed DSFCs are robust against the synchronization errors caused by the relays timing mismatches and propagation delays due to the presence of the cyclic prefix in the OFDM transmission. Also, the proposed DSFCs are robust against the relays carrier offsets since only one relay is transmitting on any subcarrier at any given instance. These properties of the proposed DSFCs greatly simplifies the system design since it is very difficult to synchronize randomly located relay nodes.

After that we addressed the problem of where to exploit diversity for multimedia transmission. We have studied the performance limit of systems that may present diversity in the form of source coding, channel coding and user cooperation diversity and their possible combinations. In the case of source coding, diversity is introduced through the use of dual-description source encoders. Channel cod-

ing diversity is obtained from joint decoding of channel coded blocks sent through different channels. We have considered user cooperation using either the amplify-and-forward or the decode-and-forward techniques. The presented study focused on analyzing the achievable performance limits, which was measured in terms of the distortion exponent. Our results show that for the relay channels, channel coding diversity provides better performance, followed by source coding diversity. For the case of having multiple relays, our results show a tradeoff between the source coding resolution and the number of relay nodes assigned to help the source node. We note that at low bandwidth it is not the channel outage event, but the distortion introduced at the source coding stage is the dominant factor limiting the distortion exponent performance. Therefore, in these cases it is better not to cooperate and use a lower distortion source encoder. Similarly, we showed that as the bandwidth expansion factor increases, the distortion exponent improves by allowing user cooperation. In these cases, the system is said to be an outage limited system and it is better to cooperate so as to minimize the outage probability and, consequently, minimize the end-to-end distortion. Depending on the operating bandwidth expansion factor, we have determined the optimal number of relay nodes to cooperate with the source node to maximize the distortion exponent.

Finally, we have considered the problem of distributed detection over wireless fading channels with the deployment of relay nodes. We have considered a system model where some sensor nodes convey more information about the state of nature to the fusion center than some other sensor nodes. We have considered the performance of two protocols, Protocol I where each sensor directly transmits its measurement to the fusion center and Protocol II where relay nodes are used instead of the sensor nodes that are less-informative to the fusion center to for-

ward the measurements of the other more-informative sensor nodes. We compare the performances of the two protocols using the probability of detection error as a performance measure. By comparing the performance of the two protocols, we can see that a tradeoff exists between the number of measurements sent to the fusion center and the reliability of the more-informative measurements. Protocol I provides the fusion center with more measurements and Protocol II has the advantage of increased reliability of the more-informative measurements. In general, if all of the sensor measurements are of equal importance then it is always better for each sensor to send its measurement to the fusion center rather than to use relay nodes. We have presented some extreme cases when one of the two protocols always performs better than the other protocol. But, for the general case having one protocol to perform better than the other one will depend on the system parameters such as the sensor node power, measurement noise variance, and communication noise variance. By deriving probability of detection error expressions we can compare the two protocols performance at any system operating parameters to decide which of the two protocols performs better.

6.2 Future Work

6.2.1 Optimal Rate Allocation for the Fast-Varying Single-Relay Channel Model

In our work, we have considered block fading channel model where the channel remains constant during the transmission of one block and varies independently from block to another. In this case, outage probability can provide a tight approximation for the block error rate [28]. For the case of fast-varying channel,

outage probability can not be used as a performance measure anymore. For this case the question is how to optimally allocate the rate between the source and the channel encoders. Over single-input single-output (SISO) channels, without any channel state information at the transmitter, the celebrated separation principle [24] holds. The separation principle states that the source and channel encoders can be separately designed without losing the optimality of the encoders. Hence, we concatenate a source encoder and a channel encoder, which will work on a rate that is arbitrarily close to but less than the channel capacity. This result is valid only under the assumption of infinite delay and infinite complexity at the receiver. Several works have considered the design of source and channel encoders under practical assumptions of finite block length finite delay and limited receiver complexities assumptions [83], [84]. These works have considered optimal rate allocation between separate source and channel encoders over binary symmetric channels (BSC) and Gaussian channels

The problem can be formulated as follows. Assuming that we have a fixed rate $r = R_s \cdot R_c$, where R_s is the source encoder rate and R_c is the channel encoder rate. For the case of a source with 0-mean and variance 1, the end-to-end distortion, in terms of mean square error, can be given as

$$\begin{aligned} D_{end-to-end} =& 1 \cdot \Pr\left(\text{channel error at rate } R_c\right) \\ &+ \left(\text{source distortion for rate } R_s\right) \cdot \Pr(\text{no channel error at rate } R_c). \end{aligned} \tag{6.1}$$

Note that (6.1) implicitly assumes that in the case of an outage the missing source data is concealed by replacing the missing source samples with their expected value (equal to zero) and we assume unit variance source (i.e., the source distortion under outage event equals 1). The objective is to minimize the end-to-end distortion

subject to a fixed rate constraint, that is

$$\min_{R_c,R_s} D_{end-to-end} \quad \textbf{subject to} \quad R_c \cdot R_s = r. \tag{6.2}$$

6.2.2 Relay Deployment for Distributed Detection in Sensor Networks with Correlated Measurements

In our work, we have considered the problem of relay nodes deployment in sensor networks under the assumption of having independent measurements at the sensor nodes. Another question to answer is how to deploy relay nodes in a sensor network if the measurements from the different sensor nodes are correlated. A new factor will come to the picture which is the measurements correlation model. In this case, how the correlation model can affect the relay nodes deployment and how to efficiently deploy the relay nodes are questions to be answered.

BIBLIOGRAPHY

[1] T. S. Rappaport, *Wireless Communications: Principles & Practice*, Prentice-Hall, 2002.

[2] J. G. Proakis, *Digital Communications*, McGraw-Hill Inc., 1994.

[3] E. Telatar, "Capacity of multi-antenna gaussian channels," *European Transactions on Telecommunications*, vol. 10, no. 6, pp. 585–595, Nov./Dec. 1999.

[4] G. J. Foschini and M. Gans, "On the limits of wireless communication in a fading environment when using multiple antennas," *Wireless Personal Communication*, vol. 6, pp. 311–335, Mar. 1998.

[5] V. Tarokh, N. Seshadri, and A. R. Calderbank, "Space-time codes for high data rate wireless communication: Performance criterion and code construction," *IEEE Trans. Info. Theory*, vol. 44, no. 2, pp. 744–765, March 1998.

[6] V. Tarokh, H. Jafarkhani, and A. R. Calderbank, "Space–time block coding for wireless communications: Performance results," *IEEE Journal on Select Areas in Communications*, vol. 17, no. 3, pp. 451–460, Mar. 1999.

[7] T. M. Cover and A. El Gamal, "Capacity theorems for the relay channel," *IEEE Trans. Info. Theory*, vol. 25, no. 9, pp. 572–584, September 1979.

[8] G. Kramer, M. Gatspar, and P. Gupta, "Cooperative strategies and capacity theorems for relay networks," *IEEE Trans. Info. Theory*, vol. 51, no. 9, pp. 3037–3063, Sept. 2005.

[9] A. Sendonaris, E. Erkip, and B. Aazhang, "User cooperation diversity, part I: System description," *IEEE Trans. Comm.*, vol. 51, no. 11, pp. 1927–1938, Nov. 2003.

[10] A. Sendonaris, E. Erkip, and B. Aazhang, "User cooperation diversity, part II: Implementation aspects and performance analysis," *IEEE Trans. Comm.*, vol. 51, no. 11, pp. 1939–1948, Nov. 2003.

[11] J. N. Laneman, D. N. C. Tse, and G. W. Wornell, "Cooperative diversity in wireless networks: Efficient protocols and outage behavior," *IEEE Trans. Info. Theory*, vol. 50, no. 12, pp. 3062–3080, December 2004.

[12] A. K. Sadek, W. Su, and K. J. R. Liu, "Multi-node cooperative communications in wireless networks," *IEEE Trans. Signal Processing*, vol. 55, pp. 341–355, Jan 2007.

[13] J. Boyer, D. D. Falconer, and H. Yanikomeroglu, "Multihop diversity in wireless relaying channels," in *IEEE Trans. on Communications*, Oct. 2004, vol. 52, pp. 1820–1830.

[14] W. Su, A. K. Sadek, and K. J. R. Liu, "Cooperative communications in wireless networks: Performance analysis and optimum power allocation," *Wireless Personal Communications*, vol. 44, no. 2, pp. 181–217, Jan. 2008.

[15] J. N. Laneman and G. W. Wornell, "Distributed space-time coded protocols for exploiting cooperative diversity in wireless networks," *IEEE Trans. Info. Theory*, vol. 49, no. 10, pp. 2415–2425, Oct. 2003.

[16] B. Sirkeci-Mergen and A. Scaglione, "Randomized distributed space-time coding for cooperative communication in self-organized networks," *IEEE Workshop on Signal Processing Advances for Wireless Communications (SPAWC)*, June 5-8 2005.

[17] P. A. Anghel, G. Leus, and M. Kaveh, "Multi-user space-time coding in cooperative networks," *International Conference on Acoustics, Speech and Signal Processing (ICASSP)*, April 6-10 2003.

[18] S. Barbarossa, L. Pescosolido, D. Ludovici, L. Barbetta, and G. Scutari, "Cooperative wireless networks based on distributed space-time coding," *in Proc. IEEE International Workshop on Wireless Ad-hoc Networks (IWWAN)*, May 31-June 3 2004.

[19] Y. Jing and B. Hassibi, "Distributed space-time coding in wireless relay networks," *the 3rd IEEE Sensor Array and Multi-Channel Signal Processing Workshop*, July 18-21 2004.

[20] D. G. Brennan, "Linear diversity combining techniques," *Proceedings of the IEEE*, vol. 91, no. 2, pp. 331–356, Feb. 2003.

[21] M. O. Hasna and M. S. Alouini, "End-to-end performance of transmission systems with relays over rayleigh fading channels," *IEEE Trans. Wireless Communications*, vol. 2, pp. 1126–1131, Nov. 2003.

[22] M. K. Simon and M. S. Alouini, "A unified approach to the performance analysis of digital communications over generalized fading channels," *Proc. IEEE*, vol. 86, no. 9, pp. 1860–1877, Sep. 1998.

[23] H. L. Van Trees, *Detection, Estimation, and Modulation Theory-Part (I)*, Wiley, 1968.

[24] T. Cover and J. Thomas, *Elements of Information Theory*, John Wiley Inc., 1991.

[25] M. Abramowitz and I. A. Stegun, *Handbook of Mathematical Functions with Formulas, Graphs, and Mathematical Tables*, New York, NY: Dover Publications, 1970.

[26] R. A. Horn and C. R. Johnson, *Matrix Analysis*, Cambridge Univ. Press, 1985.

[27] K. G. Seddik, A. K. Sadek, W. Su, and K. J. R. Liu, "Outage analysis and optimal power allocation for multinode relay networks," *IEEE Signal Processing Letters*, vol. 14, pp. 377–380, June 2007.

[28] L. Zheng and D. N. C. Tse, "Diversity and multiplexing: A fundamental tradeoff in multiple antenna channels," *IEEE Trans. Info. Theory*, vol. 49, pp. 1073–1096, May 2003.

[29] K. G. Seddik, A. K. Sadek, and K. J. R. Liu, "Protocol-aware design criteria and performance analysis for distributed space-time coding," *IEEE Global Telecommunications Conference (GLOBECOM)*, Dec. 2006.

[30] K. G. Seddik, A. K. Sadek, A. S. Ibrahim, and K. J. R. Liu, "Synchronization-aware distributed space-time codes in wireless relay networks," *IEEE Global Telecommunications Conference (GLOBECOM)*, Nov. 2007.

[31] K. G. Seddik, A. K. Sadek, A. S. Ibrahim, and K. J. R. Liu, "Design criteria and performance analysis for distributed space-time coding," *to appear in IEEE Trans. on Vehicular Technology*, 2008.

[32] K. G. Seddik and K. J. R. Liu, "Distributed space-frequency coding over relay channels," *IEEE Global Telecommunications Conference (GLOBECOM)*, Nov. 2007.

[33] K. G. Seddik and K. J. R. Liu, "Distributed space-frequency coding over amplify-and-forward relay channels," *IEEE Wireless Communications and Networking Conference (WCNC)*, March–April 2008.

[34] K. G. Seddik and K. J. R. Liu, "Distributed space-frequency coding over broadband relay channels," *to appear in IEEE Trans. on Wireless Communications*, 2008.

[35] B. Hassibi and B. M. Hochwald, "High-rate codes that are linear in space and time," *IEEE Trans. Info. Theory*, vol. 48, no. 7, pp. 1804–1824, July 2002.

[36] P. Merkey and E. C. Posner, "Optimal cyclic redundancy codes for noise channels," *IEEE Trans. Information Theory*, vol. 30, pp. 865–867, Nov. 1984.

[37] M. K. Simon and M. S. Alouini, *Digital Communication over Generalized Fading Channels: A Unified Approach to the Performance Analysis*, Wiley&Sons, Inc., 2000.

[38] S. Siwamogsatham, M. P. Fitz, and J. H. Grimm, "A new view of performance analysis of transmit diversity schemes in correlated rayleigh fading," *IEEE Trans. Info. Theory*, vol. 48, no. 4, pp. 950–956, April 2002.

[39] M. O. Damen, K. Abed-Meraim, and J. C. Belfiore, "Diagonal algebraic space-time block codes," *IEEE Trans. Info. Theory*, vol. 48, no. 2, pp. 628–636, Mar. 2002.

[40] S. M. Alamouti, "A simple transmit diversity technique for wireless communiucations," *IEEE Journ. Sel. Areas in Comm.*, vol. 16, no. 8, pp. 1451–1458, Oct. 1998.

[41] I. S. Gradshteyn and I. M. Ryshik, *Table of Integrals, Series and Products, 6th. ed.*, Academic Press, 2000.

[42] C. Schlegel and D. J. Costello Jr., "Bandwidth efficient coding for fading channels: Code construction and performance analysis," *IEEE Journal on Selected Areas in Communications*, vol. 7, no. 9, pp. 1356–1368, Dec. 1889.

[43] K. Boull and J. C. Belfiore, "Modulation schemes designed for the rayleigh channel," *in Proc. CISS92*, pp. 288–293, Mar. 1992.

[44] X. Giraud, E. Boutillon, and J. C. Belfiore, "Algebraic tools to build modulation schemes for fading channels," *IEEE Trans. Info. Theory*, vol. 43, no. 3, pp. 938–952, May 1997.

[45] J. Boutros and E. Viterbo, "Signal space diversity: A power- and bandwidth-efficient diversity technique for the rayleigh fading channel," *IEEE Trans. Info. Theory*, vol. 44, no. 4, pp. 1453–1467, July 1998.

[46] W. Su, Z. Safar, and K. J. R. Liu, "Full-rate full-diversity space-frequency codes with optimum coding advantage," *IEEE Trans. Info. Theory*, vol. 51, no. 1, pp. 229–249, Jan. 2005.

[47] Y. Jing and H. Jafarkhani, "Using orthogonal and quasi-orthogonal designs in wireless relay networks," *IEEE GLOBECOM*, Dec. 2006.

[48] T. Kiran and B. S. Rajan, "Distributed space-time codes with reduced decoding complexity," *IEEE International Symposium on Information Theory (ISIT)*, July 2006.

[49] R. A. Horn and C. R. Johnson, *Topics in Matrix Analysis*, Cambridge Univ. Press, 1991.

[50] H. Holm and M. S. Alouini, "Sum and difference of two squared correlated nakagami variates in connection with the mckay distribution," *IEEE Trans. on Communications*, vol. 52, no. 8, pp. 1367–1376, Aug. 2004.

[51] R. K. Mallik, "On multivariate rayleigh and exponential distributions," *IEEE Trans. Info. Theory*, vol. 49, no. 6, pp. 1499–1515, June 2003.

[52] J. N. Laneman, E. Martinian, G. W. Wornell, and J. G. Apostolopoulos, "Source-channel diversity for parallel channels," *IEEE Trans. Info. Theory*, vol. 51, no. 10, pp. 3518–3539, Oct. 2005.

[53] L. Ozarov, "On a source coding problem with two channels and three receivers," *Bell Sys. Tech. Journal*, vol. 59, no. 10, pp. 1909–1921, Dec. 1980.

[54] A. El Gamal and T. M. Cover, "Achievable rates for multiple descriptions," *IEEE Trans. Info. Theory*, vol. 28, no. 6, pp. 851–857, November 1982.

[55] V. K. Goyal, "Multiple description coding: compression meets the network," *IEEE Signal Processing Magazine*, vol. 18, no. 5, pp. 74–93, September 2001.

[56] W. Jiang and A. Ortega, "Multiple description speech coding for robust communication over lossy packet networks," *Proc. IEEE International Conference on Multimedia and Expo.*, vol. 1, pp. 444–447, 2000.

[57] M. Alasti, K. Sayrafian-Pour, A. Ephremides, and N. Farvardin, "Multiple description coding in networks with congestion problem," *IEEE Trans. Info. Theory*, vol. 47, no. 1, pp. 891–902, March 2001.

[58] J. Kim, R. M. Mersereau, and Y. Altunbasak, "Network-adaptive video streaming using multiple description coding and path diversity," *2003 International Conference on Multimedia and Expo. ICME03*, vol. 3, pp. 653–656, 2003.

[59] A. R. Reibman, H. Jafarkhani, M. T. Orchard, and Y. Wang, "Performance of multiple description coders on a real channel," *1999 International Conference on Acoustics, Speech and Signal Processing ICASSP99*, vol. 5, pp. 2415–2418, 1999.

[60] D. Gunduz and E. Erkip, "Joint source-channel cooperation: Diversity versus spectral efficiency," in *IEEE International Symposium on Information Theory (ISIT)*, June-July 2004, p. 392.

[61] X. Xu, D. Gunduz, E. Erkip, and Y. Wang, "Layered cooperative source and channel coding," in *IEEE International Conference on Communications (ICC)*, Seoul, Korea, May 2005, vol. 2, pp. 1200–1204.

[62] D. Gunduz and E. Erkip, "Source and channel coding for cooperative relaying," in *International Workshop on Signal Processing Advances for Wireless Communications (SPAWC)*, New York, New York, June 2005, pp. 970–974.

[63] K. G. Seddik, A. Kwasinski, and K. J. R. Liu, "Distortion exponents for different source-channel diversity achieving schemes over multi-hop channels," *IEEE International Conference on Communications (ICC)*, June 2007.

[64] K. G. Seddik, A. Kwasinski, and K. J. R. Liu, "Asymptotic distortion performance of source-channel diversity schemes over relay channels," *IEEE Wireless Communications and Networking Conference (WCNC)*, March–April 2008.

[65] K. G. Seddik, A. Kwasinski, and K. J. R. Liu, "Source-channel diversity over relay channels," *submitted to IEEE Trans. on Wireless Communications.*

[66] Z. He, J. Cai, and C. W. Chen, "Joint source channel rate-distortion analysis for adaptive mode selection and rate control in wireless video coding," *IEEE Trans. on Circuits and Systems for Video Technology*, vol. 12, no. 6, pp. 511–523, June 2002.

[67] A. Kwasinski, Z. Han, K. J. R. Liu, and N. Farvardin, "Power minimization under real-time source distortion constraints in wireless networks," in *IEEE Wireless Communications and Networking Conference (WCNC)*, New Orleans, Lousiana, March 2003, vol. 1, pp. 532–536.

[68] K. Liu and A. M. Sayeed, "Type-based decentralized detection in wireless sensor networks," *IEEE Trans. on Signal Processing*, vol. 55, no. 5, pp. 1899–1910, May 2007.

[69] J.-F. Chamberland and V. V. Veeravalli, "How dense should a sensor network be for detection with correlated observations?," *IEEE Trans. on Information Theory*, vol. 52, no. 11, pp. 5099–5106, Nov. 2006.

[70] Y. Sung, L. Tong, and H. V. Poor, "Neyman-pearson detection of gauss-markov signals in noise: Closed-form error exponents and properties," *IEEE Trans. on Information Theory*, vol. 52, no. 4, pp. 1354–1365, April 2006.

[71] J.-F. Chamberland and V. V. Veeravalli, "Decentralized detection in sensor networks," *IEEE Trans. on Signal Processing*, vol. 51, no. 2, pp. 407–416, Feb. 2003.

[72] W.-P. Tay, J. N. Tsitsiklis, and M. Z. Win, "Censoring sensors: Asymptotics and the value of cooperation," *40-th Annual Conference on Information Sciences and Systems*, pp. 62–67, March 2006.

[73] S. Appadwedula, V. V. Veeravalli, and D. L. Jones, "Energy-efficient detection in sensor networks," *IEEE Journal on Selected Areas in Communications*, vol. 23, no. 4, pp. 693–702, April 2005.

[74] P. Willett, P. F. Swaszek, and R. S. Blum, "The good, bad and ugly: distributed detection of a known signal in dependent gaussian noise," *IEEE Trans. on Signal Processing*, vol. 48, no. 12, pp. 3266–3279, Dec. 2000.

[75] V. Aalo and R. Viswanathan, "On distributed detection with correlated sensors: Two examples," *IEEE Trans. on Aerosp. Electron. Syst.*, vol. 25, pp. 414–421, May 1989.

[76] E. Drakopoulos and C.-C. Lee, "Optimum multisensor fusion of correlated local decisions," *IEEE Trans. on Aerosp. Electron. Syst.*, vol. 27, pp. 5–14, Jul. 1991.

[77] M. Kam, Q. Zhu, and W. S. Gray, "Optimal data fusion of correlated local decisions in multiple sensor detection systems," *IEEE Trans. on Aerosp. Electron. Syst.*, vol. 28, pp. 116–120, July 1992.

[78] J.-G. Chen and N. Ansari, "Adaptive fusion of correlated local decisions," *IEEE Trans. on Syst., Man, Cybern., Part C*, vol. 28, no. 2, pp. 276–281, May 1998.

[79] T. Q. S. Quek, M. Z. Win, and D. Dardari, "Energy efficiency of cooperative dense wireless sensor networks," *International Conference On Communications And Mobile Computing*, pp. 1323–1330, July 2006.

[80] K. G. Seddik and K. J. R. Liu, "On relay nodes deployment for distributed detection in wireless sensor networks," *submitted to IEEE Global Telecommunications Conference (GLOBECOM)*, 2008.

[81] K. G. Seddik and K. J. R. Liu, "Distributed detection in sensor networks: A sensor or a relay?," *submitted to IEEE Global Telecommunications Conference (GLOBECOM)*, 2008.

[82] A. Papoulis, *Probability, Random Variables, and Stochastic Processes, Third Edition*, WCB/McGraw-Hill, 1991.

[83] B. Hochwald and K. Zeger, "Tradeoff between source and channel coding," *IEEE Trans. Info. Theory*, vol. 43, no. 5, pp. 1412–1424, September 1997.

[84] B. Hochwald, "Tradeoff between source and channel coding on a gaussian channel," *IEEE Trans. Info. Theory*, vol. 44, no. 7, pp. 3044–3055, Oct. 1998.